THE UNIVERSITY
of EDINBURGH

Using CRISPR to determine the effects of mutations of PTPN22 in human T cells

Cara Bray

Thesis submitted for the degree of Doctor of Philosophy

The University of Edinburgh

2018

Declaration

I declare that this thesis has been composed solely by me and that it has not been submitted, in whole or in part, in any previous application for a degree. Except where stated otherwise by reference or acknowledgment, the work presented is entirely my own.

Cara Bray Date

For my mother

Acknowledgements

Many more people have been instrumental to the completion of this work than could possibly be named here. Be they support staff, fellow scientists, and/or dependable friends, I am grateful to the people who have made my work not only possible, but also enjoyable. In addition, I must extend special thanks to the following people:

To patient JM, whose contribution to immunology was invaluable;

To Hans Stauss and Sharyn Thomas, for helping me kick things off right;

To Rose, for the all the opportunities, resources, and guidance a fledgling scientist could ask for;

To the Zamoyska team, for discussions, insights, and laughs through good times and bad;

To my teachers at LHS, whose lessons gave me the tools and inspiration to be here today;

To my mom and dad, for good genetics and unending patience and support;

To my wonderful Joe, for encouraging, assisting, feeding, cajoling, listening, advising, and loving me every step of the way.

Abstract

The haematopoietic phosphatase PTPN22 is a key regulator in balancing immune responses between self-reactivity and tolerance. PTPN22 downregulates T cell signaling and harbors the non-HLA genetic variation most strongly associated with autoimmune disease in humans, the single nucleotide polymorphism R620W. The effect of this mutation is currently controversial due to confounding results in mouse and human models. The polymorphism is linked to increased susceptibility to autoimmunity in both human and mouse models, although the latter does depend on genetic background. However, mouse data clearly shows that the polymorphism has a loss-of-function effect on T cell signalling, whereas studies in human models largely demonstrate a gain-of-function effect for R620W. A confounding issue in human studies is that they depend on comparison of T cells from distinct individuals, on protein over-expression, or on RNA interference, techniques for which it is difficult to control for genetic and environmental variables, changes in stoichiometry, and off-target effects or incomplete knockdown, respectively. We aimed to create isogenic human cell lines with mutations in PTPN22 at the genomic level to alleviate the complications inherent in analysing human data.

In addition to autoimmune pathogenesis, we are interested in the role of PTPN22 in a cancer setting. Because PTPN22 has a strong suppressive effect on T cell responses to weak affinity antigen, which encompass most tumour antigens, we postulated that knocking out PTPN22 may better enable T cells to kill tumour cells. Furthermore, we have shown that PTPN22 knockout (KO) leads to increased IL-2 expression in mouse T cells, and that this effect is protective against TGF-β mediated suppression, a common driver of T cell inhibition in the tumour microenvironment. T cell transfer experiments in mice showed that PTPN22 KO T cells are indeed more effective at reducing tumour size. Based on these findings, we aim to determine whether PTPN22 KO in human cells confers a similar effect on signaling.

To investigate the effects of PTPN22 KO on human T cell signaling, we used CRISPR gene-editing to target PTPN22 in a Jurkat cell line. By combining this technique with lentiviral transduction of a specific T cell receptor, we generated

human cell lines which are genetically identical, save for specific alterations to PTPN22, and which can be stimulated with strong or weak cognate antigen. We found that PTPN22 KO Jurkat cells develop an enhanced activation phenotype upon stimulation, including increased IL-2 expression. Additionally, PTPN22 KO Jurkat cells show enhanced Erk signalling following stimulation with weak affinity antigen, but this difference is lost as stimulus strength increases.

CRISPR technology has presented the opportunity to create novel models of PTPN22 signalling in the context of human T cell lines. The data from these lines suggests that, unlike the R620W mutation, complete loss of PTPN22 has a comparable effect in human and mouse T cells. In conjunction with our previous findings, these results suggest that knocking out PTPN22 may lead to signalling alterations that improve adoptive T cell cancer therapy.

Lay summary

The immune system evolved to protect the body against invasion by microbes. Autoimmune disease occurs when the immune system becomes activated to cause inflammation and destruction of tissues in the absence of infection. T cells are master controllers of the immune system and are thought to play an important role in development of autoimmune disease. To better understand why some people develop autoimmunity, scientists have analysed the genomes of individuals with and without autoimmune disease. A mutation affecting protein called PTPN22 was identified as one of the strongest predisposing factors for autoimmunity in humans, however it is not clear how the function of PTPN22 is changed by this mutation to lead to autoimmune disease.

Scientists have used lab mice and human cells to study PTPN22 and understand its role in T cells and autoimmunity. Unfortunately, studies from mice do not always correspond with what we observe in humans, and in the case of PTPN22 the data is particularly contradictory. Mice that have the autoimmune-predisposing PTPN22 mutation have stronger T cell responses, which is also what is observed when PTPN22 is absent. On the other hand, T cells from human individuals with the autoimmune-predisposing PTPN22 mutation have weaker responses. There are no humans that lack PTPN22, so it is challenging to understand the role of PTPN22 in human T cells, and how it may differ from mice.

My project addresses the controversy in PTPN22 research by genetically editing human T cells to lack PTPN22, allowing us to compare human cells with and without the protein and to directly analyse the effect it has on T cell activity. My results showed for the first time that human T cells that lack PTPN22 have stronger responses, which is similar to the findings in mice. This suggests that the differences we observe between mouse and human are not due to a fundamentally distinct role for PTPN22 between the species, and lays the groundwork for fully understanding the function of PTPN22 in human T cells.

Abbreviations

AD - Addison's disease
ADAP - adhesion and degranulation-promoting adapter protein
AICD - activation-induced cell death
AIRE - autoimmune regulator
ALPS - autoimmune lymphoproliferative syndrome
AP-1 - Activator Protein-1
APC - antigen presenting cell
APS - autoimmune polyglandular syndrome
B6 - black 6
Bcl - B cell lymphoma protein
BCR - B cell receptor
bp - base pair
CARMA - CARD- and membrane-associated guanylate kinase-like domain-containing protein
CBM complex - CARMA1, Bcl10, and MALT1 complex
CD - cluster of differentiation
cDNA - complementary DNA
CFSE - carboxyfluorescein succinimidyl ester
Cp - crossing point-PCR-cycle
CRISPR - clustered regularly interspaced short palindromic repeats
Csk - C-terminal Src kinase
cTEC - cortical thymic epithelial cell
CTV - CellTrace Violet
CXCR - C-X-C chemokine receptor type
DAG - diacylglycerol
DC - dendritic cell
DMSO - dimethyl sulfoxide
DNA - deoxyribonucleic acid
EAE - experimental allergic encephalomyelitis
EDTA - ethylenediaminetetraacetic acid
eGFP - enhanced green fluorescent protein
EGR - early growth response protein
Erk - extracellular signal-regulated kinase
FACS - fluorescence activated cell sorting
FCS - fetal calf serum
FOX - forkhead box
GADS - GRB2-related adaptor downstream of Shc
GD - Graves' disease
GRB2 - growth factor receptor-bound protein 2
GSK - glycogen synthase kinase
GWAS - genome-wide association studies
HD - Hashimoto disease
HDR - homology-directed repair
HLA - human leukocyte antigen
ICOS - inducible T-cell costimulator
IFN - interferon
IL - interleukin

IMDM - Iscove's modified Dulbecco's medium
indel - insertion/deletion
IP_3 - inositol-3-phosphate
IPEX - immunodysregulation, polyendocrinopathy, and enteropathy, X-linked
ITAM - immunoreceptor tyrosine activation motifs
Itk - interleukin-2-inducible T-cell kinase
JIA - juvenile idiopathic arthritis
JNK - c-Jun N-terminal kinase
KO - knockout
LAT - linker for activation of T cells
LB - lysogeny broth
Lck - lymphocyte-specific protein tyrosine kinase
LDS - lithium dodecyl sulfate
MALT - mucosa-associated lymphoid tissue lymphoma translocation protein
MAPK - mitogen-activated protein kinases
MFI - median fluorescence intensity
MG - myesthenia gravis
MHC - major histocompatibility complex
MOG - myelin oligodendrocyte glycoprotein
MOPS -
mRNA - messenger RNA
MS - multiple sclerosis
mTEC - medullary thymic epithelial cells
mTOR - mechanistic target of rapamycin
mTORC - mTOR complex
NK - natural killer
NFAT - nuclear factor of activated T-cells
NFκB - nuclear factor-κB
NHEJ - non-homologous end joining
PAM - protospacer adjacent motif
PBS - phosphate buffered saline
PCR - polymerase chain reaction
PDK - phosphoinositide-dependent kinase-1
PFA - paraformaldehyde
PI - propidium iodide
PI3K - phosphoinositide 3-kinase
PIP_2 - phosphatidylinositol 4, 5-bisphosphate
PKC - protein kinase C
PLC - phospholipase C
PTEN - phosphatase and tensin homolog
PTPN22 - protein tyrosine phosphatase, non-receptor type 22
PVDF - polyvinylidene difluoride
RA - rheumatoid arthritis
RasGRP - RAS guanyl-releasing protein
RNA - ribonucleic acid
ROR - retinoic acid receptor-related orphan receptor
RPMI - Roswell Park Memorial Institute medium
SAg - superantigen
SDS - sodium dodecyl sulfate
SFB - segmented filamentous bacteria

SFK - Src-family kinase
sgRNA - single-guide RNA
SH2 - Src-homology 2
SHIP - SH2-containing inositol 5'-phosphatase
SHP-1 - SH2 domain-containing protein tyrosine phosphatase 1
siRNA - small interfering RNA
SLE - systemic lupus erythematosus
SLP-76 - SH2 domain-containing leukocyte protein of 76kDa
SMAC - supramolecular activation clusters
SNP - single nucleotide polymorphisms
SOS - son of sevenless homologue
STAT - signal transducer and activator of transcription
T1D - type 1 diabetes
TBE - tris-borate-EDTA
TCR - T cell receptor
Th1 - T helper type 1
Th2 - T helper type 2
Th17 - T helper 17
T_{FH} - T follicular helper
TNF - tumour necrosis factor
TRAF - TNF receptor associated factor
Treg cells - regulatory T cells
VDJ recombination - recombination of variable, diversity, and joining genes
WT - wild-type
Zap-70- Zeta-chain-associated protein kinase 70

Table of Contents

1. Introduction

The vertebrate immune system is composed of innate and adaptive branches which cooperate to protect an organism against pathogenic infection. The innate immune system serves as the first line of defense against an invading pathogen, able to recognise a broad spectrum of microbial pathogens and to rapidly initiate an immunological response[1]. Innate immune responses are also capable of activating and shaping the adaptive immune response. In contrast to innate immunity, adaptive immunity takes several days to mount a response, but adaptive responses are highly specific to the infecting pathogen. Adaptive immunity is also capable of immunological memory, allowing for rapid, specific responses upon detection of a previously encountered pathogen. T cells are key drivers of the adaptive immune response, and are able to respond to environmental signals to fill a variety of immunological roles[2]. Because of the importance of T cells in health and disease, the mechanisms that regulate T cell responses are of great interest to the immunological community.

1.1 Development and function of T cells

T cells differ from cells of the innate immune system in that their activating receptor is highly specific. In contrast to innate receptors that recognise common elements of infection, the T cell receptor (TCR) is expressed from genes that have undergone VDJ recombination of their variable (V), diversity (D) and joining (J) genes. The reassortment of receptor gene elements occurs independently in each immature cell and results in a unique sequence[3]. Mature T cells that have not been presented with their specific cognate antigen are considered to be naive, and maintain a state of homeostasis. The differentiation of a naïve T cell into an effector cell requires ligation of the TCR with an antigen of sufficient specificity as well as costimulatory signals, the cumulative effect of which must overcome the threshold of factors operating to maintain homeostasis in a naïve T cell.

However, upon ligation of the receptor with an antigen of sufficient specificity in the context of inflammation, these cells can become activated to have potent effector functions.

1.1.1 Thymic positive selection

Due to the highly destructive potential of adaptive immune responses, the repertoire of available T cell receptors is strictly controlled. The T cell receptors that exist within the periphery must be able to interact with healthy cells of the body without becoming activated to destroy them. This balance is achieved through the process of thymic selection, which requires thymocytes to express a TCR capable of low affinity interactions with self-peptide:major histocompatibility complex (MHC) in order to receive survival signals, but not high affinity interactions, which result in clonal deletion[4]. The seemingly paradoxical outcomes of TCR signalling (survival or deletion) are determined by many factors, including TCR expression level, levels of signalling molecules, APC interactions, and spatial and temporal distribution within the thymus and selection process. The progression of thymocytes through the thymus is summarized in Figure 1.

Lymphoid progenitors arise in the bone marrow. Upon migration to the thymus, thymus settling progenitor cells become early thymic progenitors. At this point in their development, the cells express no TCR or co-receptors, and are therefore considered double negative[5]. These cells undergo massive proliferation, and retain the potential to differentiate into B cells if they are experimentally transferred out of the thymus[6,7]. This expansion is important because fewer then 5% of thymocytes are estimated to survive thymic selection and become mature T cells[8]. The thymocytes receive T cell differentiation signals from thymic stromal cells.

As they move through the cortex of the thymus, double negative cells are signalled to undergo VDJ recombination and express a T cell receptor. The process of VDJ recombination randomly combines the genes of the TCR locus resulting in millions of possible variations of the TCR protein. The TCR β chain is rearranged first, and is expressed with a pre-α chain. Thymocytes with functional β chains start to proliferate, so that a successful β chain arrangement is repeated in multiple individual cells. At this stage thymocytes cease proliferation and begin to express both CD4 and CD8 co-receptors, being referred to as double positive. These cells then rearrange the genes of the TCR α chain to express a true αβ TCR. At this point, the cells are prepared to undergo positive selection. Cells that fail positive

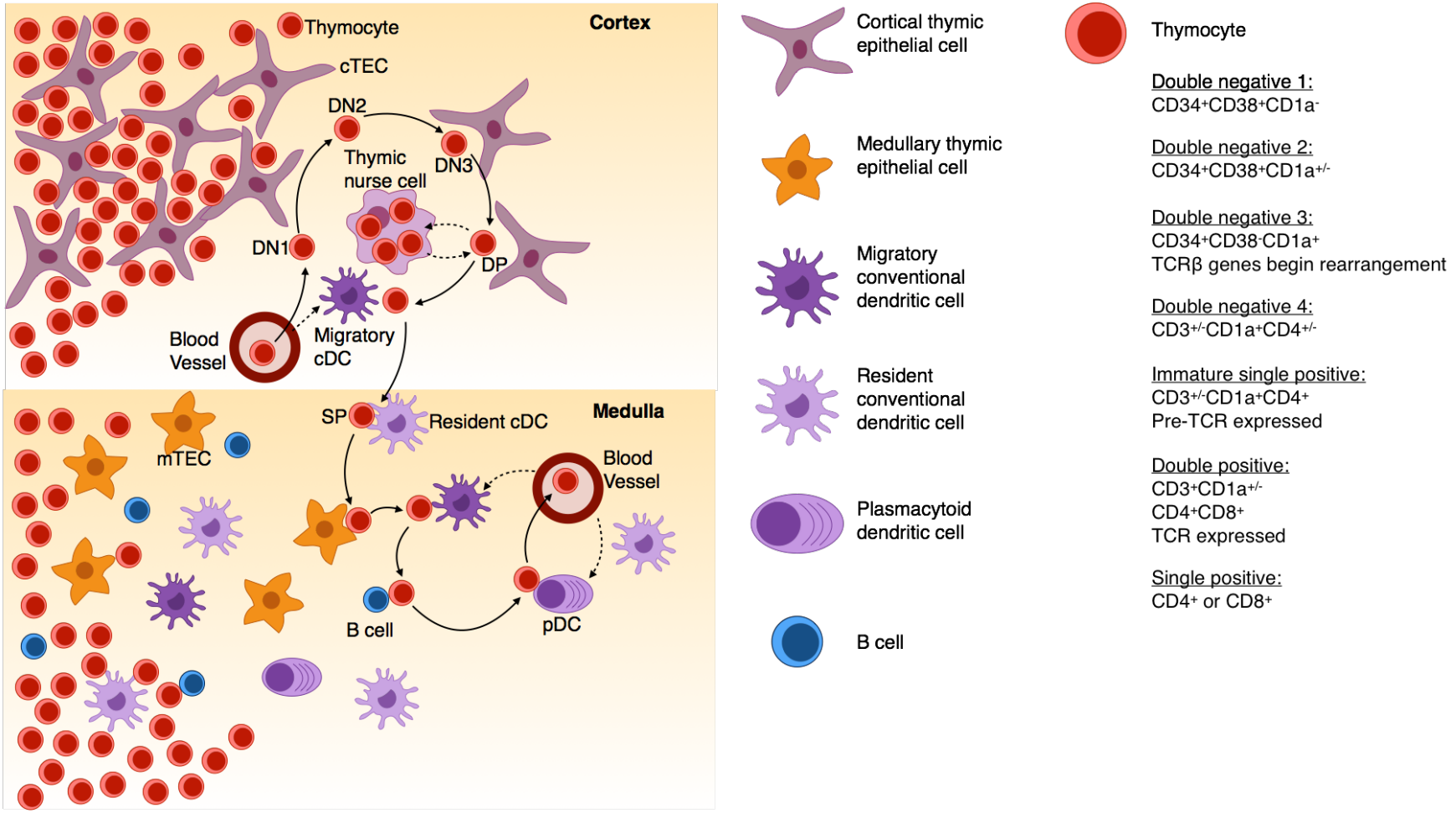

Figure 1. Thymic development of T cells. Solid arrows indicate migration of thymocytes, dashed lines are other migratory pathways. Figure adapted from Klein et al[4].

selection undergo further revision of the TCR α chain to until successful positive selection is achieved, increasing the likelihood that a successfully generated β chain will be paired with an α chain that allows it to interact with self-MHC [9]. Incomplete allelic exclusion in this process may lead to expression of two different α chains by a single cell, thereby retaining two TCRs of different affinities in an estimated 8% of peripheral T cells [10], which is a potential risk factor for autoimmunity.

Positive selection depends on the ability of a T cell to bind to a cortical thymic epithelial cell (cTEC) to receive survival signals; cells that fail to do so die by neglect. cTECs express MHC-peptide complexes to interact with the thymocyte TCR with relatively weak affinity. This step ensures that the recombined TCR has retained the ability to interact with self-MHC. Survival induced by TCR ligation appears to depend on low level, but sustained, Ca^{2+} signalling[11], and Erk signalling[12]; the latter possibly regulated in part by induction of pErk in a cytoplasmic compartment in response to low ligand affinity instead of at the plasma membrane as observed in negative selection[13]. Importantly, the strength of the TCR signal is critical, as inducing small increases in the affinity of the TCR can lead to negative selection[13], while partially inhibiting Zap-70 can convert a negatively selecting signal into a positive one [14]. It has been suggested that a mechanism in determining the strength of the signalling pathway in response to TCR ligation is the co-ligation of the TCR and its coreceptor: positive selecting ligands induce much less association of TCR and CD8 than negatively selecting ligands, meaning that Lck molecules associated with CD8 would be less able to interact with CD3 ITAMS in positive selection, thereby limiting the amplification of the TCR signal[15]. One possible way by which TCR signaling may be limited in positive selection is that thymocyte motility promotes positively-selecting transient interactions with cTECs[11]. Additionally, cTECs express relatively low levels of costimulatory molecules CD80/CD86 compared to medullary APCs involved in negative selection[11].

The protein Themis was recently identified to be critical in positive selection, but its precise role has yet to be clarified[16]. Themis appears to be important in modulating the response to weak TCR stimulation by recruitment of the negative regulator Src-homology 2 domain-containing protein tyrosine phosphatase 1 (SHP1), leading to enhanced cell survival[17,18]. During positive selection, cTECs express both MHCI and

MHCII, and present an array of peptides. cTECs express proteasomal subunit β5t, which replaces the β5i unit found in IFNγ induced immunoproteasome. β5t was found to be exclusive to cTECs in mice, and to cTECs and thymic cortex dendritic cells (DCs) in humans[19,20]. While the β5 of standard proteasomes and β5i of the immunoproteasome have activity promoting generation of peptides with hydrophobic C-terminal residues that bind MHCI with high affinity, β5t instead has weak chymotrypsin-like activity and is believed to produce peptides with weak affinity to MHCI [20]. β5t was shown to be important for positively selecting a diverse range of MHC class I-restricted TCRs, with β5t-deficient mice unable to mount a CD8 T cell response against influenza virus and experiencing severe lethality[21]. Thymocytes whose TCR that successfully binds to antigen presented by a cTEC receive survival signals through TCR signalling. Whether the thymocyte binds antigen presented in an MHCI or II context determines whether it retains the CD8 or CD4 co-receptor, respectively, through the single-positive stage.

It is not clear exactly how the decision to commit to CD4 or CD8 is made, but one attractive hypothesis is the kinetic signalling model. This model is based on the observation that CD8 transcription is downregulated upon TCR signalling, but that these cells are not yet committed. The model postulates that if signalling is maintained upon downregulation of CD8, the cells commit to the CD4 lineage; otherwise they revert to CD8 expression instead of CD4, in a process that may be interleukin (IL)-7 receptor dependent[22]. Selection of a single co-receptor following positive selection coincides roughly with the migration of the thymocyte into the medulla, though it appears that thymocytes take 1-2 more days to commit to be CD8 single positive than to be CD4 single positive[11].

1.1.2 Thymic negative selection

Single positive cells must survive negative selection. As single positive cells enter the medulla, a process dependent on upregulation of CCR7 by the thymocyte[23], they are again presented with antigen by medullary thymic epithelial cells (mTECs). It has been shown that impaired migration through the medulla results in spontaneous autoimmunity in mice[4] In contrast to the positive selection step cells that bind strongly to presented antigen receive apoptotic signals. It is not entirely clear how the signals of positive and negative selection produce such divergent results, though

experiments in different mouse strains suggested that there is a clearly defined threshold for signal strength required for negative selection[24]. mTECs and medullary DCs express much higher levels of costimulatory molecules CD80/CD86 than cTECs, which would enable them to induce stronger responses in T cells[11]. mTECs are also able to present antigen that is normally tissue-restricted through the process of promiscuous gene expression, thus exposing the thymocytes to an extensive repertoire of peripheral antigen. Promiscuous gene expression in mTECs is regulated in part by the transcription factor autoimmune regulator (AIRE), mutations or absence of which leads to autoimmunity in humans and mice[25]. Instead of binding directly to DNA like many transcription factors, AIRE promotes transcription by promoting activity of RNA polymerases that had stalled in the promoter region of genes, meaning its specificity is not to the gene itself but to the accessibility of the gene to polymerases, thus allowing AIRE to promote expression of a wide range of genes[26]. Promiscuous gene expression in mTECs during negative selection provides a thorough screen for highly auto-reactive TCRs, thereby removing cells that are likely to mediate autoimmunity. mTECs are particularly dense at the corticomedullary junction and are therefore the rare self-antigens they present are likely among the first to be encountered by thymocytes progressing from positive selection; as maturation in single positive cells was shown to lead to resistance to apoptosis via TCR stimulation, the positioning of mTECs to interact with less mature single-positive thymocytes may be important in maintaining tolerance to rare self-antigen[11].

Most dendritic cells of the thymus are found in the medulla, and make up about 0.5% of cells in the thymus[4]. Conventional DCs may be resident or migratory, with the former being somewhat more likely to reside the medulla than the latter (notably, negative selection does appear to be inducible by DCs in the cortex[4]). DCs express ICAM-1 which enables them to induce thymocyte arrest for sustained stimulation[27]. Resident cDCs tend to present antigen acquired from the thymic environment, including mTEC derived antigen, while migratory cDCs may specialise in presenting antigen from peripheral tissues and blood; although the functional consequences of these differences on thymocyte development is still open to speculation [4]. Plasmacytoid DCs have relatively poor antigen presentation, thus their role in central tolerance is only beginning to be explored, and may play a role in inducing

thymocytes to differentiate into regulatory T cells[28]. Thymic B cells are also able to induce negative selection. Although as of yet is in unclear how the contribution of B cells to central tolerance compares to that of mTECs and DCs[4], their participation in negative selection introduces a possible mechanism by which the B cell repertoire may influence the T cell repertoire.

Cells that survive both steps of thymic selection enter the periphery and are considered to be naive mature T cells. It is important to note that self-reactivity is necessary for TCR selection, and therefore T cells that react to self-antigen may be reduced by negative selection, but are not removed entirely, as self-reactive T cells are consistently detected in the periphery of healthy individuals[29]. In fact, the weak TCR:pMHC interactions required for positive selection continue to be vital to the survival of the mature T cell in the periphery, as TCR interactions with MHC promote expression of the receptors for survival-promoting cytokines, such as IL-7 and IL-15[30-33]. Self-reactivity is therefore not a mere artifact of T cell development but an element critical to their survival and function. Despite the presence of self-reactive T cells, peripheral tolerance may be maintained by a small proportion of thymocytes that become natural regulatory T (Treg) cells. The development of Treg cells specific to a given antigen was shown to depend on the tissue specificity of that antigen, as expression in organs with a role in immune defense, such as lung and intestinal tissue, was better able to elicit natural Tregs than expression of the antigen in the pancreas[34]. γδ T cells also arise from thymic development; these cells are distinct from the αβ T cells we discussed and occupy a more innate-like niche in the tissues. Thymic development also gives rise to natural killer (NK) T cells, a rare innate-like cell that may have immunoregulatory function through cytokine production. While these alternative T cell play critical roles in health and disease, the work presented here will focus on alpha-beta T cells.

1.1.3 T cell subsets

T cells encompass many subsets and thus a range of functions. Classically, T cells were differentiated by possession of a CD4 or CD8 co-receptor[2]. Upon activation the latter group differentiates into cytotoxic T cells, which are able to identify and destroy cells of the body that have been infected with virus, or which express tumour antigen. The CD8 co-receptor enables the T cell to bind to cells expressing MHC

class I (nearly all cells in the body), which presents antigen processed intracellularly. Thus, a cell that contains viral proteins presents viral antigenic peptides on the surface, which identify them to cytotoxic T cells specific to that antigen. Upon ligation of their TCR, cytotoxic T cells induce apoptosis in the target cell by releasing highly targeted granules containing granzyme B and perforin, or by engaging the Fas receptor on the target cell's surface with Fas ligand. Driving efficient killing of infected cells prevents the spread of the virus. Cytotoxic T cells also express antiviral cytokines, notably tumour necrosis factor (TNF)α and interferon (IFN)γ, which promote inflammation and activate other immune cells.

CD4 T cells are not thought to have such a direct role in cell killing. Originally dubbed "T-helper cells," these cells express dozens of different cytokines to help direct the immune response, and are also crucial in fully activating B cells. The types of cytokine expressed are highly variable depending on the microenvironmental context of the T cell's activation. For example, IL-12 and IFNγ are expressed by innate immune cells in response to intracellular pathogens[35]; these cytokines can induce a CD4 T cell to differentiate into a T helper type 1 (Th1) cell through induction of the transcription factors T-bet, signal transducer and activator of transcription (STAT)1 and STAT4[36]. Th1 cells support the cytotoxic response of CD8 T cells and macrophages by secreting IL-2, IFNγ and TNFα and β. Alternatively, the presence of IL-4 and IL-6 triggers the transcription factors STAT6 and GATA-3, leading to differentiation of the T cell towards a Th2 phenotype[36]. T helper type 2 (Th2) cells are most useful in defending against extracellular pathogens, especially by enhancing the humoural response. B cells are capable of expressing their specific antibody as IgM or IgD upon activation, but with T cell help they are able to undergo class switching and somatic hypermutation. These processes enhance the effector function of antibodies and increase their specific affinity, respectively. T follicular helper (T_{FH}) cells also help support B cell responses. T_{FH} cells express IL-21 and IL-4 and appear to be distinct from Th2 cells. Their differentiation depends on signalling by inducible T-cell costimulator (ICOS) and B cell lymphoma protein (Bcl)-6, and they migrate to the B cell follicle by upregulating C-X-C chemokine receptor type (CXCR)5 [37,38]. Finally, Th17 cells have been more recently described as a distinct T-helper cell lineage. Named for their production of IL-17, these cells develop in the presence of TGFβ, IL-6, and IL-23. Their differentiation is driven by

the transcription factor retinoic acid receptor-related orphan receptor (ROR)γt, and they are thought to be particularly important in defense against extracellular pathogens, particularly at mucosal surfaces[39]. Th17 cells are also pro-inflammatory, and have been implicated in autoimmune pathogenesis in a number of models[40,41].

Treg cells play a vital role in determining the T cell response. They can create a suppressive environment through expression of cytokines, such as IL-10 and TGF-β, and may limit the availability of stimulatory cytokines, such as IL-2, through high receptor expression[42]. Treg cells have also been reported to directly induce cytolysis in effector T cells via granzymes and perforin in a mouse tumour model, and to induce DCs to downregulate activating costimulatory molecules in vitro[43,44]. Regulatory T cells can arise naturally during T cell development or be induced by stimulation in a suppressive microenvironment or in the absence of sufficient costimulation[45]. The suppressive capabilities of Treg cells is dependent on the transcription factor forkhead box (FOX)P3.

It is likely that a variety of T cell subsets would be present in a given infection. Many of these subsets release cytokines to reinforce commitment of neighbouring T cells to the same phenotype, thereby polarising the immune response to be optimised towards a given type of infection. Upon clearance of an infection, or if an infection proves impossible to clear, the acute phase of the adaptive immune response must be downregulated. It is detrimental to maintain an environment of heightened inflammation for longer than necessary, so there exist mechanisms to downregulate the immune response and return to homeostasis. The majority of expanded T and B cells undergo apoptosis, mediated by anti-inflammatory cytokines IL-10 and TGFβ. However, a population of cells remain, forming immunological memory. These cells are characterised by long-term survival, possibly mediated by IL-7 and/or tonic TCR signaling[46,47], and the ability to rapidly produce effector cytokines upon re-exposure to their cognate antigen[48].

1.2 T cell activation

Activation of T cells is a critical event in the initiation of the adaptive immune response. Because T cells only recognise antigen in the context of MHC

presentation, their activation relies on interactions with antigen-presenting cells (APCs). An activated dendritic cell is one of the most efficient APCs, but T cells can also be activated by peptide presented by macrophages and B cells. Antigen presentation consists of a specific molecular epitope expressed in conjunction with an MHC molecule on the presenting cell's surface to be recognised by a T cell. Dendritic cells take up antigen from the periphery, but only when the microenvironment contains infection-associated signals does the cell become mature and able to express the migratory and costimulatory molecules needed to access the lymph node and fully activate T cells, such as CD80/86, interacting with CD28 on T cells, as well as TNF/TNF receptor family members[49,50]. APCs that lack the activating costimulatory molecules may instead induce an anergic state in naive T cells or even trigger differentiation into regulatory T cells, thus reinforcing immune tolerance to the given antigen[51]. Soluble peripheral antigen can also be transported into the lymph node by reticular fibers to be picked up and presentated by resident DCs located in the lymphatic sinus, a more rapid process that exposes T cells to antigen without relying on migration of DCs from the periphery, thereby initiating the T cell priming process sooner than previously believed[52,53].

T cell responses are initiated by binding of the T cell receptor to a cognate antigen peptide presented by MHC. Ligation of the T cell receptor triggers branching signalling pathways that lead to metabolic activation, proliferation, differentiation, and upregulation of effector functions (Figure 2). The outcome of T cell stimulation varies based on combinations of signals that include the strength of the activating stimulus, costimulation interactions with the antigen-presenting cell, and environmental cytokines. The integration of these signals into a phenotype appropriate to the context of activation relies on many finely regulated signalling components, the disruption of which may lead to immune dysfunction.

1.2.1 TCR binding

The T cell receptor itself is comprised of a paired alpha and beta chain which is able to bind specific antigenic peptide in the context of MHC. The TCR itself has no inherent signalling activity, but it associates with membrane-spanning CD3 molecules and dimeric ζ-chains. These associated molecules are critical for expression of the TCR complex and signalling intracellularly upon antigen binding to

the TCR. It is not entirely clear how binding of the TCR leads to signalling.. One hypothesis, the kinetic segregation model, proposes that size difference of surface molecules prevents larger negative regulators, such as the phosphatase CD45, from accessing the TCR complex when it is interacting with an APC[54]. TCR signalling molecules form clusters at the immunological synapse between the T cell and the APC[55]. These clusters are called supramolecular activation clusters (SMAC), and consist of TCR, co-receptors and co-stimulatory molecules gathered in the center of the cluster with additional signaling molecules (such as lymphocyte-specific protein tyrosine kinase [Lck] and protein kinase C [PKC]θ) surrounding them. CD45 is excluded from these structures, and is found in a surrounding outer region, unable to interact with the signaling molecules[56]. However, this idea is challenged by the finding that resting T cells show evidence of constitutive signalling that does not result in activation[57]; as the constitutive signal does not lead to TCR phosphorylation in a resting cell, it suggests that the ligands are hidden, thus supporting the model of conformational change upon TCR ligation being required to expose CD3 motifs to intracellular signalling machinery. The conformational change model suggests that binding exerts a physical force, pushing the signalling motifs of CD3 molecules further into the cytoplasm and exposing them for interaction with intracellular signalling molecules[58]. Further evidence for the conformational change model has come from detection of ligand-induced changes in the AB loop of the TCRα subunit and the H3 helis of the β subunit of specific TCRs; mutation of these regions abrogated signal transduction [59]. Xu et al. showed a close association of CD3 tyrosine residues with lipids of the plasma membrane in resting T cells using nuclear magnetic resonance, meaning that the residues involved in intracellular signalling are embedded in the membrane in the absence of TCR ligation [60]. Furthermore, Kim et al demonstrated that application of force upon the TCR can trigger stimulation using a non-agonist CD3 antibody or specific pMHC, suggesting that the TCR can act as a mechanosensor, translating

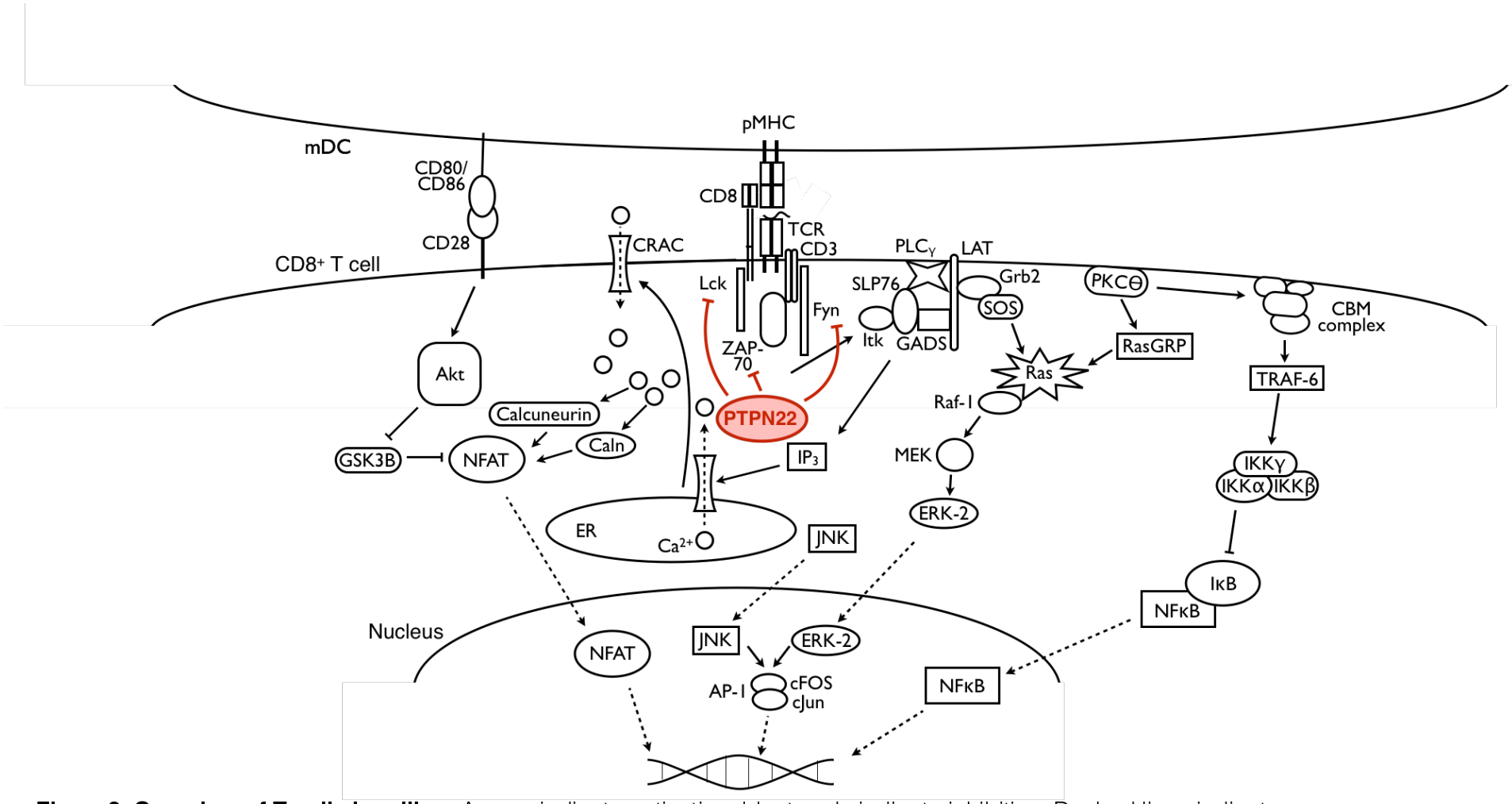

Figure2. Overview of T cell signalling. Arrows indicate activation, blunt ends indicate inhibition. Dashed lines indicate translocation.

mechanical force into signalling output[61]. While the contribution of kinetic segregation is not precluded by the conformational change model, the evidence is convincing that mechanical forces and biochemical changes are important for initiation of TCR signalling.

The result of TCR ligation is phosphorylation of immunoreceptor tyrosine activation motifs (ITAMs) on the cytoplasmic tails of the CD3 molecules. Phosphorylation is carried out by Src-family kinases (SFKs), notably Lck, which associates with CD4 and CD8 coreceptors, and Fyn, which associates with CD3 chains[62]. Lck contains a tyrosine residue, Y505, that inhibits the protein when phosphorylated. In the absence of Y505 phosphorylation, Lck undergoes auto-phosphorylation of Y394, which enhances its activity in phosphorylating ITAMs and downstream targets.

Phosphorylated ITAMs serve as docking sites not only for Lck and Fyn, but also for Zeta-chain-associated protein kinase (Zap)-70, which, upon phosphorylation by Lck, triggers the assembly of the proximal signalling complex by phosphorylating linker for activation of T cells (LAT) and SH2 domain containing leukocyte protein of 76kDa (SLP-76) [63-66]. LAT contains many tyrosine resides, enabling it to recruit key signalling proteins such as GRB2-related adaptor downstream of Shc (GADS) (associated with SLP-76), PLCy, and Grb2 (associated with SOS)[66,67]. SLP-76 in turn recruits Vav1, interleukin-2-inducible T-cell kinase (Itk), Nck, and adhesion and degranulation-promoting adapter protein (ADAP). Recruitment of these molecules to the signalling complex leads to their activation by other molecules in the complex, which in turn drives the propagation of the activating signal throughout the cell.

1.2.2 Distal T cell signalling pathways

Proximal TCR signalling leads to downstream effects via a number of branching distal signalling pathways. One of the key drivers of downstream signalling is Phospholipase C (PLC)Y, which cleaves membrane-bound phosphatidylinositol 4, 5-bisphosphate (PIP_2) into inositol-3-phosphate (IP_3) and diacylglycerol (DAG). IP_3 binds to channels in the endoplasmic reticulum and triggers the release of intracellular calcium stores, depletion of which triggers the influx of extracellular calcium through Ca^{2+} release-activated Ca^{2+} (CRAC) channels in the plasma membrane, enabling intracellular calcium levels to remain elevated for 1-2 hours[68].

Calcium depletion in the ER is sensed by STIM1, which multimerises upon loss of its bound Ca^{2+} and translocates to be proximal to the plasma membrane. STIM 1 facilitates clustering of Orai1 to form the pore of the CRAC channel[69]. The influx of calcium ions activates calmodulin, leading to activation of calcineurin, which dephosphorylates the transcription factor NFAT, enabling NFAT to enter the nucleus[66].

DAG is able to activate PKCθ and RAS guanyl-releasing protein (RasGRP). RasGRP is the critical activator of Ras, and is itself activated through phosphorylation by PKCθ following its recruitment to the plasma membrane by DAG[70]. The Ras/Extracellular Signal-regulated Kinase (Erk) pathway may also be activated by son of sevenless homologue (SOS), although SOS signalling cannot compensate for RasGRP deficiency[70,71]. Ras activation of Raf-1 leads to activation of Mitogen-activated protein kinases (MAPK1/2), which activates Erk1/2. This pathway leads to the phosphorylation of the transcription factor Elk, which induces expression of cFos, a constituent of the critical transcription factor Activator Protein-1 (AP-1). Activated PKCθ also triggers the formation of the CBM complex (consisting of CARD- and membrane-associated guanylate kinase-like domain-containing protein [CARMA]1, Bcl10, and Mucosa-associated lymphoid tissue lymphoma translocation protein [MALT]1), which activates TNF receptor associated factor (TRAF)-6. This leads to the ubiquitination of IκB by releasing inhibition of the IκB kinase (IKK) complex. IκB is normally in complex with NFκB; its degradation releases NFκB and allows it to translocate to the nucleus[66].

Another indispensable pathway in T cell activation is mechanistic target of rapamycin (mTOR) signalling, a key regulator of cell growth, metabolism, and proliferation[72]. mTOR deletion in mouse CD4 T cells reduced their ability to differentiate into Th1, Th2, or Th17 cells when stimulated in the appropriate conditions. The cells instead gained Treg markers, thereby demonstrating a role for mTOR in integrating environmental cues into the T cell signalling pathway[73]. mTOR activation in stimulated T cells was shown to be enhanced by the presence of the cytokines IL-1, IL-2, IL-4, IL-12, and IFNγ[74]. mTOR signalling is accomplished via two mTOR complexes, mTORC1 and mTORC2. mTORC1 activity is downstream of Phosphoinositide 3-kinase (PI3K), which activates phosphoinositide-dependent

kinase (PDK)1 and leads to phosphorylation and activation of Akt. Notably, two regulators of PI3K, phosphatase and tensin homolog (PTEN) and SH2-containing inositol 5'-phosphatase (SHIP1), are absent in Jurkat cells, meaning the threshold for PI3K activity is lowered and PI3K-Akt pathway is dysregulated in these cell lines[56,75]. There is evidence that Akt activity may not be required for mTORC1 activation, suggesting some redundancy in mTORC1-activating kinases activated by PDK1[76]. The specific signals upstream of mTORC2 are still being actively investigated, with one group showing that mTORC2 is activated upon association with ribosomes[77], and another demonstrating its inhibition by cell stress via GSK-3β, which also inhibits Akt[78]. The best described substrates for mTORC1 are ribosomal S6 kinase and 4 elongation factor-binding protein 1, enabling it to promote protein translation, while mTORC2 modulates cytoskeletal organisation and survival by phosphorylating the signalling proteins PKCα and Akt[79].

1.2.3 T cell costimulation

The outcome of TCR stimulation depends on the strength of signalling through the TCR as well as the presence of costimulatory factors and cytokine signals in the environment. Information from each of these signals is interpreted and integrated into an appropriate response.

One of the best characterised costimulatory pathways is that of signalling through CD28. Costimulation is required for TCR ligation to produce an effector response; in the absence of costimulation, stimulated T cells may die or become anergic and unresponsive[80]. CD28 signalling is important for production of IL-2, the survival factor Bcl-x, and promotes signalling throughout other TCR pathways. CD28 on resting T cells binds to CD80 or CD86 on activated dendritic cells, which triggers phosphorylation of the cytoplasmic tail of CD28. These phosphorylation events allow for the subsequent steps of CD28 signalling, including the binding of PI3K, and enhancement of the PI3K-driven pathways described above, and recruitment of Akt, which has been shown to promote both NFκB and NFAT transcription factor activation, resulting in pro-survival factors and IL-2 expression[70]. The intracellular tail of CD28 can also bind other adaptor proteins involved in T cell signalling, such as GADS and GRB2, which leads to activation of JNK and cJun activity via Vav, a GRB2 binding partner[56]. By modulating interactions with key molecules of TCR

signalling, CD28 has a profound effect on the outcomes of T cell stimulation.

Activated CD28 enhances TCR signalling past the threshold needed for the cell to gain effector functions, but is not sufficient for differentiation into different T cell subsets. This process depends on specific cytokines produced in response to different types of infection, as described above.

1.3 Autoimmune disease

Autoimmunity occurs as a result of the adaptive immune system becoming inappropriately activated to attack healthy tissues of the body. Autoimmune diseases can affect a wide range of organs and cell types, and can vary dramatically in effect and severity in affected individuals. Progression of autoimmune disease often requires a number of steps and different cell types. It is believed that autoimmune responses require an environmental trigger to break tolerance on a predisposing genetic background. Diseases of autoimmune classification affect roughly 3-5% of people in the US, but, worryingly, incidence of autoimmune diseases may also be increasing in the Western world[81]. Autoimmune diseases represent a significant societal burden and understanding their pathogenesis is critical for preventing their development and improving treatments.

1.3.1 Pathogenesis of autoimmune disease

Similar to protective immune responses, autoimmune responses are thought to be driven by T cells. Thymic selection deletes the TCRs that interact too strongly with self-antigen, however weakly interacting TCRs may escape. In fact, all individuals harbour T cell receptors with self-reactive capacity within their repertoire, however peripheral tolerance mechanisms typically prevent these from becoming activated. In autoimmune disease, this tolerance is lost and the destructive power of the immune system is directed towards antigens of the self.

Overcoming peripheral tolerance mechanisms may occur through a combination of various specific circumstances. One suggested triggering event is infection: the normal course of response to infection involves increased inflammation and the activation of dendritic cells to better stimulate T cells. Without activation, DCs

instead trigger anergy or tolerance in T cells. It is possible that DCs present not only antigen of the pathogen, but also self-antigen from the infection site, thereby inadvertently stimulating self-reactive T cells in the context of inflammation. T cells may also respond to a foreign antigen that is similar to a self-antigen, in a phenomenon known as molecular mimicry. Infection can also lead to tissue injury, which, in the case of immune privileged sites, may expose self-antigen for which no tolerising events have occurred[82]. It has also been suggested that the expression of multiple TCRs on a single cell (which may occur if two alpha chains are positively selected during thymic development[10]) may enable a cell to be activated to fight infection while also bearing a receptor that recognises self-antigen. In addition to infection, man-made interventions may be associated with autoimmune disease, such as certain vaccinations, although this occurrence is exceedingly rare[83]. B cells may also play a role in induction of autoimmunity. Development of experimental allergic encephalomyelitis (EAE) in a mouse model required the presence of B cells when mice were vaccinated with myelin oligodendrocyte glycoprotein (MOG) protein, but B cells were dispensable upon vaccination with MOG peptide; B cells may therefore have a capacity to stimulate autoreactive T cells in the context of certain antigens[84]. Further evidence for the critical role of B cells in autoimmunity is found in the efficacy of Rituximab, an antibody directed against CD20 which depletes naive and memory B cells, and has been approved for treatment of rheumatoid arthritis, with efficacy demonstrated in a number of other autoimmune diseases[85].

In any case, self-antigen is unlikely to be able to be cleared, and normal down-regulation of the immune response cannot occur (except in specific cases, such as pancreatic islet cell destruction in T1D). This situation leads to chronic inflammation and tissue destruction as the immune system attempts in vain to destroy the offending antigen. Progression to full autoimmune disease severity typically takes time. One way the disease state may be exacerbated is through epitope spreading to recruit additional T cells distinct from those already active[86]. Epitope spreading may be mediated by B cells presenting new peptide from native antigen to T cells[87]. B cells can also contribute to the exacerbation of autoimmunity through somatic hypermutation and isotype switching of autoantibodies.

1.3.2 Role of the microbiome in autoimmune disease

Clearly environmental triggers cannot bear sole responsibility for autoimmune disease, or the prevalence would be far higher. The currently accepted model is that environmental triggers will lead to autoimmune disease only in individuals with certain predisposing traits. Traditionally, the alternative to environmental factors were genetic factors, and while these still make a major contribution to autoimmune susceptibility, we must also consider the possible role of the microbiome, which straddles the border between extrinsic and intrinsic factors.

The population of commensal bacteria that make up an individual's gut microbiome are proving to be vital in regulating the development and homeostasis of the immune system[88]. Germ-free mice showed accumulation of NKT cells and increased inflammatory disease, which was mitigated when the mice were colonised with conventional bacteria at a young age, but not when colonised as adults[89]. Similarly, germ-free mice have been shown to have reduced lymphoid organ development in the intestinal mucosa[90]. Segmented filamentous bacteria (SFB) were shown to be crucial for the development of Th17 and Th1 versus Treg cells in the gut[91]. The microbiome is likely to have a role in both protection by and regulation of the immune system, which means dysbiosis has the potential to contribute to autoimmune disease. For example, a significant reduction in specific phyla of commensals was observed in Crohn's disease and ulcerative colitis patients, though it is unknown whether this effect is causative[92]. Murine rheumatoid arthritis models showed reduced pathology in germ free mice, which increased in severity upon introduction of SFBs, an effect which correlated with increased TH17 activity[93]. While the field is still very new, evidence is rapidly accumulating to support the importance of commensal bacteria in regulating functions of the immune system.

1.3.3 HLA associations with autoimmune disease

Twin studies provided early evidence that autoimmune diseases have a genetic component, with disease concordance at least four times higher in monozygotic twins than dizygotic twins[94], although the degree of inheritability varies considerably between specific diseases[95]. More recently, genome-wide association studies (GWAS) have enabled us to identify individual alleles which may contribute to autoimmune susceptibility. These genes provide important clues to the mechanisms

underlying autoimmunity.

By far the clearest genetic contribution to autoimmune disease is in the human leukocyte antigen (HLA) genes, with nearly every autoimmune disease having an association with certain HLA genes[96]. The human gene pool contains thousands of different alleles for the HLA gene complex. HLA genes determine the specific MHC molecules expressed on an individual's cells, and therefore the type of peptide antigens that can be presented on their surface. Different MHC molecules are able to bind and present different ranges of peptides, meaning that the adaptive immune systems of different individuals may recognise and respond to wholly diverse antigens, even from the same pathogen. The HLA gene complex contains three major loci encoding MHC class I genes (called A, B and C) and three pairs of genes encoding MHC class II (DR, DP, DQ). There are also a number of MHC II chaperone genes, DM, DOα and DOβ, which are important in epitope selection for peptide binding to MHC II. An analogous role is carried out for MHC I by the proteins TAP, tapasin, and ER folding factors ERp57 and ERAAP, which load MHC I molecules with peptides derived from the 26S proteasome [97]. Variations in the genes involved in antigen presentation can have a vital role in autoimmune susceptibility.

The degree of redundancy in MHC presenting genes enables individuals' MHC to bind to a wider range of peptides than if our genes encoded only one type of MHC class I or II, and increased heterozygosity may lead to stronger cellular immune responses, as HLA homozygosity was found to correlate with reduced lymphocyte proliferation in response to vaccination compared to heterozygotes[98,99]. The number of loci also allows plenty of room for diversity between individuals, as it is extremely unlikely for unrelated individuals to share an identical HLA genotype. This heterogeneity is valuable not only for the individual, but also for the fitness of the species as a whole in resisting infection by pathogens[100]. Maintaining HLA diversity has even been suggested to be a key factor in human sexual selection. Such behaviour has been reported in other vertebrates, but human studies have yet to reach a consensus[101-103]. Regardless of how the diversity is maintained, it is clear that HLA genes have a significant impact on determining immune responses.

The antigens that have been found to drive autoimmunity are relatively restricted.

They must be presented somewhat rarely, possibly found at immune-privileged sites, or responsive T cells would be clonally deleted during thymic development. At the same time, they must be presented sufficiently to trigger T cell effector functions. In keeping with this idea, distinct individuals with a given autoimmune condition may have mounted immune responses against the same self-antigen, as observed in Celiac disease[104]. The antigenic self-peptide must be able to be presented in the context of an MHC molecule, so an individual's HLA genes highly affect the likelihood of their T cells ever encountering such an antigen. Alternatively, it is possible that certain MHC molecules can bind an autoimmune-associated antigen weakly, allowing for positive selection but not sufficient for negative selection. In this case, an individual might have a disproportionate number of self-reactive T cell receptors in their periphery. Another possibility is that certain MHC molecules are less adept at producing Treg populations during thymic selection, thereby weakening peripheral tolerance mechanisms[96].

It can be difficult to disentangle the individual contributions of MHC class I and class II genes because of linkage disequilibrium throughout the HLA region, but some associations have been identified[96]. Type 1 diabetes (T1D)-associated HLA alleles include DRB1*03, DRB1*04, and B*39, with variations in the *DQB1* and *HLA-A* loci being associated with either protection or increased susceptibility. RA and Graves' Disease (GD) have been linked to a number of *DRB1* alleles, with the latter also having shown associations with certain *HLA-C* and *-B* alleles. Multiple sclerosis (MS) is associated with DR15, as well as A*0301, with A*0201 apparently conferring a protective effect. The complexity of the HLA region makes it challenging to disentangle the effects of individual alleles on autoimmune susceptibility, but the associations identified may help inform the mechanisms of disease progression.

1.3.4 Non-HLA genes in autoimmune disease

HLA genes undoubtedly play an important role in shaping our immune systems, but they are far from the sole genetic player in autoimmune susceptibility. Monozygotic twins have more similar incidences of autoimmunity than HLA-matched siblings, so other elements of the genetic landscape must play a role.

Single-gene autoimmune diseases are rare, but do exist within the human gene

pool. One classic example is mutations in the AIRE gene, which was identified to be the cause of autoimmune polyglandular syndrome (APS) type 1. This syndrome is characterised by hypoparathyroidism, adrenal failure, and chronic mucocutaneous candidiasis[105]. An investigation into how mutations in AIRE lead to mutli-organ autoimmunity revealed that the protein is crucial in presentation of tissue-restricted self-antigens during thymic selection. The lack of presentation of self-antigens means that negative selection against these antigens cannot occur, and thus mature T cells are able to enter into the periphery which then mediate autoimmunity, with symptoms of APS type 1 typically arising in infancy[106].

Immunodysregulation, polyendocrinopathy, and enteropathy, X-linked (IPEX) is a very rare, severe autoimmune disorder which was linked to mutations in the gene FOXP3, which is critical for Treg function. The disease manifests in infancy and is lethal if untreated, with symptoms characteristic of over-activation of the immune system, including dermatitis, diabetes mellitus, thyroiditis, hemolytic anemia, diarrhea, and severe responses to viral infection[106].

Patients with autoimmune lymphoproliferative syndrome (ALPS) were found to harbor mutations in Fas, Fas-ligand, or the associated apoptosis pathway. Symptoms of ALPS include lymphadenopathy, splenomegaly, hypergammaglobulinemia, and frequently hemolytic anemia and thrombocytopenia. It is not yet clear precisely how disruption of apoptosis leads to these symptoms, but current hypotheses suggest aberrant regulation of self-reactive lymphocytes[106].

While study of monogenic autoimmune diseases can provide valuable insights into normal and disrupted immune function, they account for a very small proportion of all autoimmune diseases. The vast majority of autoimmune diseases are thought to be multifactorial, which makes it much more difficult to identify the individual causative factors. GWAS are a tool to identify the gene alleles shared by patients with autoimmune disease by screening large cohorts of individuals. It is important to note that only those alleles that are frequent enough in the population to achieve significance will be reported by these studies. GWAS studies are also only recently beginning to consider copy number variants, which may contribute to disease heritability[107]. Nonetheless, the genes that have been identified by GWAS studies

provide useful information in understanding complex autoimmune pathogenesis.

Perhaps unsurprisingly, many of the genes indicated by GWAS studies are involved in T cell and B cell signalling. In most cases, individual genes make only a minor contribution to risk of autoimmune disease, with all but the strongest associations conferring an odds ratio between 1.1 and 1.5[108]. The odds ratio refers to how likely a carrier of a risk allele is to develop a disease compared to someone who does not carry the allele. For rare diseases, such as autoimmune diseases, the odds ratio can be interpreted as an approximation of the relative risk that the allele confers[109]. For example, an odds ratio of 1.5 for a gene associated with a disease with a global incidence of 1% suggests that the disease incidence among carriers of that gene increases to 1.5%. The immune system contains many redundant checks to reduce risk of autoimmunity, so a combination of factors are likely to be required to break tolerance. Many of the genes identified are linked to multiple—but not all—autoimmune diseases, suggesting that certain autoimmune diseases share mechanisms of pathogenesis, but that these mechanisms are not necessarily conserved across every disease. Roughly half of the >40 genome regions linked to autoimmunity are associated with more than one disease. A number of genes reported to have associations with autoimmune diseases are listed in Table 1[110].

Table 1. Non HLA genetic markers of autoimmune diseases. AD: Addison's disease, GD: Graves' disease, HD: Hashimoto disease, JIA: juvenile idiopathic arthritis, MS: multiple sclerosis, RA: Rheumatoid arthritis, SLE: systemic lupus erythematosus, T1D Type 1 diabetes. Adapted from Sjakste et al[110].

Gene	Protein function	Associated diseases
PTPN22	Inhibits T-cell activation, contributes to TCR, B cell receptor, and toll-like receptor signalling in immune cells,	RA, SLE, T1D, HD, GD, vitiligo[111]
STAT 4	Involved in JAK-STAT signalling in spermatozoa, myeloid cells, and T cells. STAT 4 is activated by tyrosine phosphorylation in response to IL-12 treatment of T cells,	RA, SLE, Sjögren's syndrome, JIA, GD, myasthenia gravis[112,113]
CTLA-4	Cell surface molecule involved in regulating TCR signalling	RA, SLE, T1D, AD, Vitiligo, MS, HD[114]
TRAF1/C5	Involved in TNF signalling. TRAF1 is implicated in cell growth, proliferation, apoptosis, bone turnover, cytokine activation.	RA[115,116]
PADI4	Mediates the citrullination of histones in T cells, B cells, neutrophils, eosinophils, monocytes. Targeted by RA autoantibodies.	RA[115,117]
MIF	T cell cytokine, inhibits migration of macrophages and promotes macrophage accumulation in delayed-type hypersensitivity reactions.	T1D, RA[118]
UBASH3A	Involved in growth factor withdrawal-induced apoptosis in T cells. A suppressor of TCR signalling.	T1D[119,120]
STAT3	Activated in response to IFNs, EGF, IL5, IL6, HGF, LIF and BMP2. Acts as transcription activator and plays a key role in many cellular processes such as cell growth and apoptosis.	MS[121]
CLEC16A	A transmembrane calcium- dependent (C-type) lectin-like receptor	MS, RA, T1D[122]
CAPSL	Calcium sensor and calcium signal modulator.	T1D[123]
RGS1	Regulator of G protein signalling	T1D, MS[123]
ZMIZ1	Regulates the activity of various transcription factors, including Smad3/4, and p53. May also play a role in sumoylation.	T1D, MS[123]
TNFSF14	Costimulatory factor for the activation of lymphoid cells, stimulates the proliferation of T cells, and apoptosis of various tumour cells.	T1D, MS[123]
VCAM1	Cell surface sialoglycoprotein expressed by cytokine-activated endothelium. Mediates leukocyte-endothelial cell adhesion and signal transduction.	T1D, RA[123]
SOXB	Transcription factor involved in the regulation of embryonic development and in the determination of the cell fate.	T1D, MS[123]
Pvt1 oncogene	Oncogene, associated with several types of cancer and renal diseases.	T1D, RA[123,122]

1.4 Negative regulators establishing TCR signalling thresholds

T cells are potent drivers of autoimmune responses. To limit the possibility of their inappropriate activation, T cells express many negative regulators of TCR signalling, which maintain a threshold of signalling required to overcome homeostasis.

CD45 is a highly abundant trans-membrane phosphatase that is critical in determining T cell responses to TCR stimulation. CD45 regulates SFKs directly, though there is evidence that it has both positive and negative regulatory capacity, and has been shown to dephosphorylate both Lck Y394 and Y505[124,125]. CD45 has an important role in determining the signalling threshold required for T cell activation by downregulating the Y394 on constitutively active Lck in resting T cells. Thus T cells are able to maintain a state of signalling readiness with a baseline level of active Lck without pushing the cell into a stimulated state. It has been hypothesised that CD45 is essential as a positive regulator in early T cell signalling, but may act as a negative regulator at later timepoints[126]. Another feature of CD45 is that it has several isoforms that vary upon T cell stimulation, but the function of these remains unclear.

In addition to CD45, Lck and other early signalling molecules are regulated by a number of intracellular kinases and phosphatases, such as C-terminal Src kinase (Csk), protein tyrosine phosphatase, non-receptor type 22 (PTPN22), and SHP-1.

The intracellular phosphatases SHP-1 (PTPN6) and SHP-2 (PTPN11) contribute to T cell signalling regulation. SHP-1 acts predominately as a negative regulator and is thought to act on SFKs, and in vitro studies have shown that SFKs are efficient substrates for SHP-1[127,128]. THEMIS was shown by Paster et al to bind constitutively to either SHP-1 or SHP-2 in T cells and thymocytes, in a complex mediated by GRB2. Furthermore, knockdown of THEMIS resulted in a similar phenotype to SHP-1 knockdown, including increased CD3 phosphorylation, Erk activation, and CD69 upregulation in response to TCR stimulation. SHP-1 knockout cells were also demonstrated to be resistant to proliferation suppression by Tregs, and to have enhanced Akt signalling. These data suggest that SHP-1 plays an important role in

regulating T cell signalling thresholds in a THEMIS-dependent manner.

In contrast to the widely accepted role of SHP-1 as a negative regulator, the role of SHP-2 in T cells is unclear. SHP-2 forms associations with ITAMs of activated T cells[129], suggesting it plays a role in the TCR signalling pathway, however studies in transgenic mice lacking SHP-2 have produced contradictory results. Mice which lack SHP-2 in T cell lineages showed reduced TCR-driven proliferation, and reductions in expression of IL-2, CD25, and CD69 upon stimulation with anti-CD3[130], which supports the hypothesis that SHP-2 promotes TCR signalling. However, Zhang et al showed that CD4 tumour-associated T cells that lacked SHP-2 had elevated expression of inflammatory cytokines IL-6, TNFα, and IFNγ, suggesting that SHP-2 has a role in negative regulation of these cytokines[131]. While the effects that SHP-2 has on T cell signalling have yet to be fully understood, these studies underline the complex roles of intracellular phosphatases in TCR regulation and T cell function.

Csk is a kinase thought to act antagonistically to CD45 by phosphorylating Y505 on Lck on resting T cells. Manz et al. developed a mutant version of mouse Csk that is susceptible to small molecule inhibition[132]. Their data showed that inhibition of Csk reduced phosphorylation of Lck Y505 in mouse T cells at rest and upon stimulation with anti-CD3. This reduction correlated with increased Lck Y394 phosphorylation and, to a lesser degree, phosphorylation of Zap-70 Y319, a target of active Lck. Zap-70 phosphorylation did not appear to have significant downstream effects at rest, as measured by LAT, PI3K, and Erk phosphorylation, but upon stimulation these proteins were significantly more phosphorylated at early timepoints in cells with inhibited Csk compared to active Csk. These data suggests that Csk has a role in resting T cells, but that other negative regulators contribute to maintaining the resting state. Strikingly, Manz et al observed that activation (as measured by CD69 expression) is particularly enhanced by Csk inhibition when the cells were stimulated with weak peptide, suggesting that, like PTPN22, Csk is important in regulating T cell responses to weak peptide[132].

The final class of negative regulators are ubiquitin ligases. The Cbl family proteins are E3 ubiquitin ligases which play a role in regulating T cell responses through degradation of targets, including the TCRζ chain, Zap-70, LAT, and Vav[66].

Knockouts of c-Cbl or Cbl-b demonstrated increased proliferation and IL-2 expression, and, as well as a failure to down-regulate surface expression of TCR[133,134], demonstrating the importance of ubiquitin ligases in the regulation of TCR signalling.

1.4.1 PTPN22

The non-HLA genetic factor most strongly associated with autoimmune disease is the single nucleotide polymorphism (SNP) in the protein PTPN22, which changes arginine 620 to tryptophan, PTPN22 R620W. This polymorphism was one of the first genes to be convincingly linked to autoimmunity, and indeed it has the strongest genetic association with autoimmune disease outside of HLA. The odds ratio for RA and T1D in individuals homozygous for PTPN22 R620W is 3-4, with heterozygotes still having a two-fold risk of disease[108].

In 2004 interest in PTPN22 increased manyfold, following the discovery that a human polymorphism resulting in a single amino acid substitution in the protein is associated with Type I Diabetes[135]. Following this finding, the polymorphism was soon investigated in the context of other human autoimmune diseases, and was found to have strong associations with rheumatoid arthritis[136], systemic lupus erythematosus[137], and Graves' disease[138]. Further association studies soon revealed that the polymorphism is strongly implicated in multiple autoimmune diseases affecting varied organs, but has no association with certain other diseases, notably multiple sclerosis, and psoriasis[139-141]. It has even been suggested that PTPN22-R620W may have a protective effect in context of Behcet's disease and Crohn's disease[142,143]. The degree to which PTPN22-R620W varies in its contribution to different diseases suggests that rather than enacting widespread and constant changes, such as globally increasing inflammatory responses, PTPN22 plays a complex role in different immune landscapes, likely by influencing certain cell types important in different disease contexts.

1.4.2 PTPN22 structure

24 exons make up the *PTPN22* gene in humans. Full-length PTPN22 in humans is 807 amino acids long and 91.7 kDa. The protein consists of three broad domains: the catalytic domain, the interdomain, and C-terminal domain, which contains four

proline-rich regions that mediate protein-protein interactions (Figure 3). Mouse PTPN22 shares roughly 80% homology with the human protein, with the majority of the differences located in the interdomain (Figure 4). The crystal structure of the catalytic domain of PTPN22 has been solved, revealing that the catalytic loop has an atypical open state, which must be closed for phosphatase activity[144].

Six isoforms of PTPN22 have been reported and the functions of these are largely unknown, with the notable exception of isoform 6, reported to be a negative regulator of the full-length protein[145]. Different ratios of isoform 2 to full-length protein were also reported in RA patients compared to healthy controls[146]. Another group reported differences in both splice ratios and total protein levels in SLE patients[147]. The different isoforms may well have important implications for the function of PTPN22, unfortunately the varied isoforms of PTPN22 appear to be a species-specific feature of the human protein; making mouse models of little use in this capacity.

The proline-rich regions garner much attention because it is the site of the R620W mutation, a C to T transition in Exon 14, which leads to a substitution of arginine to tryptophan in the first of four proline-rich regions. These regions mediate the interactions of PTPN22 with other proteins, most notably Csk. Normally, 5% of Csk is reported to interact with up to 50% of PTPN22 in T cells; the SNP significantly reduces the association of PTPN22 with Csk, with PTPN22-R620 pulling down with nearly 3 times as much Csk as PTPN22-W620 by immunoprecipitation[136]. The functional significance of this interaction and its reduction is still under study.

1.4.3 Biochemistry, function and signalling of PTPN22

PTPN22 is an intracellular phosphatase that negatively regulates signalling by dephosphorylating tyrosine residues of signalling proteins, chiefly Lck, Fyn, and Zap-70, but also possibly the CD3 chains, Vav, c-Cbl, and others. Csk associates with PTPN22; as they both negatively regulate Lck, it was initially suggested that their complexing allowed them to act synergistically [141,148] but the significance of the association between Csk and PTPN22 remains controversial. Vang et al. found that PTPN22 association with Csk was reduced upon TCR stimulation, and that PTPN22 was found in lipid rafts, where SKFs are localised, only after TCR stimulation,

independently of Csk[149]. They proposed that the Csk-PTPN22 complex sequesters PTPN22 away from target proteins, and that only disassociation of the proteins upon stimulation allows PTPN22 to access its substrates. These observations were made using human cells, however no such compartmentalisation was found in mouse cells[150]. Other groups also did not confirm that TCR ligation reduced PTPN22-Csk interaction, finding that it was either unchanged or increased[151,152]. Burn et al used superresolution imaging to show that PTPN22 existed in clusters in resting human primary T cells, which then dispersed upon LFA-1 stimulation to localise at the plasma membrane. They found that PTPN22 co-precipitated with Csk in resting cells, and that the association was increased upon LFA-1 stimulation[153]. Other effects of Csk-PTPN22 interaction have also been suggested, including that Csk and PTPN22 mediate positive or negative regulation of each other when complexed[151,154] or that association with Csk protects PTPN22 from degradation by calpain[155], although the latter hypothesis seems unlikely as other groups do not report changes in PTPN22 levels correlated with Csk binding[156]. Distinct activities by different splice forms of PTPN22 could explain some of the discrepancies in the data, as little is known about the six isoforms, save for one that appears to act as a negative regulator of full-length PTPN22[145], and none have been reported in mice.

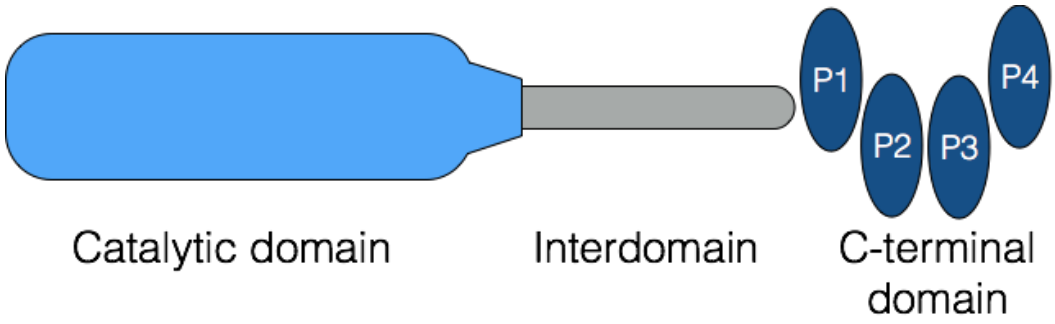

Figure 3. Structure of PTPN22.

Figure 4. Protein alignment of human and mouse PTPN22. Protein sequences were alined using BLAST by NCBI (https://blast.ncbi.nlm.nih.gov/Blast.cgi). The catalytic domain is highlighted in blue, the interdomain is in grey, and the C-terminal domain is in red. R620 is indicated from below by an asterisk (*). Amino acid numbers are listed at the beginnings and ends of each line, and the third line is made up of homologous amino acids. Plus signs (+) indicate a conservative amino acid difference. Dashes (-) are used if one sequence is missing the analogous amino acids.

1.4.4 Understanding the link between PTPN22 and autoimmunity

PTPN22 was first characterised in haematopoietic cells in 1992 by Matthews, et al[157]. In subsequent years, studies by Andre Veillette's lab showed PTPN22 to associate with the negative T lymphocyte regulator Csk[158], and that this complex has a negative regulatory function in T cell signalling through inhibition of Src-family kinases Lck, Fyn, and Zap-70[154]. Mice with PTPN22 knocked out (KO) showed enhanced T cell activation accompanied by increased antibody production[159]. Knockout mice also exhibited increased disease on autoimmune-predisposed backgrounds, but PTPN22 KO alone appeared insufficient to cause spontaneous autoimmunity without additional predisposing genetic factors[159-161]. It has also been reported that regulatory T cells are enriched in PTPN22 KO animals, but data conflicts on whether this difference stems from altered thymic signalling, and also does not agree on whether peripheral Treg cells are more potent suppressors of effector functions[162-164]. Genetic background of the animals may contribute to this disagreement, and additional work is required to reach a consensus on how PTPN22 is affecting T cell tolerance.

PTPN22 is known to be a negative regulator of T cell receptor signalling, however the specific role of the polymorphism in autoimmune susceptibility is still elusive, due in no small part to a divergence in results between mouse and human models. A major challenge in PTPN22 research is the fact that mouse models of the polymorphism have differed significantly from human models. In fact, while most mouse models report the polymorphism to have a loss-of-function effect, many human studies conclude the exact opposite. A comparison of the polymorphism data generated in mouse and human models is discussed in more detail in Chapter 3. A possible confounding factor may be the apparent difference in splice variants expressed between the species, as it has been suggested that one variant found in humans but not in mice has a direct negative regulatory effect on PTPN22 itself, and its activity was altered by the R620W polymorphism[145]. It is also possible that the contribution of PTPN22 to autoimmunity lies not in its activity in a single effector cell, but in altering the interactions between cells; for example a reduction in the effectiveness of Treg cells could promote autoimmunity by reducing the signalling threshold required to activate effector cells.

One possible explanation for the increased susceptibility to autoimmune disease is that PTPN22-R620W affects central tolerance to allow more autoreactive T and B cells to survive. Such an effect could explain the increased susceptibility to only select diseases, as PTPN22-R620W could expand the lymphocyte repertoire in a non-random manner, however studies on this topic have produced conflicting results. Increased numbers of CD4/CD8 cells in the periphery have been reported in knockout mice, however the role of PTPN22 in thymic selection in mice varies depending on the genetic background, from no observed effects to enhanced positive selection[159,165,166]. In contrast, B cell positive selection does appear to be enhanced in a B cell-intrinsic manner in mice and humans carrying the risk variant, leading to a greater proportion of polyreactive B cells[167-169]. Given the similarities between B and T cell signalling and development, it seems likely that T cell selection is affected by PTPN22 R620W, but perhaps is not detectable by current assays, whereas B cell receptor affinity can be assessed using antibody assays such as ELISA. The fact that no changes in peripheral B cell numbers were observed in variant mice[159,160] suggests that increased selection does not necessarily disrupt homeostatic numbers of lymphocytes in mice less than six months of age[156], therefore detection of changes to T cell selection may require more precise assays to be developed to analyse the T cell repertoire. As B cells are unable to express high affinity class-switched antibody without T cell help, the expansion of the peripheral B cell repertoire would have limited autoimmune potential without a similar expansion in the T cell compartment.

The story of PTPN22 R620W in B cell signalling is similar to that of T cell signalling. Arechiga et al showed that B cells from human individuals who were heterozygous for PTPN22 R620W had reduced proliferative capacity and reduced phosphorylation of the activating kinase, Syk[170]. In contrast, Dai et al showed a slight increase in proliferation in B cells derived from mice carrying the analogous polymorphism and found that even restricting the polymorphism to the B cell lineage was sufficient to cause splenomegaly in aged mice[156]. In addition, greater numbers of germinal centre B cells have been reported in PTPN22$^{-/-}$ mice[155], and Metzler et al found that among mouse B cells homozygous for the variant of PTPN22, those with self-reactive BCRs were selectively shuttled into the follicular zone, potentially increasing

the likelihood of the development of autoimmune germinal centres[167]. Taken together, these reports indicate that B cell immunity is regulated by PTPN22 from development to activation, and that PTPN22 R620W leads not only to a more autoreactive B cell repertoire, but also to an increased likelihood of autoreactive B cells receiving T cell help. However, the specific signalling events that lead to such predispositions in mice are still unknown, and may differ from humans.

PTPN22 is expressed in other haematopoietic cells, and innate immune responses may be critical in establishing environmental signals that promote autoimmunity. In innate myeloid cells PTPN22 is reported to promote signalling by pathogen recognition receptor pathways that lead to expression of type I interferons, suppressors of inflammation[171]. PTPN22 R620W was unable to upregulate type I interferons, and the polymorphism was linked to greater arthritis scores in mice. PTPN22 R620W could therefore lead to enhanced inflammatory responses, potentially promoting autoimmunity. Dendritic cells are also intrinsically tied to T cell function. Zhang et al found that expression of costimulatory molecules was increased in mice carrying the polymorphism[155], but Clarke et al recently reported no changes in the ability of PTPN22$^{-/-}$ or PTPN22 R619W DCs to uptake antigen or stimulate T cells[172]. Based, on these results it is impossible to conclude whether or not PTPN22 R620W contributes to autoimmunity through regulation of DCs. Further studies investigating the role of PTPN22 in non-T cells are needed to fully elucidate their role in autoimmune pathogenesis.

1.4.5 Population genetics of PTPN22

Although the PTPN22 R620W polymorphism was identified as a factor of disease predisposition, the prevalence of the allele suggests that there is selective pressure to maintain it within the population. The incidence of the autoimmune-predisposing PTPN22 allele varies between populations, found in up to 17% of individuals with Northern European heritage[108], but with a greatly reduced frequency in Asian and African populations. Lins et al reported an allele frequency of only 0.014 in African American populations, while it was nearly ten times as common in European Americans, with an allele frequency of 0.133[173]. Given the importance of allele frequency in GWAS data, as well as the complex impact of genetic background on immunity, it is unsurprising that different populations also report differences in

degree of association of PTPN22 R620W with various autoimmune diseases. One possible explanation for the frequency of the PTPN22 R620W allele is that the enhanced immune signalling increases protection from infectious diseases[95]. An analysis of genes associated with Crohn's Disease demonstrated that PTPN22-R620W correlates with reduced susceptibility to protozoa[174], although it is unlikely for such infections to be the source of significant selective pressure in Northern European populations. PTPN22 R620W has also been reported to reduce the risk of pulmonary tuberculosis in a Colombian population[175], however no such link was found in Iranian or Brazilian populations[176,177]. Thus, the reason for maintenance of the PTPN22 R620W allele in certain populations is still an open question.

Other SNPs of PTPN22 have also been reported, although they are rarer than PTPN22 R620W across different populations, which makes associations more difficult to determine conclusively. PTPN22-R263Q is a loss-of-function variant that affects the catalytic domain of the protein, and has been reported to be protective against RA and SLE[178-180], but may also increase susceptibility to pulmonary tuberculosis[181].

1.5 Project aims

Many of the difficulties in describing the mechanisms of PTPN22 function are rooted in inherent variation between mouse and human studies. A major challenge in reconciling human and mouse studies is that human individuals are highly genetically varied compared to lab mice, and are affected by different disease states, environments, and lifestyles. Thus, there is inherent difficulty in comparing results generated in genetically diverse human individuals to findings from inbred lab mice, which have a restricted range of genetic variance; this important difference alone may account for the discrepancies between mouse and human data. There are also some differences in the immune systems of mice compared to humans, such as an increase in the percentage of lymphocytes compared to neutrophils in the blood, significantly higher proportion of $CD28^+$ T cells, altered mechanics of calcium flux, and an array of chemotactic and signaling molecules that are absent in mice yet expressed in humans[182]. Furthermore, evidence is accumulating that the function of the immune system—including development of autoimmune disease—is

highly affected by commensal bacteria in the gut micro-biome and by bystander chronic infections, factors which are highly divergent between laboratory mice and human subjects[183]. It is therefore unsurprising that complex immunological phenomena like the development of allergy or autoimmune disease are found to be divergent between mice and humans. While mouse models have undoubtedly contributed enormously to our understanding of the immune system as a whole, it is hardly straightforward to convert findings in mice into discoveries in man.

Therefore, to address the controversy surrounding the role of PTPN22 in human T cell signalling, we decided to create a novel human PTPN22 KO model. The development of CRISPR technology allowed us to induce specific mutations at the genome level, enabling the creation of isogenic human T cell lines, genetically identical save for mutations in PTPN22. These models also eliminate the need to overexpress the protein of interest or attempt to inhibit it through siRNA or chemical drugs, eliminating other confounding factors that have limited previous human studies. These cell line models could provide valuable insight into the cell-intrinsic signalling effects of PTPN22 in human T cells.

2. Materials and methods

2.1 Cell lines

TCR^- Jurkat cells and Phoenix Ampho cells were obtained from Hans Stauss, University College London. T2 cells were obtained from Paul Travers, at the MRC Centre for Regenerative Medicine, Edinburgh.

2.2 Cell Culture

Complete Iscove's Modified Dulbecco's Medium (IMDM) (Sigma Aldrich, I3390)
+ 5% Heat inactivated Fetal Calf Serum (FCS) (Gibco, 10500-064, Lot 08G3560K)
+ 100U/mL Streptomycin (Gibco, 15140-122)
+ 100µg/mL Penicillin (Gibco, 15140-122)
+ $2x10^{-3}$ M L-Glutamine (Gibco, 25030081)
+ $5x10^{-5}$ M β-2-Mercaptoethanol (Fluka BioChemika, 63689)

Dulbecco's Phosphate Buffered Saline (Sigma Aldrich, D8537)

Trypsin EDTA 1x (Phoenix Ampho cells only) (Gibco, 25200056)

Cells were maintained in complete IMDM. Cells were incubated in a Thermo Scientific Hera Cell 150 CO_2 incubator at at 37ºC, 5% CO_2 unless otherwise specified. Cell cultures were split 3 times per week, and maintained between $2x10^5$ and $2x10^6$ cells/mL. Unless otherwise specified, cells were centrifuged at 310 x g for 3min.

2.2.1 Mycoplasma

Screening for mycoplasma was carried out every six months using MycoAlert Mycoplasma Detection Kit (Lonza). Infected lines were isolated and treated using complete IMDM supplemented with 100 µg/mL Plasmocure (Invivogen) for two weeks.

2.3 Transduction of Jurkat cells

2.3.1 Phoenix Ampho cell transfection

Complete Roswell Park Memorial Institute (RPMI) medium

+ 5% Heat inactivated Fetal Calf Serum (FCS)
+ 100U mL^{-1} Streptomycin
+ 100µg mL^{-1} Penicillin
+ $2x10^{-3}$ M L-Glutamine

$2x10^6$ Phoenix ampho cells were plated in 8 mL of IMDM media in 10 cm Petri dishes and incubated overnight. The following day media was exchanged with 5 mL complete IMDM 30 minutes prior to transfection. Transfection was carried out using Fugene HD transfection reagent (Promega).

Fugene Transfection mix
Solution A:
10 µl FuGENE HD Transfection Reagent (Promega, E2311)
150 µl OPTI-MEM 1x medium (Gibco, 31985-062)

Solution B
1.5 µg pCL Ampho Retrovirus Packaging Vector (Novus Biologicals, NBP2-29541)
2.6 µg DNA
made up to to 50 µL with dH_2O

Solution A and B were mixed and incubated at room temperature for 20 minutes. The transfection mix was subsequently added dropwise to the prepared Phoenix Ampho cells, with gentle agitation. Cell culture media was replaced with 5 mL complete RPMI after one day and further incubated for 24 hours. Virus supernatent was prepared by removing media from Phoenix Ampho cells and centrifuging it at 485 x g for 5 minutes to remove cells and debris for use in Jurkat cell transduction.

2.3.2 Jurkat cell transduction

To prepare for transduction, 24-well not treated tissue culture plates (Corning CLS3738) were coated with 750 µl/well RetroNectin Recombinant Human Fibronectin Fragment (100 µg/mL, Takara Bio, T100B) suspension and incubated at room temperature for 3 hours. Excess retronectin was removed and wells were blocked with 500ul/well filter sterilised PBS containing 2% BSA for 30 minutes at room temperature. Following blocking, BSA solution was removed and wells were washed twice with 1 mL PBS.

$5x10^5$ Jurkat cells were pelleted and resuspended in 1 mL virus supernatant, then plated onto retronectin-coated wells. The plate was then centrifuged at 860 x g for

90 minutes at 32ºC with no brake. After centrifugation, virus supernatant was removed and replaced with 1 mL complete RPMI. Cells were cultured for 3 days before analysis of TCR expression by flow cytometery.

2.4 CRISPR gene editing of Jurkat cells

2.4.1 Ligation of guide sequences into Cas9 expression vector

Guide sequence single-strand DNA oligos were purchased from Invitrogen (see Table 1 for sequences) and Cas9 plasmids Px330 and Px461 were purchased from Addgene (plasmid #42230 and 48140, respectively).

Plasmid Bbs1 restriction digestion was carried out in a solution of:

2 µL Bbs1 (5000 U/mL) (New England Biolabs, R0539)
2 µL plasmid (2 µg/µL)
4 µL NEB Restriction Buffer 1.1 (10x) (New England Biolabs)
36 µL dH_2O

The restriction digest was incubated for two hours at 37ºC.

Single strand DNA oligo pairs were annealed in a PCR tube containing:

1 µL forward oligo (100 µM)
1 µL reverse oligo (100 µM)
1 µL 10x T4 ligation buffer (New England Biolabs)
0.4 µL T4 PNK (New England Biolabs)
6.5 µL dH_2O

Tubes were incubated in a PCR machine for 30 minutes at 37ºC, 5 minutes at 95ºC, and reduced to 25ºC at a rate of 5ºC/minute.

Plasmid DNA was purified from restriction digest reaction using Geneclean II kit (Fisher Scientific) according to manufacturer protocol for purifying DNA from solutions. Plasmid DNA concentration was measured using a Nanodrop 1000 spectrophotometer (Thermo Scientific).

Ligation reaction of the plasmids and guide oligos contained:

1 µg digested plasmid
1 µL oligo duplex (diluted 1:200)
5 µL 2x Quickligation buffer (New England Biolabs)
1 µL Quick ligase (New England Biolabs)
made up to 11 µL with dH_2O

Ligation reaction was incubated for 15 minutes at room temperature.

2.4.2 Bacterial transformation with Cas9 expression vector

100 µL competent XL1 E. coli were thawed on ice. 10 µL of ligation reaction from section 2.4.1 was added. Bacteria were incubated on ice in the presence of ligation reaction for 75 minutes before being heat shocked for 3 minutes in a waterbath at 42ºC, then were transferred back to ice for a further 3 minutes. Subsequently 500 µL of lysogeny broth (LB) was added to each culture and incubated for 40 min at 37ºC. Cultures were then spread on plates with agar and ampicillin (Sigma-Aldrich) and incubated overnight.

Bacterial colonies were picked and expanded in 10 mL LB overnight at 37ºC with shaking at 240 rpm. DNA preps from colonies were carried out the following day using the QIAprep Spin Miniprep Kit (QIAGEN, 27104). Correct oligo insertion into plasmid was screened for by restriction digest before being confirmed by both PCR and Sanger sequencing.

Restriction digest
1 µL BbsI
1 µL AgeI
2 µL New England Biolabs buffer 1
1 µL plasmid
15 µL dH_2O

Tubes were incubated for 50 minutes at 37ºC and run on a 0.8% agarose gel at 80 V for 70 minutes.

PCR reaction
1 µL plasmid reverse primer (10 µM) (Invitrogen)
1 µL single-strand sense guide oligo
2 µL 10x PCR reaction buffer (Invitrogen)
1 µL $MgCl_2$ (Invitrogen)
1 µL Deoxynucleotide Solution Mix (Promega)
0.4 µL Taq DNA polymerase recombinant (5 U/µl) (Invitrogen)
13.6 µL dH_2O
1 µL plasmid template

PCR programme (BIO-RAD T100 Thermal Cycler)
94ºC for 3 minutes
34 cycles of:
    94ºC for 1 minute
    56ºC for 30 seconds
    72ºC for 1 minute
72ºC for 10 minutes

Hold at 4ºC

Products were resolved on a 2% agarose gel run at 120 V for 30 minutes.

2.4.3 Amaxa transfection

In accordance with manufacturer recommendations, $1x10^6$ Jurkat cells were electroporated with 2 µg total plasmid in 100 µL Cell Line Nucleofector Solution V (Lonza). Cells were electroporated using the Amaxa Biosystems Nucleofector II (Lonza) set to programme X-001 to maximise viability and then gently transferred by Pasteur pipette onto a 12-well plate containing 1 mL warm culture media without antibiotics for incubation for 48 hours before sorting.

2.4.4 Neon transfection

$1x10^6$ Jurkat cells were electroporated with 10 µg total plasmid in 100 µL buffer R (ThermoFisher Scientific, MPK10096). The electroporation station was prepared with buffer E2, and cells were electroporated with 3 pulses of 1350 volts for 10 milliseconds. Cells were then immediately transferred onto a 6-well plate containing 2 mL warm culture media without antibiotics. Cells were incubated for 48 hours before sorting.

2.4.5. Sorting of transfected cells

Transfected Jurkat cells were sorted using a BD FACS Aria IIu with BD FACSDIVA v6 software (BD Biosciences). Cells were transferred from cell culture wells into a 15 mL centrifuge tube and washed twice with PBS before resuspension in IMDM supplemented with 1% FCS. Cells were either bulk sorted into centrifuge tubes or single cell sorted onto round bottom 96-well plates, both containing FCS + 10% penicillin and streptomycin. After sorting, 3x volume complete IMDM without antibiotics was added to wells, and cells in tubes were centrifuged at 140 x g and resuspended in 2 mL complete IMDM and seeded onto a 6-well plate for incubation.

2.5 Human PTPN22 knockout screening

2.5.1 PTPN22 Exon 1 PCR AvaII digestion

DNA lysis buffer

30mM Tris HCl (Fisher Scientific)
10mM EDTA (Sigma Aldrich)
0.1% SDS (Fisher Scientific)
0.5% Tween 20 (Scientific Laboratories Supplies)

$2x10^6$ cells were pelleted and resuspended in 200 µL DNA lysis buffer + 0.2 µL Proteinase K (800 U/mL, New England Biolabs). Samples were incubated for 15 minutes at room temperature, followed by 5 minutes at 55ºC and 10 minutes at 98ºC.

0.1 volumes 3M Na Acetate were added to each tube, followed by 2.5 volumes ice cold 100% ethanol (VWR Chemicals). Tubes were stored overnight at -20ºC, then centrifuged at 17,000 x g for 10 minutes in a benchtop centrifuge at 4ºC. Supernatant was removed, and pellets were washed twice in 500 µL 70% ethanol. After the final wash, ethanol was fully removed and pellets were allowed to air dry before resuspension in water. PTPN22 Exon 1 primers were chosen using the NCBI/Primer Blast tool (https://www.ncbi.nlm.nih.gov/tools/primer-blast/).

PCR reaction
1 µL forward PTPN22 Exon 1 primer (10 µM) (Table 1)
1 µL reverse PTPN22 Exon 1 primer (10 µM) (Table 1)
2.5 µL 10x PCR reaction buffer
1 µL $MgCl_2$
1 µL Deoxynucleotide Solution Mix
0.5 µL Taq DNA polymerase recombinant (5 U/µl)
17 µL dH_2O
1 µL DNA template

PCR programme
94ºC for 3 minutes
34 cycles of:
    94ºC for 1 minute
    60ºC for 30 seconds
    72ºC for 2 minute
72ºC for 10 minutes
Hold at 4ºC

To each tube of PCR product, 0.5 µL of AvaII restriction enzyme (10,000 U/mL, New England Biolabs) was added directly and incubated at 37ºC for two hours. Products of PCR and digestion were run on a 2% agarose gel at 120 V for 30 minutes.

2.5.2 TOPO Sequencing of PTPN22 Exon 1

TOPO Cloning reaction
1 µL TOPO vector (ThermoFisher Scientific)
1 µL salt solution (ThermoFisher Scientific)
1 µL PCR reaction
3 µL H_2O

The TOPO TA Cloning Kit with PCR 2.1-TOPO (ThermoFisher Scientific) was used to separate alleles of Jurkat clones for sequencing. The PTPN22 Exon 1 region of each clone was amplified by PCR using *Taq* polymerase (as described in section 2.5.1), of which 5 µL was reserved for TOPO cloning and the remainder was resolved on an agarose gel to confirm that the expected PCR product was amplified. XLI E. coli were transformed and plasmid DNA was isolated from bacterial colonies as described in section 2.5.2.

Sanger sequencing was carried out by Edinburgh Genomics. Sequence of each TOPO cloning colony was verified using both M13 forward and M13 reverse sequencing primers (Thermo Fisher Scientific). Sequencing mixes consisted of 1 µL primer (3.2 µM) and 5 µL plasmid miniprep (100-200 ng).

2.5.3 Western Blotting

Protein lysis buffer
0.15 M NaCl (Sigma-Aldrich)
50 mM Tris HcL (pH 7.5)
2 mM EDTA
1% Triton X-100 (Fluka BioChemikal)
0.5% n-Dodecyl β-D-Maltoside (Merck Millipore)
Added fresh before use:
- 1 mM Sodium Orthovanadate (Sigma-Aldrich)
- 1x Protease Inhibitors (Sigma-Aldrich P8340)
- 1 mM Sodium Fluoride (Sigma-Aldrich)

Transfer Buffer:
24 mM Tris base pH 7.5 (Fisher Scientific)
192 mM glycine (Fisher Scientific)
20% methanol (Fisher Chemical)
Made up to 1 L with H_2O

Blocking Buffer:
5 mL Odyssey Blocking Buffer (LI-COR Biosciences)
5 mL PBS

To create cell lysate for Western blotting, Jurkat cells were counted and washed twice in PBS. $5x10^6$ cells were lysed in 50 µL of protein lysis buffer and incubated on ice for 20 minutes. Lysed cells were centrifuged at 13,000 RPM for 5 minutes to pellet nuclei, and supernatant was transferred into a fresh tube. 15 µL of protein lysate was combined with 5 µL NuPAGE LDS Sample Buffer (ThermoFisher Scientific) + 10% β-2-Mercaptoethanol, and tubes were boiled for 10 minutes at 95ºC.

Protein lysate was resolved by migration on a 10 or 15 1.0 mm well 4-12% Bis-Tris gels (Novex, NP0321BOX, NP0323 BOX) in 1x NuPAGE MOPS SDS Running Buffer (Novex, NP0001) using an Invitrogen Mini Gel Tank (ThermoFisher Scientific). Running Buffer (Novex, NP0001) was used to thoroughly wash wells of the gel and 3 µL Precision Plus Protein Standards (Biorad 161-0373) was loaded into the first well. 15-18 µL of sample was loaded into the remaining wells, depending on well size used. Protein migration was run at 4ºC at 70 V for 15 minutes, followed by 140 V for 60 minutes.

Protein transfer onto a polyvinylidene difluoride (PVDF) membrane (Immobilon IPFL00010) used the Mini Trans-Blot Cell transfer system (Biorad Laboratories). The PVDF membrane was first activated by soaking in 100% methanol for several minutes, and transfer of proteins from migration gel onto the PVDF membrane was carried out using and sponges and Whatman filter paper was soaked in transfer buffer prior to assembly of the transfer sandwich:

Negative plate
Sponge
Whatman
Protein gel
PVDF membrane
Whatman
Sponge
Positive plate

Transfer was carried out at 4ºC with stirring at 100 V for 105 minutes. After transfer was complete, membrane was transferred into a 50 mL centrifuge tube and incubated in blocking buffer for 30 minutes at room temperature with gentle agitation. Primary antibodies (Table 2) were diluted 1:1000 in Odyssey Blocking Buffer + PBS containing 0.1% Tween 20 and incubated with membrane overnight at

4ºC with agitation. The following day, membranes were washed in four times in 50ml PBS containing 0.4% Tween 20 for at least 5 minutes per wash at room temperature with agitation. Secondary antibodies (Table 2) were diluted 1:20,000 in Odyssey Blocking Buffer + PBS containing 0.1% Tween 20 and 0.01% SDS and incubated with membrane for 30 minutes at room temperature with agitation. After incubation with secondary antibodies, membranes were washed four times in PBS containing 0.4% Tween 20 before scanning on a LI-COR Odyssey CLx (LI-COR Biosciences). Blot analysis annotation was performed using Image Studio Lite software (LI-COR Biosciences).

2.6 Tax TCR Jurkat cell stimulation

2.6.1 Peptides

pTax: LLFGYPVYV
pHuD: LGYGFVNYI

Stimulating peptides were purchased from ThermoFisher Scientific at >96% purity. Peptides were dissolved in DMSO, then diluted 1:1 in PBS to a final concentration of 2 mM. Peptide aliquots were prepared to prevent excessive freeze/thaw cycles, and stored at -20ºC.

2.6.2 T2 loading

Exogenous peptide bound to surface HLA of cultured T2 cells were stripped by washing cells in serum-free IMDM and incubating in 0.13 M citric acid prepared in PBS[184]. Cells were incubated in acid for 2 minutes on ice, then 10 mL of serum-free IMDM were added. Cells were pelleted and washed twice in 5 mL serum-free IMDM before peptide pulse.

T2 cells were subsequently incubated with 100 µM peptide for 2 hours at 37ºC. Peptide loaded T2 cells were then washed in PBS to remove excess peptide and plated with Jurkat cells on a 96-well plate. $2x10^4$ - $3x10^6$ T2 cells were cultured with $2x10^5$ Jurkat cells, and plates were incubated at 37ºC for the period of stimulation.

2.6.3 Plate-bound DimerX

DimerX I (BD Biosciences) was incubated with 160 molar excess of peptide, in accordance with BD Biosciences recommendation. DimerX and peptide were incubated overnight at 37ºC before being bound to tissue culture plate.

After initial titration to ascertain maximal CD69 expression after 24 hours (Chapter 4, Figure 1) 20µg/ml was used as the highest concentration of DimerX+peptide conjugate stimulations. 50 µL of 20 µg/mL DimerX+peptide diluted in PBS was distributed into each well of a flat-bottom 96-well tissue culture plate and incubated overnight at 4ºC. Excess DimerX+peptide conjugate was removed prior to stimulation, and $3x10^5$ Jurkat cells suspended in complete IMDM containing 2µg/mL anti-CD28 were seeded into a single well, centrifuged for 10 seconds, and incubated at 37ºC for the period of stimulation. For periods of stimulation shorter than 30 minutes, cells were incubated in a 37ºC water bath; for longer periods plates were placed in a tissue culture incubator.

2.6.4 Plate-bound anti-CD3 antibody

50 µL of 20 µg/mL anti-CD3ε antibody (clone OKT3, Biolegend) diluted in PBS was distributed into each well of a flat bottom 96-well tissue culture plate and incubated overnight at 4ºC. The concentration of anti-CD3 was chosen to match the concentration of DimerX that was found to give maximum stimulation. Unbound antibody was removed immediately prior to stimulation, and $3x10^5$ Jurkat cells suspended in complete IMDM containing 2 µg/mL anti-CD28 were seeded into each well. Plates were centrifuged for 10 seconds, and incubated at 37ºC for the period of stimulation. For periods of stimulation shorter than 30 minutes, cells were incubated in a 37ºC water bath; for longer periods plates were placed in a tissue culture incubator.

2.7 Flow cytometry

2.7.1 Surface staining of whole cells

FACS buffer
1x PBS
2% FCS
0.2% Sodium azide

Analysis of cell surface markers by flow cytometry was carried out in non-sterile round bottom 96-well plates. Cells were washed in 200 µl FACS buffers before staining with relevant antibodies (listed in Table 2) in a total volume of 30 µl at 4^{o}C for 20 minutes. After the incubation period, plates were centrifuged and excess antibody removed. Cells were subsequently washed in 200 µl FACS buffer before being resuspended in 100 µl for acquisition on MACSQUANT Analyzer 10 flow cytometer (Miltyeni Biotec).

To assess cell viability, a LIVE/DEAD Fixable Dead Cells Stain (ThermoFisher Scientific) reconstituted in DMSO was diluted 1:1000 in PBS. Cells that had been stained with surface antibody and washed were resuspended in diluted LIVE/DEAD stain and incubated for 10 minutes at room temperature. The stain was then removed by centrifugation and resuspended in PBS for flow analysis.

Plates were kept on an ice block for the duration of their acquisition using the MACSQuant Analyzer. Calibration of the machine was performed prior to acquisition using MACSQuant Calibration Beads (Miltenyi Biotech, 130-093-607), and fluorescence compensation was carried out using single stain controls. Acquisition data was analysed using FlowJo version 8.7 (Becton, Dickinson and Company).

2.7.2 Annexin V staining

Cells in a round bottom 96-well plate were washed once in PBS, then once in 1X eBioscience Binding Buffer for Annexin V (Thermo Fisher, BMS500BB), and resuspended in 100 µL Binding Buffer. 5 µL fluorochrome-conjugated Annexin V was added to each well, and the plate was incubated for 15 minutes at room temperature. Cells were then washed once in Binding Buffer resuspended in 190 µL Binding Buffer. 10 µL Propidium Iodide (20 µg/mL) was added to each well immediately before acquisition for flow analysis.

2.7.3 CellTrace Violet/CFSE staining

5 mM Stock solutions of CellTrace Violet or CFSE were created by dilution in DMSO. Cells were counted and 1x10^{6} cells were centrifuged in 15 mL centrifuge tubes and washed 4x in 5 mL of PBS. Cells were subsequently resuspended in 1 mL

PBS. CellTrace Violet or CFSE dilutions were made up at 1000x working concentration, with additional serial dilutions as needed, and 1 µL was added to cell suspensions. The highest working concentration used in any experiment was 50 nM. Cells were incubated for 20 minutes at 37ºC, then 5 mL complete IMDM was added to each tube. Tubes were kept on ice for 10 minutes before centrifugation and removal of media. Cells were washed twice in PBS before differently stained lines were combined into groups for use in experiments.

2.7.4 Intracellular staining

All cell surface stains were performed prior to starting this protocol. Cells in 96-well plates were washed twice in 100 µL FACS buffer. Remaining FACS buffer was removed by centrifugation, before fixation and permeabilisation in 100 µL BD Cytofix/Cytoperm (BD554722) was added to each well. Plates were incubated for 15 minutes at 4ºC and wells were subsequently washed in 1x BD perm wash buffer. Antibodies (Table 2) were diluted in 1xBD perm wash buffer and incubated with cells for 20 minutes at 4ºC. After staining, wells were washed in Perm/Wash and cells were resuspended in FACS buffer for flow analysis.

2.7.5 Phosphoprotein flow cytometry

To analyse phosphoproteins by flow cytometry, cells on 96-well plates were fixed in 2% PFA and incubated for 15 minutes at 37ºC. Cells were pelleted by centrifugation and PFA removed, then 100 µL prewarmed BD Phosflow Lyse/Fix (BD558049) was added to each well and plates were incubated for 10 minutes at 37ºC. Plates were centrifuged again to remove Lyse/Fix, and 200 µL BD Phosflow Perm I (BD557885) was added to each well. Plates were incubated for 20 minutes at room temperature, then Perm I buffer was removed by centrifugation. Flow cytometry antibodies were diluted in Perm I. Primary antibody was added to wells, and incubated for 20 minutes at 4ºC. Primary antibody was removed by centrifugation, and secondary antibody was added and incubated for 20 minutes at 4ºC. After staining, wells were washed with 150 µL Perm I and resuspended in FACS buffer for flow analysis.

2.7.6 Nucleus flow cytometry

Sucrose Buffer A
10mM HEPES pH 7.8

8 mM $MgCl_2$
320 mM Sucrose
0.1% Triton-X 100
1x Protease Inhibitor

Sucrose Buffer B
10mM HEPES pH 7.8
8 mM $MgCl_2$
320 mM Sucrose
1x Protease Inhibitor

FACS Buffer+$MgCl_2$
1X PBS
2% FCS
8mM $MgCl_2$

PERM buffer
1X PBS
2% FCS
8mM $MgCl_2$
0.3% Triton-X 100

Sucrose Buffer A and B were prepared fresh. Cells used for nuclear flow cytometry were transferred into 1.5 mL Eppendorf tubes and pelleted by centrifugation. Samples were kept on ice unless otherwise noted for the remainder of the process. Cell pellets were resuspended in 250 µL chilled Sucrose Buffer A and incubated for 15 minutes. Samples were then centrifuged at 2000 x g for 10 minutes at 4ºC. Supernatant was removed, and cells were washed in 250 µL chilled Sucrose Buffer B and centrifuged at 2000 g for 10 minutes at 4ºC. After two 250 µL washes in Sucrose Buffer B, nuclei were fixed by resuspending sucrose buffer B containing 4% paraformaldehyde. Resuspended samples were incubated for 25 minutes at room temperature, protected from light.

Fixed nuclei were washed once with FACS buffer supplemented with $MgCl_2$ and centrifuged at 1000 x g for 5 minutes at 4ºC, then washed once with PERM buffer and centrifuged at 1000 x g for 5 minutes at 4ºC. Nuclei were stained with flow cytometry antibodies diluted in PERM buffer for 20 minutes. PERM wash was repeated before staining with secondary antibodies, when necessary. After staining, samples were washed once in FACS buffer containing $MgCl_2$ and resuspended in FACS buffer containing $MgCl_2$ for flow analysis.

2.8 Calcium flux measurement

2.8.1 Indo-1 loading

$1x10^6$ cells were stained with CFSE as described in section 2.7.3 prior to loading with Indo-1, AM, cell permeant (ThermoFisher Scientific). Indo-1 was initially reconstituted in DMSO to a final concentration of 1 mM. Cells were resuspended in 1 mL of warm PBS and 1 µL of 1 mM Indo-1 was added. Cells were incubated with Indo-1 for 30 minutes at 37ºC. Loading was quenched by adding 5 mL IMDM + 1% FCS to each tube. Cells were washed once in 5 mL IMDM + 1% FCS before being resuspended in 800 µL RPMI + 1% FCS supplemented with Ca^{2+} for acquisition.

2.8.2 Acquisition

Indo-1 loaded cells were acquired using a BD LSR II Special Order System with BD FACSDIVA v8 software (BD Biosciences). The violet:blue emission ratio of unstimulated samples were adjusted to 50,000, in accordance with manufacturer recommendations (BD LSR II user guide, BD Biosciences). Unstimulated samples were acquired for 45 seconds, then a 15 second break in acquisition was taken to add 16 µL anti-CD3 (clone OKT3, Biolegend) to stimulate cells. The remaining sample was allowed to run for 14 minutes and 45 seconds. At this point, a further 15 second break was taken to add 10 µL ionomycin (1 µg/mL, Sigma-Aldrich) and the remaining sample was run for and additional 60 seconds. Acquisition data was analysed using FlowJo version 8.7.

2.9 Quantitative PCR

2.9.1 RNA isolation

Cells were transferred to 1.5 mL Eppendorf tubes and pelleted by centrifugation and media was removed. Pellets were resuspended in 500 µL Trizol and vortexed for 10 seconds. 100 µL chloroform was added and tubes were vortexed again for 10 seconds, then incubated at room temperature for 3 minutes. Tubes were then centrifuged at 17,000 x g in a benchtop centrifuge at 4ºC for 10 minutes. Centrifugation caused separation of the samples into organic and aqueous phases, and the aqueous phase was removed into a fresh tube (approx 200-250 µL). An equal volume of RNase-free isopropanol (VWR chemicals) and 1 µL of Glycoblue was added to each tube. Samples were kept at -20ºC for 1 hour, then centrifuged at

17,000 x g at 4ºC for 20 minutes. Isopropanol was removed, and pellets were washed once with RNase-free 70% ethanol. Pellets were air dried before resuspension in 20 µL RNase-free water and RNA concentration was checked by Nanodrop.

2.9.2 cDNA synthesis

Pre-Reverse Transcription reaction
1 µL oligo (dT)20 Primer (ThermoFisher Scientific)
1 µL Deoxynucleotide Solution Mix (Promega)
1 µg RNA
made up to 11 µL with H_2O

Reverse Transcription reaction
4 µL 5X first-strand buffer (ThermoFisher Scientific)
1 µL 0.1 M Dithiothreitol (ThermoFisher Scientific)
1 µL RNase inhibitor (ThermoFisher Scientific)
1 µL SuperScript III Reverse Transcriptase (ThermoFisher Scientific)

1 µg of RNA was used for each reverse transcription reaction. Pre-reverse transcription reactions were prepared in PCR tubes and incubated for 6 minutes at at 65ºC, and then left on ice for one minute before addition of reverse transcription reagents. Tubes were then incubated for 50 minutes at 50ºC, then 15 minutes at 70ºC, and finally 5 minutes at 4ºC. After completion of reverse transcription, 0.5 µL of RNAse H (5,000 U/mL, New England Biolabs) was added to each tube.

2.9.3 SYBR Green qPCR

SYBR Green reagent mixture
10 µL 2x SYBR Green QPCR master mix (Agilent)
0.4 µL Forward Primer (10 µM) (Table 1)
0.4 µL Reverse Primer (10 µM) (Table 1)
4.2 µL H_2O
5 µL cDNA template

180 µL of RNase-free water was added to each 20 µL cDNA product before use as qPCR template. SYBR Green reagents were aliquoted across a 96-well qPCR plate (Roche Molecular Diagnostics) and an adherent film was applied to make wells airtight. Roche LightCycler 480 II (Roche Molecular Diagnostics) was programmed to perform 40 cycles after an initial 3 minute incubation at 95ºC. Each cycle included

5 seconds at 95ºC followed immediately by 10 seconds at 60ºC, with a ramp rate of 4.4ºC/second. Cp values were exported from Light Cycler 480 Software 1.5 (Roche Molecular Diagnostics) and analysed using Microsoft Excel 2011 (Microsoft Office). Where applicable, qPCR products were run on a 10 well Novex 6% TBE Gel (ThermoFisher Scientific, EC6265BOX).

2.10 Statistical analysis

Statistical analyses were performed in Prism 7 (Graphpad Software Inc). Comparisons of two samples used unpaired T tests with Holm-Sidak multiple comparisons correction. A p-value less than 0.05 was considered significant. Significance was denoted in figures as follows: ns = not significant, *p < 0.05, **p < 0.01, ***p < 0.001.

Table 1. Primer and oligo sequences

CRISPR guide oligos	Ex 1-6	CACCG ACTTCTGCAGAATTTCTCTT TGG
		AAAC AAGAGAAATTCTGCAGAAGT C
	Ex 1-7	CACC GGAGTTTGCCAATGAATTTC TGG
		AAAC GAAATTCATTGGCAAACTCC
	Ex 1-8	CACCG ACCCTGAGAGGGTCACATAC AGG
		AAAC GTATGTGACCCTCTCAGGGT C
PCR primers	PTPN22 Exon 1	TTTGCTGAGAAGGAAGGCACT
		GCAAACCACTCAGAGAAGTCAAA
qPCR primers	GAPDH	ATGACATCAAGAAGGTGGTGAAG
		CTGTTGAAGTCAGAGGAGACCAC
	7SK	CATCCCCGATAGAGGAGGAC
		GCGCAGCTACTCGTATACCC
	SDHA	GAGGCAGGGTTTAATACAGCA
		CCAGTTGTCCTCCTCCATGT
	EGR-1	CTTCAACCCTCAGGCGGACA

	GGAAAAGCGGCCAGTATAGGT
cJun	CCTTGAAAGCTCAGAACTCGGAG
	TGCTGCGTTAGCATGAGTTGGC
cFos	CCGGGGATAGCCTCTCTTACT
	CCAGGTCCGTGCAGAAGTC

Table 2. Antibodies. Working concentrations are given in µg/ml when manufacturer reports antibody concentration, otherwise concentrations are given as dilution factor used.

Specificity	Clone	Host	Application	Working concentration	Catalogue Number
α-tubulin	TU-02	Mouse	Western blot	0.4 µg/ml	Santa Cruz Biotechnology sc8035
β-actin	13E5	Rabbit	Western blot	1:1000	Cell Signalling Technology 4970
CD3	OKT3	Mouse	T cell stimulation	plate: 20 µg/mL Ca^{2+} flux: 10 µg/ml	BioLegend 317302
CD3	OKT3	Mouse	Flow cytometry	0.25 µg/ml	eBioscience 45-0037-41
CD69	FN50	Mouse	Flow cytometry	1:200	BD Biosciences 560711
cFos	2G2	Mouse	Flow cytometry	1:100	Novus Biologicals NBP2-37492
DimerX I	Human HLA-A2:Ig Fusion Protein	(Mouse)	T cell stimulation	20 µg/mL	BD Biosciences 551263
Erk1/2	polyclonal	Rabbit	Flow cytometry	1:200	Cell Signalling Technology 9102
Erk 1/2 pY204	197G2	Rabbit	Flow cytometry	1:200	Cell Signalling Technology 4377
IL-2	MQ1-17H12	Rabbit	Flow cytometry	0.25 µg/ml	Biolegend 500328

Specificity	Clone	Host	Application	Working concentration	Catalogue Number
Lck	polyclonal	Rabbit	Flow cytometry, Western blot	1:200	Cell Signalling Technology 2752
Lck pY394 (p-Src Family Y416)	polyclonal	Rabbit	Flow cytometry	1:200	Cell Signalling Technology 2101
Lck pY505	polyclonal	Rabbit	Flow cytometry	1:200	Cell Signalling Technology 2751
NFAT	D43B1	Rabbit	Flow cytometry	1:50	Cell Signalling Technology 14324
NFkB	E379	Rabbit	Flow cytometry	0.625 µg/ml	Abcam ab190589
PTPN22	polyclonal	Goat	Western blot	0.2 µg/ml	R&D Systems AF3428
PTPN22	D6D1H	Rabbit	Western blot	1:1000	Cell Signalling Technology 14693
TCR Vβ13.1	IMMU 222	Mouse	Flow cytometry	1:200	Beckman Coulter IM2292
zap-70	D1C10E	Rabbit	Flow cytometry, Western blot	1:200	Cell Signalling Technology 3165
Zap-70 pY493	polyclonal	Rabbit	Flow cytometry, Western blot	1:200	Cell Signalling Technology 2704
Secondary Antibodies					
Goat secondary	polyclonal	Donkey	Western blot	0.1 µg/ml	Life Technologies A21084
Mouse secondary	polyclonal	Goat	Flow cytometry	5 µg/ml	Life Technologies A11001
Mouse secondary	polyclonal	Goat	Western blot	0.05 µg/ml	LI-COR 926-32210
Rabbit secondary	polyclonal	Goat	Flow cytometry	4 µg/ml	Invitrogen A21245
Rabbit secondary	polyclonal	Goat	Western blot	0.1 µg/ml	Life Technologies A21109

3. Development of isogenic human cell lines with mutated PTPN22

3.1 Introduction

The haematopoeitic phosphatase PTPN22 has one of the strongest associations with autoimmune disease of any human gene outside of HLA[185,186]. The single-nucleotide polymorphism R620W has been linked to increased susceptibility to autoantibody-driven autoimmunity, such as type 1 diabetes, rheumatoid arthritis, systemic lupus erythematosus, and Graves' Disease[135-138]. The fact that HLA has the strongest genetic association with these diseases indicates that T cells are critical in pathogenesis of autoimmunity[187], most likely because the development of high-affinity autoantibodies by B cells requires T cell help[188].

In T cell signalling, PTPN22 is considered to be a negative regulator, dephosphorylating activating residues on the signalling molecules most proximal to the T cell receptor. It associates with another negative regulator, the kinase Csk[158], but the consequences of this interaction are still under debate[149]. What is known is that the PTPN22 R620W SNP affects the region of PTPN22 that mediates interaction with Csk, and reduces the interaction significantly.

3.1.1 PTPN22 in mice and men

One of the most challenging aspects of PTPN22 R620W research is a lack of consensus between data generated in different models. Mouse models consistently show that the equivalent mutation, R619W, is a loss-of-function mutation in T cells; in contrast a gain-of-function effect was reported in most studies using human T cells. In both cases, the SNP was associated with increased susceptibility to autoimmune disease, although this varied in mice depending on the genetic background[155,156], and on the ethnic population studied in humans.

Zhang et al. found that T cells from C57 Black 6 (B6) mice with the analogous R619W polymorphism exhibited enhanced T cell activation, as expected from a loss-of-function mutation in a negative regulator of T cell activation[155]. They

observed greater T cell numbers in spleen and thymus in R619W mice, higher ratios of effector/memory to naive as measured by CD62L/CD44 surface staining, and increased expression of CD69 and CD25 compared to wild-type (WT) mice. They were also able to detect prolonged phosphorylation of PTPN22 targets Lck Y394 and Zap-70 Y319 after stimulation with CD3/CD28. They explained these findings by showing an increase in calpain-mediated degradation of PTPN22 with the SNP, and showed a similar effect in Jurkat cells transfected with expression vectors of WT or R620W PTPN22.

Dai et al. released a study several years later using independently-generated knock-in mice on a B6x129/sV genetic background, a background which is prone to developing spontaneous autoimmunity[156]. While they corroborated the findings of Zhang et al. such as expanded T cell populations and enhanced signalling, including increased calcium flux and IL-2 expression, they found that the variant protein was not subject to increased rates of degradation compared to the wild-type. Importantly, they also reported higher levels of autoantibodies, and increased rates of spontaneous and induced autoimmunity. These mouse models, while demonstrating some variation, clearly show the R619W polymorphism to be a loss-of-function mutation, resulting in enhanced T cell signalling in mice.

Human individuals carrying the R620W allele have some similarities with R619W mice, including a susceptibility to autoimmune disease and accumulation of effector/memory T cells in the periphery, as well as autoreactive B cells. However, a closer look at T cell signalling revealed a more complicated landscape. Contrary to the mouse results, CD4 cells isolated from humans with the polymorphism were found to have reduced proliferation and calcium flux in response to CD3/CD28 stimulation[189,190]. They were also reported to have reduced CD25 expression, as well as a trend towards reduced cytokine production, including IL-2 and IL-4, with the most significant difference in IL-10. In contrast, loss of PTPN22 by siRNA knockdown of PTPN22 in human PBMCs and Jurkat cells was reported to lead to an increase in IL-2 production relative to untargeted cells[191]. Taken together, these studies suggested that the R620W polymorphism constitutes a gain-of-function, with T cells exhibiting reduced activation when the polymorphism is present, which is the opposite effect from when the protein is reduced.

Further evidence for R620W as a gain-of-function polymorphism is found in overexpression studies. Human primary cells and Jurkat cells showed PTPN22-R620W to be more effective at downregulating the NFAT/AP-1 pathway[192], and to have reduced Lck phosphorylation[151] (although the latter did not correlate with reduced Zap70 phosphorylation). However, conclusions are further complicated by the fact that in certain circumstances the human polymorphism mimics the mouse polymorphism or the protein knockout. Metzler et al found that in both human and mouse, B cell selection was similarly affected to generate more autoreactive B cells[167]. Burn et al found that the human polymorphism appeared to have a loss-of-function effect, associated with stronger signalling in primary T cells stimulated with LFA-1[153]. Evidence from these studies shows that although PTPN22 R620W autoimmune susceptibility is consistent between mouse and human models, the specific biochemical mechanisms driving it are distinct and complex.

A significant challenge in understanding the relation between mouse and human models is that human studies have thus far been conducted either in genetically distinct individuals, used overexpression vectors, or achieved knockdown through siRNA complexes. These techniques present unique difficulties compared to studies in lab-bred mice. Using cells from humans inevitably carries the complication of genetic variation between individuals, as well as uncontrollable environmental effects accumulated over years. At the same time, overexpression of a protein in a cell alters the normal stoichiometry of the protein relative to its binding partners and other members of the signalling pathway, and can change protein:protein interactions. Interpreting results from siRNA studies also brings with it the caveats of possible off-target effects and of incomplete reduction of the target protein, as well as the confounding factor of Toll-like receptor stimulation[193]. The aim of this thesis is to address the controversy between mouse and human data by generating isogenic human cell lines with mutations in PTPN22.

3.1.2 CRISPR technology

The advent of CRISPR technology offers a rapid, inexpensive route for genetic engineering[194]. The technique uses bacterial endonucleases, most commonly Cas9 from *Streptococcus pyogenes*, to introduce breaks in DNA strands. The enzyme is targeted to a specific DNA sequence by an associated single-guide RNA (sgRNA)

consisting of a scaffold and a 20-nucleotide guide RNA sequence. The purpose of the enzyme in nature is to provide bacterial adaptive immunity by recognising and digesting foreign DNA sequences present in the cell, such as those derived from bacteriophages. The guide sequence is variable, and will direct the enzyme to bind to a sequence of complementary DNA. In order for the endonuclease to bind and cleave the DNA molecule, the recognised DNA sequence must be followed by a protospacer adjacent motif (PAM) sequence. In the case of Cas9, the required PAM sequence is -NGG, meaning Cas9 can theoretically be directed to any site in a genome that contains -NGG. In the human genome, this means that Cas9 can be targeted to every 8 base pairs (bp) of the human genome, on average[195]. Thus, a PAM site is rarely far from a given region of interest.

Upon binding to a DNA molecule, Cas9 creates a double-strand break. The cut is made three bp upstream of the PAM sequence, and exposes the ends of the DNA strands, triggering DNA repair. DNA damage can be repaired by non-homologous end joining (NHEJ) or homology-directed repair (HDR) in the presence of a homologous DNA template. NHEJ results in deletions or insertions, whereas HDR is a much more precise, yet infrequent, event, and has been used to achieve specific gene edits. Compared to HDR, NHEJ is much more likely, and can lead to knock out of a protein, as the random insertions/deletions (indels) may cause frameshift mutations and premature stop codons.

3.1.3 Jurkat T cells

Jurkat T cells were selected for this project due to the relative ease of handling them compared to primary human T cells[196]. Isolated in 1977 from an ALL patient, much of our knowledge of T cell signalling is based on work in Jurkat cells[197]. While Jurkat cells may not exactly recapitulate human T cell signalling, they are very well-characterised, to the point that their entire genome has been analysed for abnormalities[198]. Notably, they lack PTEN and SHIP and may have altered levels of other signalling molecules compared to primary cells[75]. However, they are diploid and relatively stable, are homozygous for the major allele of PTPN22, and express it along with all of its known interactors[199]. These facts, coupled with the significant differences in cost and challenge compared with primary cells, made Jurkat cells an appropriate choice for this work.

The vast majority of human T cell models use superantigen (SAg) stimulation, such as CD3/CD28 antibodies. These stimuli produce responses through the same pathways as cognate antigen stimulation, but are fundamentally different in binding behaviour. Importantly for PTPN22 investigations, our lab has demonstrated that PTPN22 is most important in discriminating responses to weak antigens[200], a type of interaction which cannot be replicated by SAgs and instead requires a known cognate antigen. Based on this observation, we decided to transduce our cell line model with a known TCR that can be stimulated with cognate antigen of varying specificity, which has not previously been possible in a human model of PTPN22 mutation.

GWAS studies have identified PTPN22 as a critical phosphatase in regulating immune responses. Due to the lack of human PTPN22 knockout data, we used CRISPR to produce isogenic Jurkat cell lines with the *PTPN22* gene disrupted or intact at the genome level. The lines can also be stimulated specifically with cognate antigen with different degrees of affinity. These lines represent a novel method to investigate the role of PTPN22 in human T cell signalling.

Our recent work with mouse knockout cells has also demonstrated that the absence of PTPN22 in T cells improves tumour killing[201]. Given that adoptive T cell therapy has recently been approved for treating human cancers[202], PTPN22 could prove a valuable target in enhancing cancer therapy. Human PTPN22 KO cell lines are the first step in validating such a method.

3.2 Results

3.2.1 Genotyping and verification of Jurkat PTPN22 expression

Before beginning work with CRISPR, I had to establish a suitable parent cell line. I first needed to confirm that Jurkat cells are homozygous for the major allele of PTPN22. The R620W SNP has a phenotype even in the heterozygote state, so it was important to ensure that the unaltered control cell lines would have normal PTPN22 function.

Genetic screening for the R620W SNP is carried out by PCR of the R620W region followed by restriction digest with XCMI. The SNP introduces an XCMI cut site, which allows XCMI to cleave the 215 bp polymerase chain reaction (PCR) product into segments of 170 and 45 bp. These segments can be visualised by gel electrophoresis and are distinct from the uncut product, which remains if there is at least one allele which lacks the R620W SNP. XCMI screening showed that Jurkat cells are indeed homozygous for the major allele of PTPN22 (Figure 1a). The 215 bp product remains completely intact after incubation with XCMI, so neither allele contains an XCMI cut site. The heterozygous control on the same gel shows XCMI digestion of one allele, while the other remains uncut, confirming that the XCMI enzyme is able to cleave the PCR product only when the SNP is present.

I next performed a Western blot to verify that Jurkat cells express PTPN22 protein (Figure 1b). A band was detected at the appropriate molecular weight of 97kD in the lane containing Jurkat cell lysate. The band was absent in the negative control lane containing lysate from an equal number of 293T cells, which are human embryonic kidney cells not expected to express PTPN22, suggesting that the 97kD band is indeed PTPN22 and not a result of non-specific binding. Both lanes do contain a non-specific band that is detectable just under the molecular weight of PTPN22. While detection by Western blot is not a requisite for a protein to have a biological effect, sufficient expression of a protein by the parent cell line makes it much easier to later confirm protein knockout in daughter lines by directly checking for loss of protein expression.

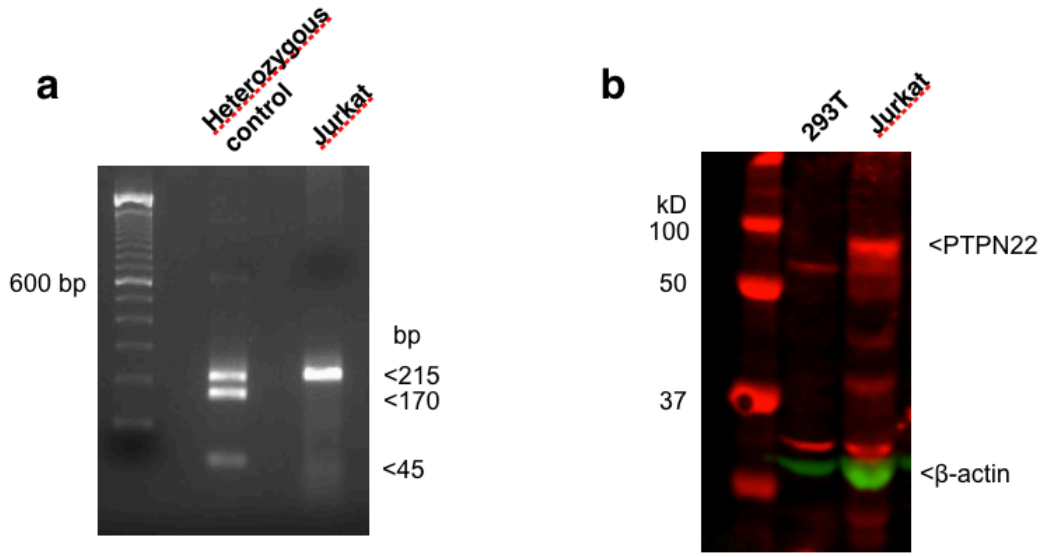

Figure 1. Jurkat cells express the major variant of PTPN22. (**a**) Jurkat genotyping was done by PCR followed by XCMI digest. The major allele produces a 215 bp band, while the R620W polymorphism produces 170 and 45 bp bands. (**b**) PTPN22 expression was tested by Western Blot. Whole cell lysates from Jurkat cells or non-haematopoeitic 293T cells were probed for PTPN22 and B-actin.

3.2.2 Transduction of Jurkat cells with Tax TCR

The cognate antigen of the endogenous Jurkat TCR is unknown. Most publications circumvent this issue by using (SAg) stimulation, such as anti-CD3/anti-CD28, PHA/PMA, or PDBU/ionomycin. However, these types of stimulus operate through different mechanisms than peptide/MHC, and may not be truly representative of physiological signalling mechanisms. Furthermore, we have previously reported that the involvement of PTPN22 varies with strength of antigen stimulation, a distinction that could be lost with stimulation by SAgs.

Because we are interested in the role of PTPN22 in weak cognate interactions, we decided to transduce our cell line with a known TCR of that could be stimulated with weak or strong peptides. We used a line of Jurkat cells that lacks endogenous TCR expression to eliminate any possible effects of an additional TCR on signalling stoichiometry, and avoid the possibility of incorrect alpha/beta chain pairings.

We transduced JRT3-T3.5 Jurkat cells, which lack the TCR beta chain, with a specific T cell receptor that recognises pTax, an HLA-A2 restricted peptide derived from human T-cell lymphotropic virus. The Tax TCR also recognises with weaker affinity the peptide pHuD (from Hu-antibody associated paraneoplastic neurological syndromes). The TCR transduction was carried out in collaboration with Hans Stauss, as described[203]. Cells were bulk sorted for TCR expression by flow cytometry (Figure 2a), and then the sorted population was cloned by limiting dilution and each clonal population expanded. Using a line isolated from a single cell reduces the genetic variability between subsequent daughter lines, including the possibility of highly varied CD3 expression following TCR transduction.

In order to select which TCR-transduced clone to use as a parent line, I tested each of them for surface CD3 expression as well as responsiveness to pTax stimulation. CD3 and TCR can only be stably expressed on the cell surface when they are present together in a complex, so levels of CD3 on a cell surface can be considered equivalent to TCR expression. For this experiment, Jurkat cells were co-cultured with T2 cells pulsed with pTax peptide. T2 cells are a lymphoblast line that expresses HLA-A2, but lacks a peptide transporter involved in antigen processing

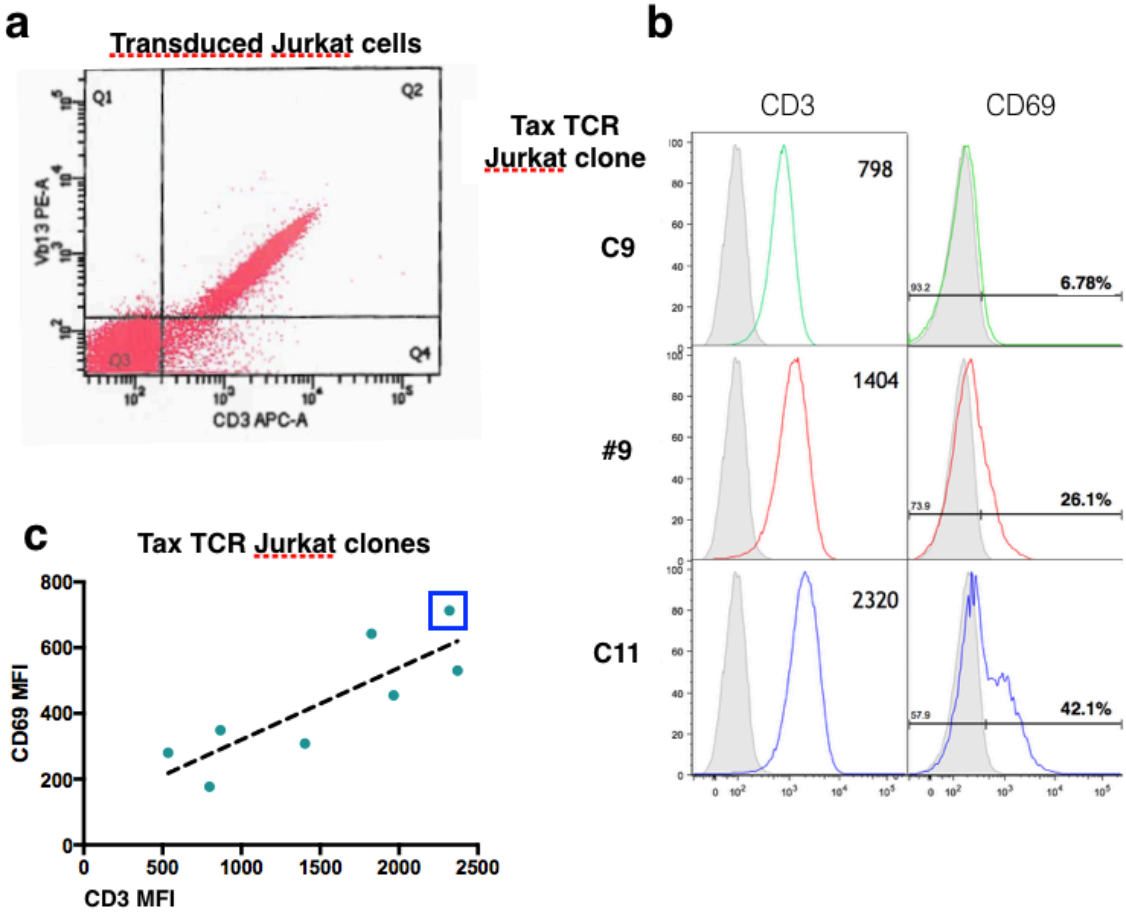

Figure 2. Selection of Tax TCR Jurkat line. (**a**) Tax TCR-transduced Jurkat cells were sorted by flow cytometry based on expression of Vβ13 TCR chain and CD3. Sorting was performed 72 hours after transduction. (**b**) CD69 and CD3 expression was evaluated by flow cytometry. CD3 expression of unstimulated cells is compared to unstained controls (grey). Numbers indicate MFI of stained samples. CD69 expression of cells stimulated for 24 hours with pTax peptide is compared to unstimulated controls (grey). Numbers indicate percentage of cells that are CD69 positive. Three representative clonal cell lines are shown. (**c**) MFI of CD3 expression and CD69 upregulation were found to correlate across eight cell lines tested. The blue square indicates Jurkat Tax TCR clone C11.

and is thus unable to load endogenous protein for MHC class I presentation[204]. This means the surface HLA-A2 is able to pick up the pTax peptide when it is present in the culture media, and to present it in MHC:peptide complexes to Jurkat cells. Jurkat and pTax-loaded T2 cells were co-cultured for 24 hours before antibody staining for flow cytometry.

When analysing CD69 surface expression by flow cytometry, I observed that Jurkat clones with higher CD3 expression showed correspondingly increased upregulation of CD69 (illustrated for three clones in Figure 2b). This correlation was found to give a linear relationship for each of the clones I tested (n=8) (Figure 2c). The capacity for a cell line to produce a strong response to cognate peptide is important when trying to detect subtle signalling effects or to analyse responses to much weaker peptides. Thus, clone C11 (blue square, Figure 2c) was selected to continue with CRISPR work because it had the highest MFI of CD3 surface expression as well as the greatest degree of CD69 upregulation in response to pTax.

3.2.3 Exon 1 PCR screen design

CRISPR knockout efficiency varies, but is almost never affects 100% of a transfected population. Because I would be trying to choose mutated cell lines from potentially hundreds of clones, I needed a rapid, simple way to screen for indels at the genomic level. Following genomic screening, clones would be selected for lower throughput Western blot screening to check for loss of protein expression. Genomic screening would be useful as a first step to analyse many clones to estimate gene editing efficiency and select likely candidates for further study.

I opted for a PCR screen with restriction digest because PCR is simple, cheap, and well-established. I used NCBI/Primer-BLAST to select primers that would create a PCR product longer than 400 base pairs. The size of the product would reduce the likelihood that a large deletion could knock out a primer site or reduce the product to <100 bp, which becomes difficult to detect on a gel or read by Sanger sequencing. The PCR product spans PTPN22 exon 1 as well as two restriction sites for AvaII, which create products differing in length by at least 40 base pairs (240,

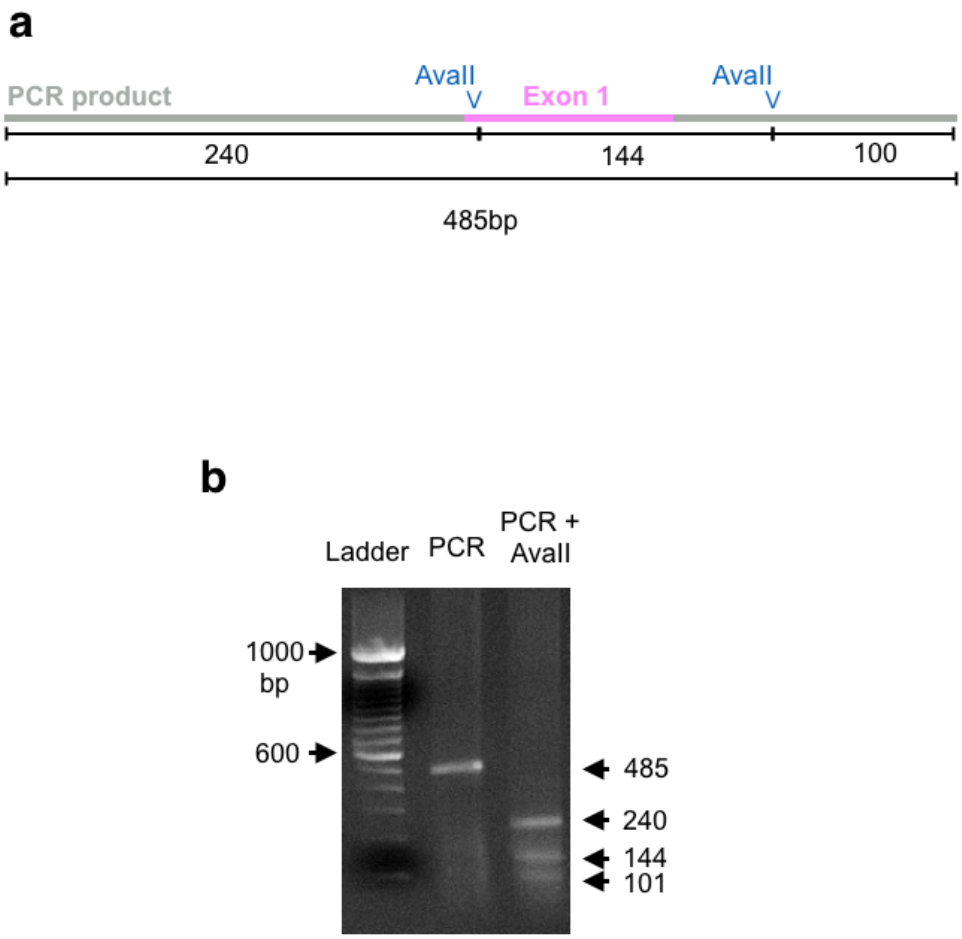

Figure 3. PCR screen development. (**a**) 485 bp product spanning human *PTPN22* Exon 1 contains two AvaII restriction sites. (**b**) Uncut PCR product and AvaII digested PCR product were run on an agarose gel.

144, 101 bp) (Figure 3a), and are thus easily distinguishable on a gel (Figure 3b). One AvaII restriction site involves the start codon, thus loss of that site could be a good indicator that the cell line would no longer be able to express PTPN22.

3.2.4 CRISPR guide RNA design

Guide design is an important determinant in maximising Cas9 efficiency and minimising off-target effects[205,206]. I selected four guides that had "green" quality scores from the Zheng Lab off-target prediction tool (http://crispr.mit.edu/) to reduce the likelihood of introducing insertions or deletions in the genome outside of our region of interest. The guides were selected in pairs with cut sites within 15 bp of each other for potential use with the nickase version of Cas9. The nickase was created to further reduce off-target editing by creating cuts on only one DNA strand, so that only when two guide sequences are recognised in the same region of DNA does a double-strand DNA break occur. As double-strand breaks are needed to expose the DNA strand to loss or addition of nucleotides, this method reduces the likelihood of creating off-target indels. Use of the nickases effectively doubles the specificity of Cas9, but requires two sgRNAs with high activity to create indels efficiently[207].

We targeted exon 1 in order to mimic the mouse Ptpn22 KO used in our lab, in which exon 1 has been excised. The guide pairs I selected targeted either the start codon at the beginning of exon 1 or the region within 10 bp downstream from the end of exon 1 (Figure 4). Exon 1 of human PTPN22 spans only 87 bp, which is short enough that most or all of it could be deleted by CRISPR targeting.

At the time of performing these experiments, plasmid CRISPR transfections were better optimised than protein or RNA transfections, and there were readily available and affordable reagents from Addgene in a number of formats, including plasmids encoding antibiotic resistance cassettes or fluorescence markers. We purchased DNA oligonucleotides based on our guide sequences to clone into the plasmids, allowing our sgRNA to be expressed from the same promoter as the Cas9 protein. I followed the protocol described by Ran, et al[194] to anneal the guide sequence DNA oligos into plasmids from Addgene, and performed a bacterial transformation into

Figure 4. *PTPN22* Exon 1 PCR region and CRISPR guide sequences. Exon 1 is highlighted in pink. SgRNA recognition sites are indicated by blue constructs, with associated PAM sites indicated in green. AvaII restriction sites are also indicated.

XLI E. coli with the resulting plasmids. Single colonies were expanded and screened by restriction digest; if the guide sequence is inserted, it disrupts a BbsI site (data not shown).

Different guide sequences have varying on-target efficiency[205]. To test which of the guides we selected had efficient Cas9 cutting activity, I transfected each of them into 293T cells, human cells which can be transfected more easily than Jurkat cells. Due to the relative difficulty of transfecting Jurkat cells by electroporation, screening Jurkat populations is labor intensive and time consuming: populations must be enriched or even grown up from single cells because the resolution of our bulk population screens is not clear enough to evaluate cutting efficiency. However, 293T cells can be transfected with highly efficient Fugene transfection, and bulk populations screened directly by PCR and restriction digest within a couple of days of transfection. 293T screening allowed me to verify whether or not each sgRNA was capable of directing any endonuclease activity in human cells (Figure 5).

I observed changes in the band pattern of the PCR product and the AvaII restriction digest following transfection of 293T cells with CRISPR plasmids. Interestingly, I did not observe any consistent large, uncut bands following AvaII digest, suggesting that small deletions around the AvaII restriction sites were not a common occurrence. Larger bands can be seen in the heavily loaded lanes 6, 7, and 8. As lane 6 was not transfected with any CRISPR plasmids, any residual uncut product may be due to incomplete digestion by AvaII over the two hour incubation. Another possible explanation could be that the band is a weak, nonspecific PCR product, but as no such band is visible in the corresponding uncut PCR lanes, this seems unlikely. Lanes 7 and 8 show the larger band of similar intensity to the mock transfection group, despite less DNA being loaded, so it is possible that the reduction of the 144 bp band in those lanes can be attributed to loss of the AvaII site located near the start codon. If this is the case, however, it is a relatively uncommon occurrence, as the larger band is weak compared to the other bands.

The most common result from transfection with different guides was shifts or

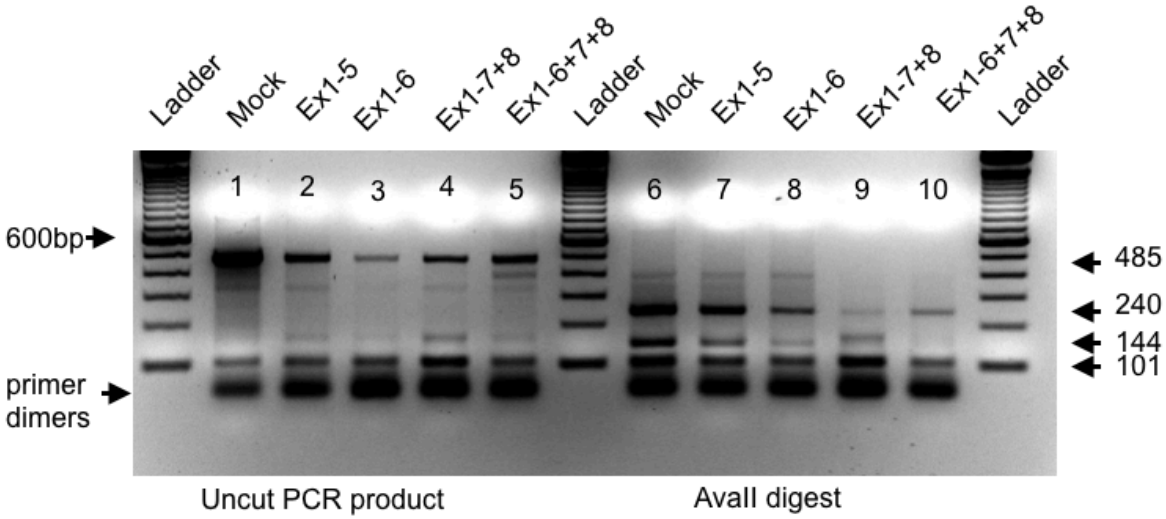

Figure 5. CRISPR guide sequence efficiency testing. Jurkat cells underwent Amaxa transfection under one of the following conditions: No exogenous DNA added (mock), plasmid containing guide Ex1-5, plasmid containing Ex1-6, two plasmids containing Ex1-7 and Ex1-8, three plasmids containing Ex1-6, Ex1-7 and Ex1-8. Lanes 1-5: Uncut PCR product. Lanes 6-10: PCR product digested by AvaII restriction enzyme.

changes in intensity of the 144 bp band upon AvaII digestion, evident to some degree across all CRISPR conditions (lanes 7-10). This consistency was reassuring, as the 144 bp band represents the exon 1 region. CRISPR-driven indels would cause the length of that region to vary between the different cells of the transfected population, meaning that we would expect to see the intensity of the single wild-type band reduced. In lane 9, the 144 bp band appears to be slightly larger, suggesting that the region may be subject to insertions more commonly than deletions under those transfection conditions. In lane 10, the 144 bp band is no longer visible. There is also no larger uncut band visible, suggesting that the loss of the 144 bp band is not due to loss of the restriction site, but instead to sufficient deletions in the exon 1 region that a band of the expected size can no longer by detected. This hypothesis is supported by the corresponding uncut PCR product in lane 5, which is the only lane to show evidence of consistent and large enough deletions to create a shifted band without AvaII digestion.

Based on the fact that lanes 5 and 10 showed the most striking changes, I decided to use guide Ex1-6 in combination with 1-7 and 1-8. Ex1-5 showed the least amount of difference to the mock transfected group, so I elected not to use it. Instead I used Ex1-6 with the wild-type version of Cas9, plasmid Px330, and Ex1-7 and 1-8 each in the nickase version, plasmid Px461. The latter plasmid also carries an enhanced green fluorescent protein (eGFP) reporter construct on the same promoter as the gRNA and Cas9 (Figure 6).

3.2.5 CRISPR plasmid transfection and indel screening

Electroporation is a widely used method of T cell transfection. We initially used Amaxa electroporation, but later switched to Neon electroporation due to its reported efficacy in Jurkat transfections[208]. In our hands, the Neon system produced much higher rates of cell survival 48-hours following transfection, increasing from 10% (Figure 7a) to 60-80% survival (Figure 7b). Additionally, Neon transfection with the CRISPR plasmids alone led to greatly increased GFP expression compared to Amaxa transfection with the same constructs. Cell number, concentration of plasmid, and electroporation settings all followed manufacturer recommendations as described in Chapter 2. These transfections are transient, so that Cas9 and GFP

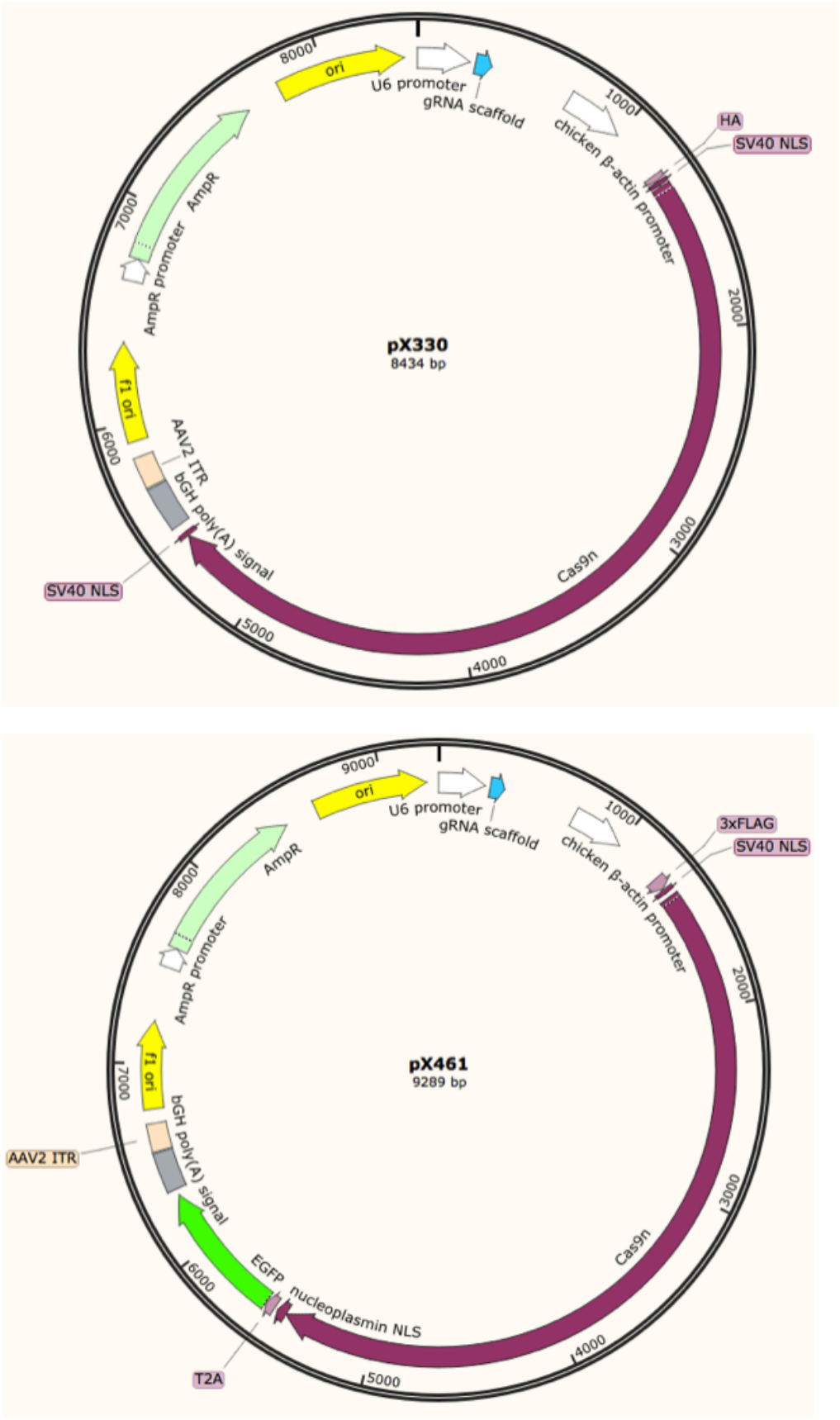

Figure 6. Addgene CRISPR plasmid maps. Guide sequences were ligated into plasmids px330 and px461 for transfection in Jurkat cells.

expression begins to decline 2-3 days following transfection (data not shown).

48-hours following transfection, cells were sorted based on GFP expression from a reporter construct either coded within the CRISPR plasmids or on an independent plasmid which was co-transfected. Upon PCR/AvaII screening, I observed that co-transfections led to greater numbers of GFP-positive cells, but that this GFP expression did not correlate with an increased rate of indels; out of 50 tested clones, none of them showed any changes at the PCR level (Figure 7c). However, GFP expression following transfection with Px461 and no additional reporters did correlate with increased indel formation, although many fewer cells were recovered; from three clones tested, two of them showed loss of an AvaII restriction site (Figure 7d). Based on this finding I repeated the transfection using the Neon system without using co-transfection with a GFP vector.

GFP-positive cells were sorted as single cells or as bulk populations to be frozen and cloned using limiting dilution in order to expand genetically homogenous daughter cell lines derived from a single cell. The Neon system gave far better transfection efficiency than the Amaxa protocol, allowing me to sort three different populations based on levels of GFP expression (Figure 7b). I also sorted cells that had been transfected with only a GFP vector, designated the “mock” group. Like the CRISPR lines, this group had undergone Neon electroporation, expression of a foreign construct, cell sorting and growing from a single clone, but never expressed Cas9, and therefore was expected to be as genetically identical as possible to the untransfected parent line.

CRISPR and mock-transfected Jurkat cell lines were grown from single cell clones over a period of 3-4 weeks before undergoing screening and further selection. CRISPR populations were checked for indel formation by PCR screen, and cell lines with clear shifts were chosen to undergo further screens. Similarly to the tests in 293T cells, a significant number of clones showed large shifts in the exon 1 PCR product even before digestion with AvaII. I found that high and medium levels of GFP expression correlated with increased rate of large indels on at least one allele

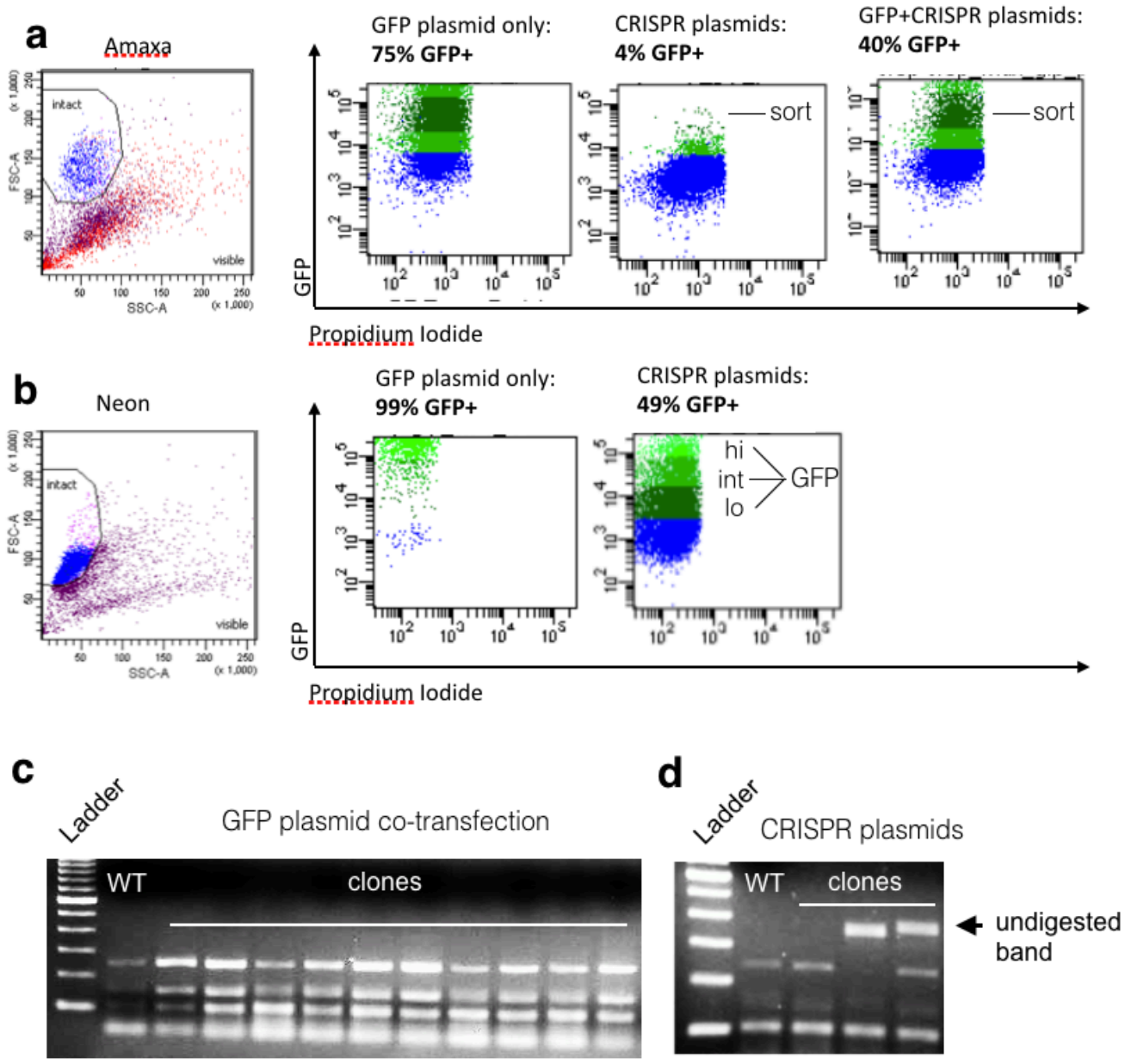

Figure 7. Cell sorting following *PTPN22* Exon 1 CRISPR of Jurkat cells.
Cells were sorted 48-hours after transfection using (**a**) Amaxa or (**b**) Neon electroporation. Forward and side scatter plots of cells transfected without DNA are shown. Blue events on the FSC/SSC plotes are included in the "intact" gate for further analysis. GFP expression is shown for transfection with a GFP reporter plasmid only, CRISPR plasmids only, or both a GFP reporter and CRISPR plasmids together. Events considered GFP negative are blue. GFP positive cells were sorted as a single group (Amaxa) or separated into high, intermediate, and low GFP expressing groups (Neon). (**c** and **d**) After sorting, clones transfected by Amaxa with (**c**) CRISPR plasmids and a GFP reporter or (**d**) CRISPR plasmids only were screened for indels by exon 1 PCR and AvaII digestion.

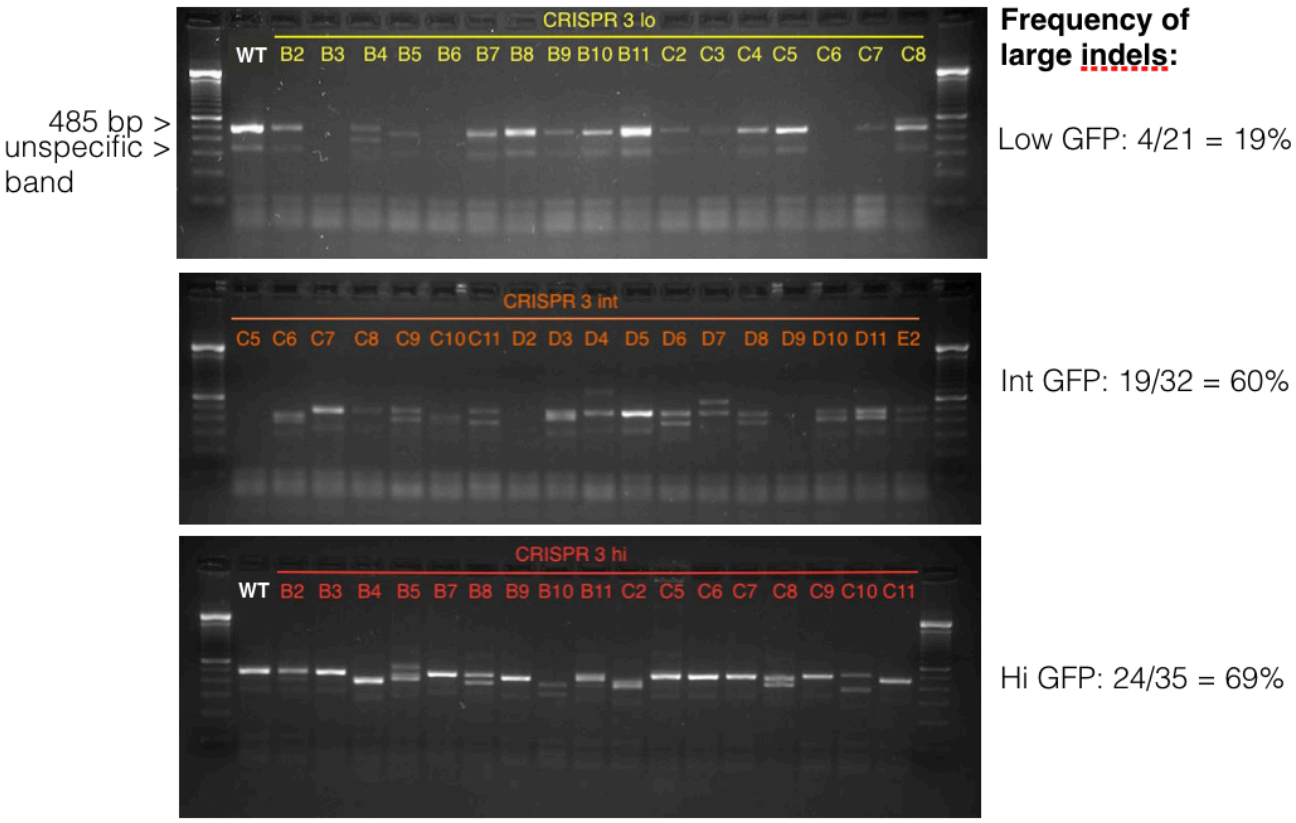

Figure 8. PCR screen of *PTPN22* Exon 1 CRISPR Jurkat clones. C11 Jurkat cells were transfected with CRISPR plasmids using Neon electroporation and sorted by high, intermediate, and low GFP expression. Clonal populations were expanded and screened for indels by PCR. One representative gel is shown for each sorted group. Large indels were detected by shifts in the main band size compared to wild-type control (WT). Frequency of large indels was determined by dividing the number of clones with shifted bands by the total number of clones screened for each sorted group.

(>60%) compared to low levels of GFP (<20%) (Figure 8). A recently developed technique that could be used to more accurately assess indel frequency is droplet digital qPCR, which uses duplexed primer probes to distinguish WT amplicon product from product containing a deletion. Using this technique yields accurate indel frequency information from small amounts of DNA, reducing the amount of time needed to grow up large volumes of cells merely for screening purposes [209].

Because we previously observed that large differences in Tax TCR expression correlate with changes in activation readouts (Figure 2), I took steps to ensure that the clones chosen to undergo further screening expressed similar CD3 levels to the parent line. Both the mock clones and the CRISPR clones were tested for CD3 surface expression levels by flow cytometry and compared to CD3 expression of the parent line. CD3 median fluorescence intensity (MFI) values were normalised by forward scatter MFI to account for differences in cell size, and only cell lines for which normalised values were within 10% of the parent line were kept for further screening (Figure 9a). The range of CD3 expression of selected clones is shown in Figure 9b.

Cell lines were then subjected to Sanger sequencing to more accurately analyse the mutations introduced by CRISPR. We used the TOPO cloning technique to separate alleles for individual sequencing. In this method, PCR product is annealed into the TOPO 2.1 bacterial vector. The open vector contains a 3' T-overhangs, which enable ligation of PCR products carrying non-template adenosines on the 3' end due to amplification by *Taq* polymerase. The closed plasmid carries an ampicillin resistance gene, allowing for selection and expansion of E.coli colonies that contain a plasmid with a PCR product. For each cell line I sequenced, I selected six bacterial colonies in order to increase likelihood of both alleles being represented.

The sequencing data (Figure 10) shows that deletions of >50 bp are well-represented, with short sequence alterations often found near the deletion site. Deletions frequently span the latter 75% of exon 1, with only a few instances of a disrupted start codon. Occasionally, deletions occurred in the centre region of exon 1, with both Cas9 cut sites remaining intact; this is likely due to more accurate repair of the damaged region by homologous recombination using the other allele.

To confirm protein expression was lost due to the genomic changes, Western blotting was carried out (Figure 11). PBMCs were restimulated for 24 hours to increase PTPN22 expression, five days after initial isolation and expansion, at which

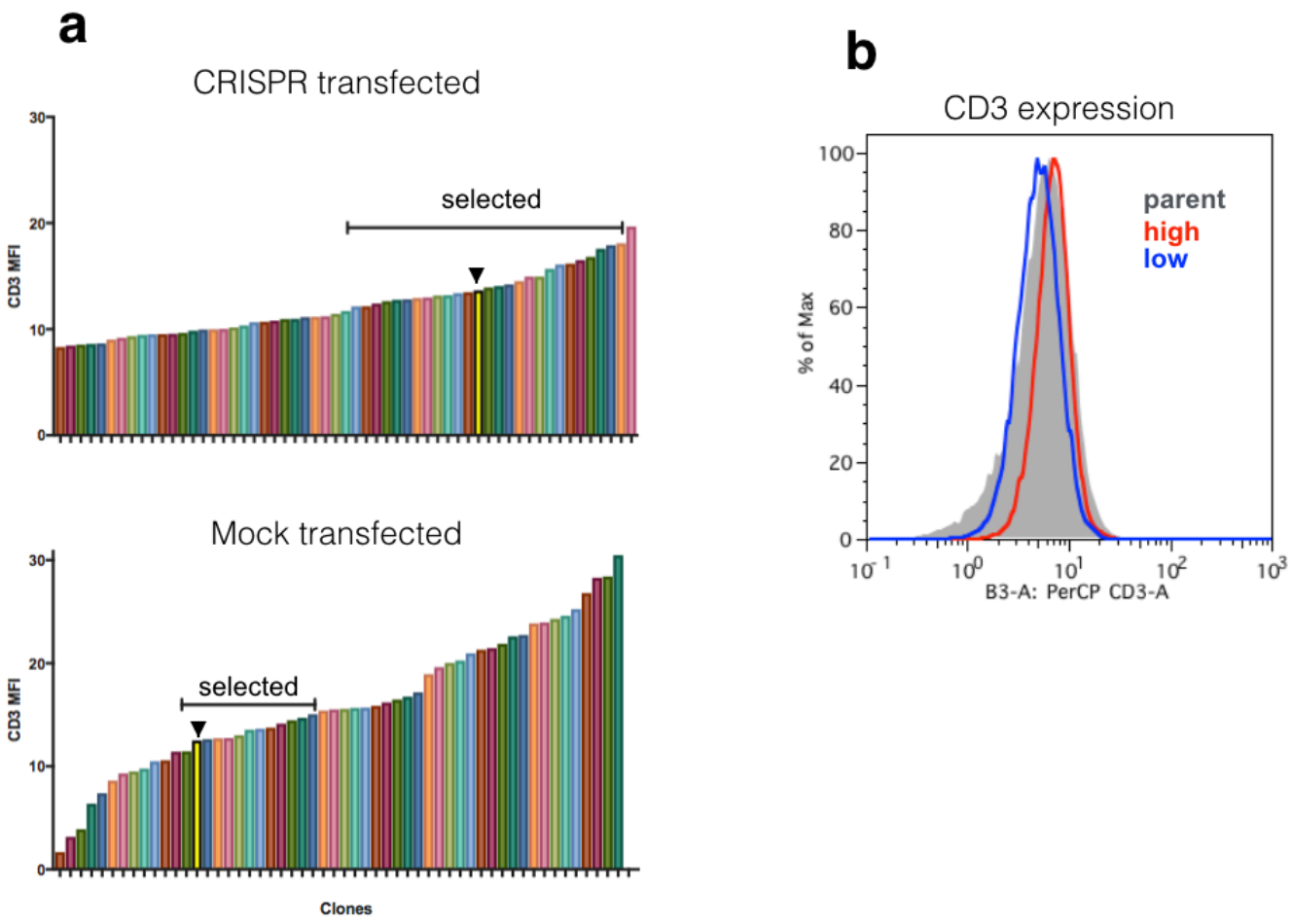

Figure 9. Selection of Jurkat clones by CD3 expression. (**a**) Clonal lines of C11 Jurkat cells that had been transfected with CRISPR plasmids or with a GFP reporter plasmid were checked for CD3 expression by flow cytometry and compared to the parent line (yellow bar, indicated by arrow). Clones with an MFI within 10% of the parent line were selected. (**b**) Histogram demonstrating the range of CD3 expression of selected clones. The C11 parent line is shown in grey, with the highest selected CRISPR clone in red and the lowest selected clone in blue.

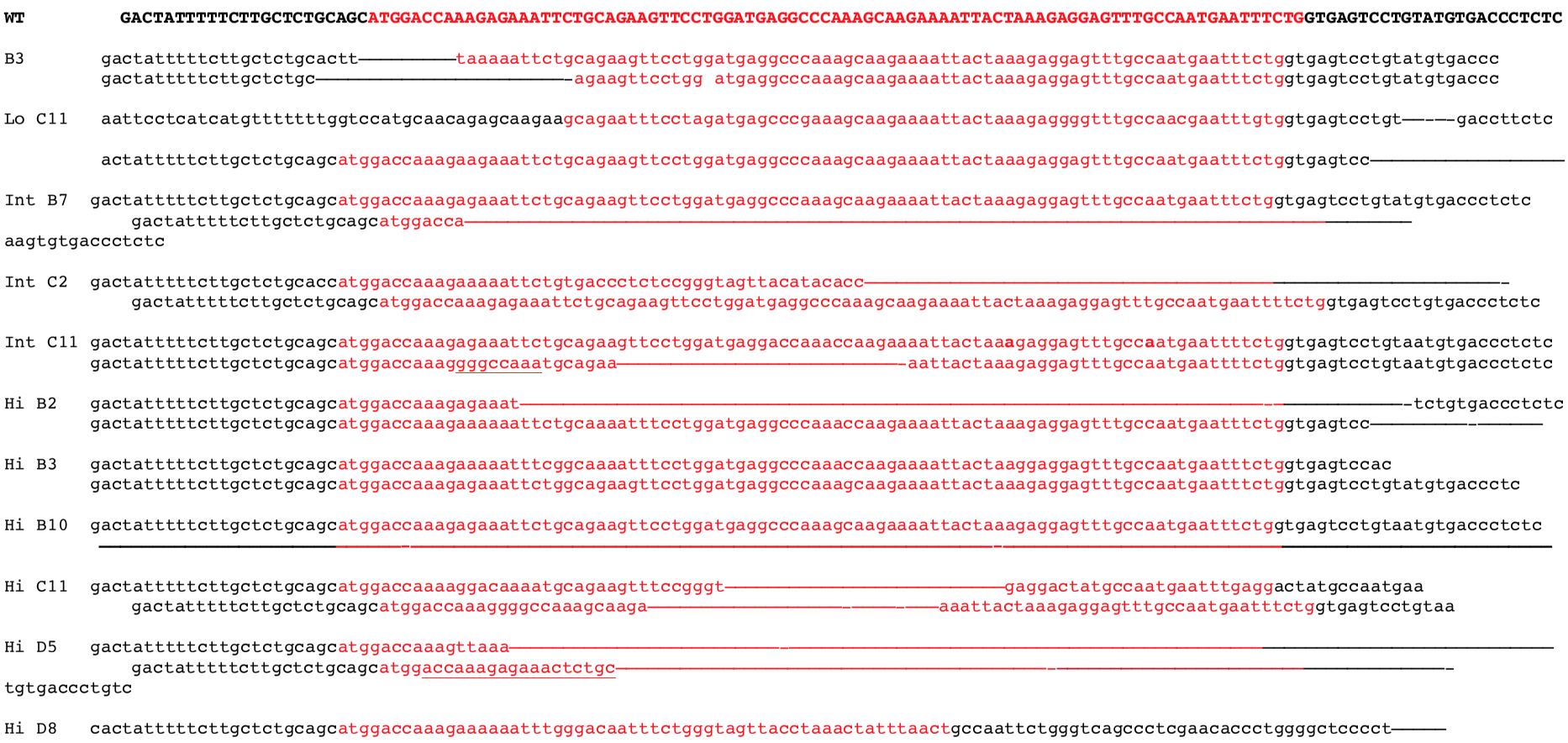

Figure 10: Sequences of *PTPN22* Exon 1 CRISPR Jurkat clones. PTPN22 Exon 1 region of selected Jurkat clonal cell lines were sequenced using Topo cloning and Sanger sequencing. The canonical human sequence is labeled “WT”. Exon 1 is indicated in red. Solid lines represent deletions.

point they express both more PTPN22 and more protein in general per cell than resting Jurkat cells. The membrane was probed with an antibody against the central region of PTPN22 and with an antibody against the housekeeping gene α-tubulin as a loading control. I later also probed the membrane using another antibody against PTPN22 that recognises the N-terminal region to check for truncated forms of PTPN22 (data not shown). The additional antibody did not lead to any new bands detected in lanes lacking full-size PTPN22, suggesting that the genomic deletions occur early enough in the protein sequence that no truncations of PTPN22 are being expressed. Based on the Western blot results, I selected six PTPN22 knockout clonal lines (KO) and five mock transfected wild-type clonal lines (WT) for use in further experiments with the untransfected parent line.

3.2.6 Characterisation of clones in the steady state

Importantly, PTPN22 WT and KO cell lines in the steady state were morphologically indistinguishable by microscope and flow cytometry (Figure 12a). Baghbani, et al reported that suppression of PTPN22 by siRNA led to apoptosis in Jurkat cells[210], but the viability of my PTPN22 KO cell lines was unchanged, suggesting that their observations were due to a confounding factor unrelated to PTPN22 expression. As Jurkat cells do not rely on TCR signalling for normal growth, we did not expect loss of PTPN22 to have any impact on their behaviour in culture. I observed similar levels of cell death, and the rate of cell growth was identical between WT and KO lines under normal culture conditions, when measured by daily counts (Figure 12b).

I also found that abundance of the TCR proximal signalling molecules Lck and Zap-70 was consistent between mock and CRISPR lines (Figure 12). These proteins are involved in some of the earliest steps of TCR signalling, and are also known to be direct targets of PTPN22. The similar levels of these proteins between WT and KO lines means that any differences observed should be due to the presence or absence of PTPN22, and not to changes in the stoichiometry of other signalling molecules.

These observations were reassuring that PTPN22 was not impacting the cells in their normal state, and that any changes in response to stimulation would be due to

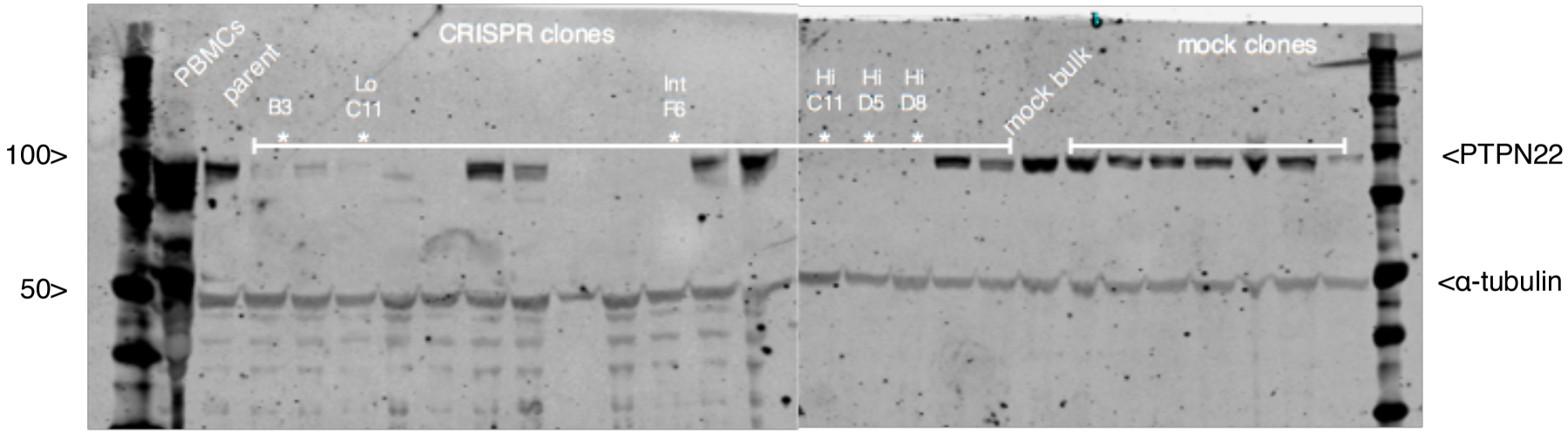

Figure 11. Western blot of *PTPN22* Exon 1 CRISPR Jurkat clones. Whole cell lysate from $1x10^6$ cells was loaded in each lane for screening for PTPN22 by Western blot. 'Parent' refers to untransfected C11 Jurkat parent line. 'Mock bulk' refers to sorted mock transfected cells that have not been cloned. Clonal lines that were chosen for further study are indicated by stars. Clone designations of each line are given.

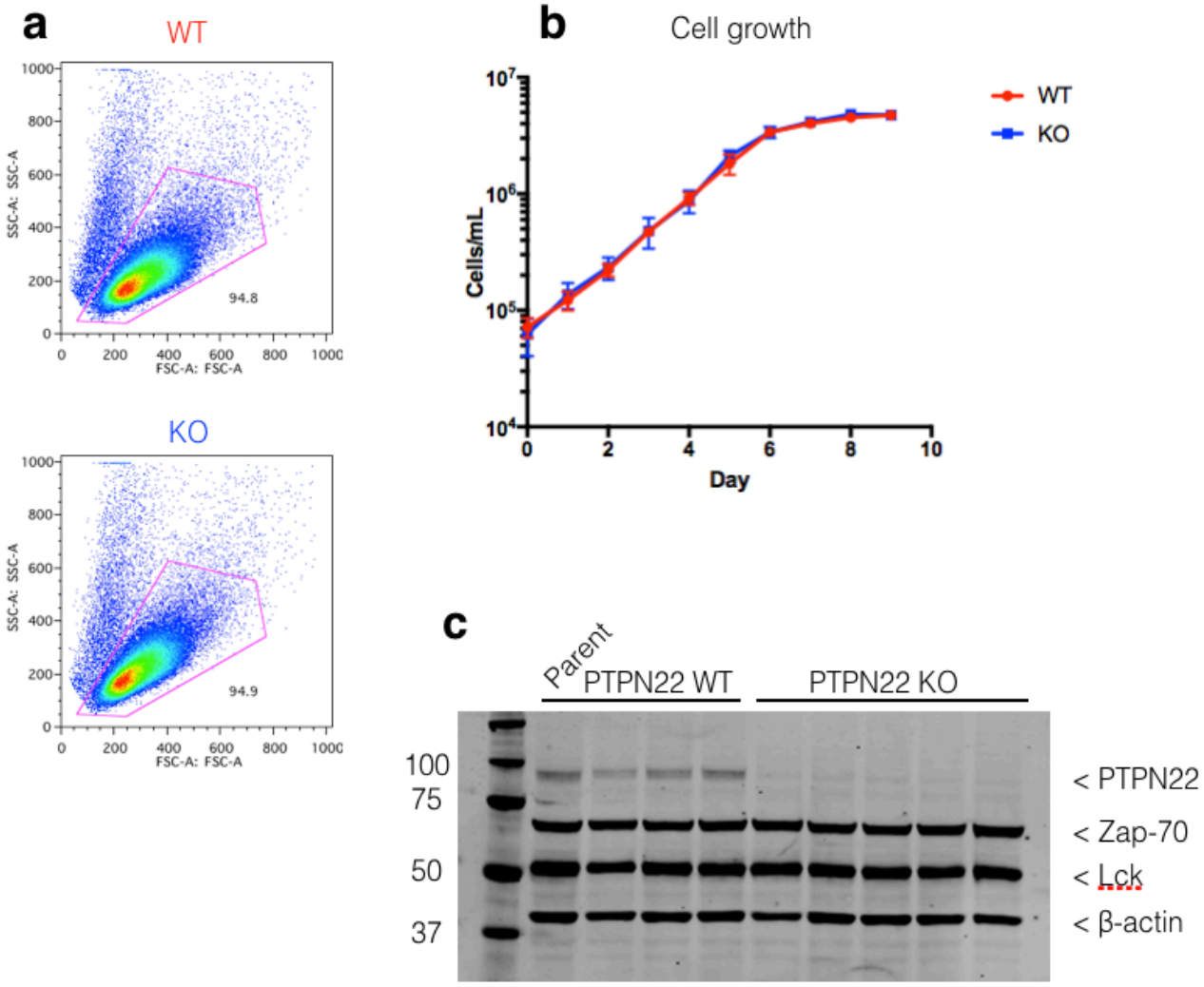

Figure 12. Steady state analysis of *PTPN22* Exon 1 CRISPR Jurkat clones. (**a**) Size and granularity of cells in culture was observed by flow cytometry by foward scatter and side scatter, respectively. Plots are representative of more than 10 experiments. (**b**) Growth of cells was monitored by daily counting using a Casy Cell Counter. Three lines per group were grown in 24-well plates in triplicate wells. (**c**) Western blot of PTPN22 and early T cell signalling molecules. Whole cell lysate from $1x10^6$ cells of each clonal line was loaded per well.

alterations in TCR signalling, rather than differences in the condition of the cells prior to the experiment.

3.3 Discussion

We created isogenic PTPN22 KO human T cell lines in order to address the complications contributing to the controversy between mouse and human studies of PTPN22 function. The CRISPR technique enabled the introduction of genome mutations, so that we did not need to rely upon siRNA or protein overexpression to identify the role of our protein of interest. Also we could ensure that our cell lines were clonally derived, eliminating confounding genetic or environmental factors.

Jurkat cells are a single cell type and are not subject to interactions with Tregs or other cells. It is possible that the phosphatase has different roles in specific cell lineages. They also lack the capacity to differentiate into specialised effector cells. However, many of our outstanding questions about PTPN22 pertain to the TCR signalling pathway itself, which has been very well characterised in Jurkat cells. PTPN22 KO Jurkat lines are well-suited to address the discrepancies observed in mouse and human signalling studies.

One concern about using gene-editing technology is the possibility of off-target effects. We reduced the impact of potential CRISPR off-targets on our results in three ways: (1) we used an off-target prediction tool to ensure that our guides had low homology with other regions of the genome, (2) we used the Cas9 nickase along with the wild-type to reduce the likelihood of non-specific double-strand breaks, and (3) we selected six different clonal cell lines for each genotype, so that it would be unlikely that the same off-target effect would be present in every line across the group. A control group that had been through the same procedures for transfection and selection was also developed. The cell lines were grown from single cell clonal populations and were screened by PCR and Western blot. Each line was also selected to have similar levels of CD3 expression relative to the parent line, and the lines demonstrated identical growth rates and expression of Lck and Zap-70 while at rest. These steps give me confidence that the results reported in chapters 4 and 5 can be attributed to loss of PTPN22 expression.

CRISPR technology has advanced considerably since the inception of this project three years ago. Were I to begin today, I would transfect with protein instead of plasmids, as the former has been shown to be more efficient in primary cells, our eventual targets[208]. There are also a number of databases now with predesigned guide RNAs that are optimised according to more recent knowledge about off-target tendencies and optimising efficiency, and many kits exist that expedite the process from design to selection, from the several months experienced here to a number of days or weeks.

Nonetheless, I was able to achieve an indel frequency of >60%, which enabled me to select a number of clones with the PTPN22 KO genotype and which were carried forward for biochemical and functional analysis as described in the following chapters. This protocol has also informed work using CRISPR to knock out PTPN22 in primary cells which is now an ongoing technique in the lab and which we aim to use to augment adoptive T cell therapy. The PTPN22 KO Jurkat cell lines developed here represent a novel and powerful tool in understanding the role of PTPN22 in human T cell signalling.

4. Effect of PTPN22 on T cell effector molecules

4.1 Introduction

The development of PTPN22 KO Jurkat clones presented a novel opportunity to investigate the effects of loss of PTPN22 on human T cell signalling. In order to determine how PTPN22 influences T cell responses to antigen, we stimulated PTPN22 WT and KO Jurkat clones with cognate peptide and evaluated their upregulation of CD69 and production of IL-2, and their susceptibility to activation-induced cell death (AICD).

4.1.1 Effector functions of Jurkat T cells

Jurkat cells were derived from an acute lymphoblastic leukemia patient in 1977[211]. They have been widely used since then as a model of T cell signalling, a role they continue to occupy today despite well-known divergences in growth and cytokine production upon stimulation compared to normal human primary cells. They offer several advantages over primary cells: because of their historical widespread use, characteristics of Jurkat cells are well documented in literature[197], and immortalised cell lines in general are much simpler to work with compared to primary cells, as they grow continuously without cytokines, are easier to transfect, do not require isolation from other haematopoetic cells, and are not subject to the heterogeneity observed in cells isolated from human donors[212].

As with all scientific models, however, there is a trade-off for the convenience offered by Jurkat cell lines: they differ considerably from primary human T cells in terms of steady-state activity and protein expression upon stimulation. For example, the fact that Jurkat cells divide independently of TCR stimulation means they cannot be used to study the proliferation response to TCR signalling. Another very important distinction between Jurkat cell signalling and that of primary cells is that Jurkat cells do not differentiate upon stimulation the way we expect of normal T cells: although their lineage is from a CD4 T cell, they frequently lack CD4 expression and do not adopt typical activation phenotypes in the form of T helper cell cytokine profiles. There is significant variation in the behaviour of Jurkat lines used by different groups, with some groups reporting cytokine production upon

stimulation including IL-6, IL-8, IL-10, or IFNγ, and others reporting no detection of any of these[75,213,214]. Despite this variability, IL-2 is a consistently reproducible cytokine readout for Jurkat cell activation[75], reflective of the fact that high IL-2 production was the factor for which the line was originally selected[215].

4.1.2 Interleukin-2

The cytokine now known as IL-2 was initially described as a "T cell growth factor," [216,217] but is now known to have additional crucial functions besides promoting expansion of T cells[218]. For example, in the 1980s IL-2 was shown to also act as a growth factor for NK cells and B cells[215,219]. Paradoxical roles for IL-2 were later discovered in its ability to promote AICD in murine T cells upon subsequent stimulation[220], and in the phenotype of IL-2 KO mice, which develop lymphoid hyperplasia and autoimmune disease [221,222]. An explanation for the unexpected result that loss of IL-2 in vivo enhanced T cell activity was found in the discovery that IL-2 also promotes activity and homeostasis of Treg cells in the periphery; reintroduction of IL-2 into IL-2 KO mice re-established the absent population of CD4 Treg cells and rescued the autoimmune phenotype[223]. IL-2 is a critical component of the immune system, not only for promoting immune cell responses to infection but also in the maintenance of immune homeostasis.

4.1.3 CD69

CD69 is a surface molecule commonly used as an early marker for activation in T cells, as it is detectable on the cell surface within 2-3 hours of stimulation[224]. Constitutive expression of CD69 was reported in lymphoid precursors and mature thymocytes[225], but it does not appear to be critical for T cell maturation, as CD69 KO mice did not exhibit any aberrations in T cell development[226]. CD69 is present on tissue-infiltrating T cells, and may have a role in promoting tissue retention by participating in a complex that negatively regulates S1P1, a surface molecule that mediates T cell tissue egress[227]. However, Esplugues et al showed that CD69 deficiency in a mouse tumour model led to increased accumulation of T and NK cells in the tumour compartment, suggesting CD69 may have a negative regulatory role on T cell activity which the authors attributed to a loss of TGF-β signalling, normally initiated by CD69 engagement[228]. Further evidence of the negative regulatory functions of CD69 is that lack of CD69 has also been shown to enhance

inflammation in several mouse models of disease[229-232]. A possible mechanism for negative regulation by CD69 became apparent with the recent discovery of Galectin-1 as a counter receptor for CD69; the interaction of Galectin-1 (expressed by dendritic cells) and CD69 appears to inhibit Th17 polarisation[233]. As Th17 cells contribute to tissue inflammation, their lack of inhibition could account for the increased inflammation observed in the absence of CD69. Additional ligands for CD69 have yet to be described, but recent evidence has made it clear that despite the historical role for CD69 as a marker for activated T cells, CD69 has a negative regulatory effect on T cell functions.

4.1.4 AICD

AICD is a regulatory mechanism by which stimulated T cells undergo apoptosis, and plays a role in maintaining both central tolerance and peripheral tolerance, as well as controlling lymphocyte numbers in response to a pathogen. In peripheral T cells, AICD is largely dependent on Fas/Fas ligand interactions. Binding of Fas by FasL on a neighbouring cell (or from the same cell[234]) triggers recruitment of the Fas-associated death domain, which leads to activation of caspase-8 and the caspase cascade[235]. Mice with defects in Fas or FasL suffer from lymphoproliferation and autoimmune disorders, as do humans with defects in Fas signalling machinery, underlining the importance of these interactions to immune regulation[236-238].

Both Fas and FasL are expressed at low or undetectable levels on resting T cells, but are upregulated upon stimulation[239], meaning activated T cells have a self-limiting mechanism. Norian et al showed that FasL expression in primary mouse cells increased upon prolonged exposure to antigen, up to 72 hours[240], suggesting that AICD becomes a more prevalent mechanism as stimulation time increases. However, it was shown in mouse T cell hybridomas that both Fas and FasL are upregulated within a few hours of stimulation, with peak Fas and FasL expression detected at 2 and 4 hours post-stimulation, respectively; this data suggested that transformed T cells may be more susceptible to AICD than primary cells[234].

Selecting an appropriate readout for any scientific model requires an understanding of the characteristics and limitations of that model. In order to study the effects of PTPN22 KO on T cell signalling using Jurkat cells, I assayed the T cell responses

that are reliably consistent across all Jurkat clones: IL-2 upregulation, CD69 expression, and AICD. These experiments laid the groundwork to understanding how loss of PTPN22 influences T cell signalling.

4.2 Results

4.2.1 Development of pTax stimulation protocol

I initially used the lymphoblast T2 cell line to present pTax to my TCR transduced Jurkat lines, however results were complicated to analyse due to the fact that it was challenging to distinguish between the stimulator and responder cells during analysis by flow cytometry. I therefore developed a method of stimulation with the pTax peptide in the context of HLA-A2 that did not require presentation by another cell line.

DimerX is comprised of two human HLA-A2 molecules fused to mouse IgG (Figure 1a). I followed manufacturer instructions (described in Chapter 2) to load pTax, an HLA-A2-restricted peptide, into the binding groove of DimerX. To test whether DimerX loaded with pTax was able to stimulate Jurkat T cells carrying the Tax TCR, I used a standard plate-coating protocol to bind either anti-CD3 or DimerX+pTax to the bottom of 96-well plates. Cells were cultured in wells containing anti-CD3, DimerX+pTax, or PHA for 24 hours, then analysed by flow cytometry. We observed no significant differences in FSC/SSC profiles from cells stimulated with CD3 or with DimerX+pTax, and CD69 upregulation was similar in all three groups (Figure 1b).

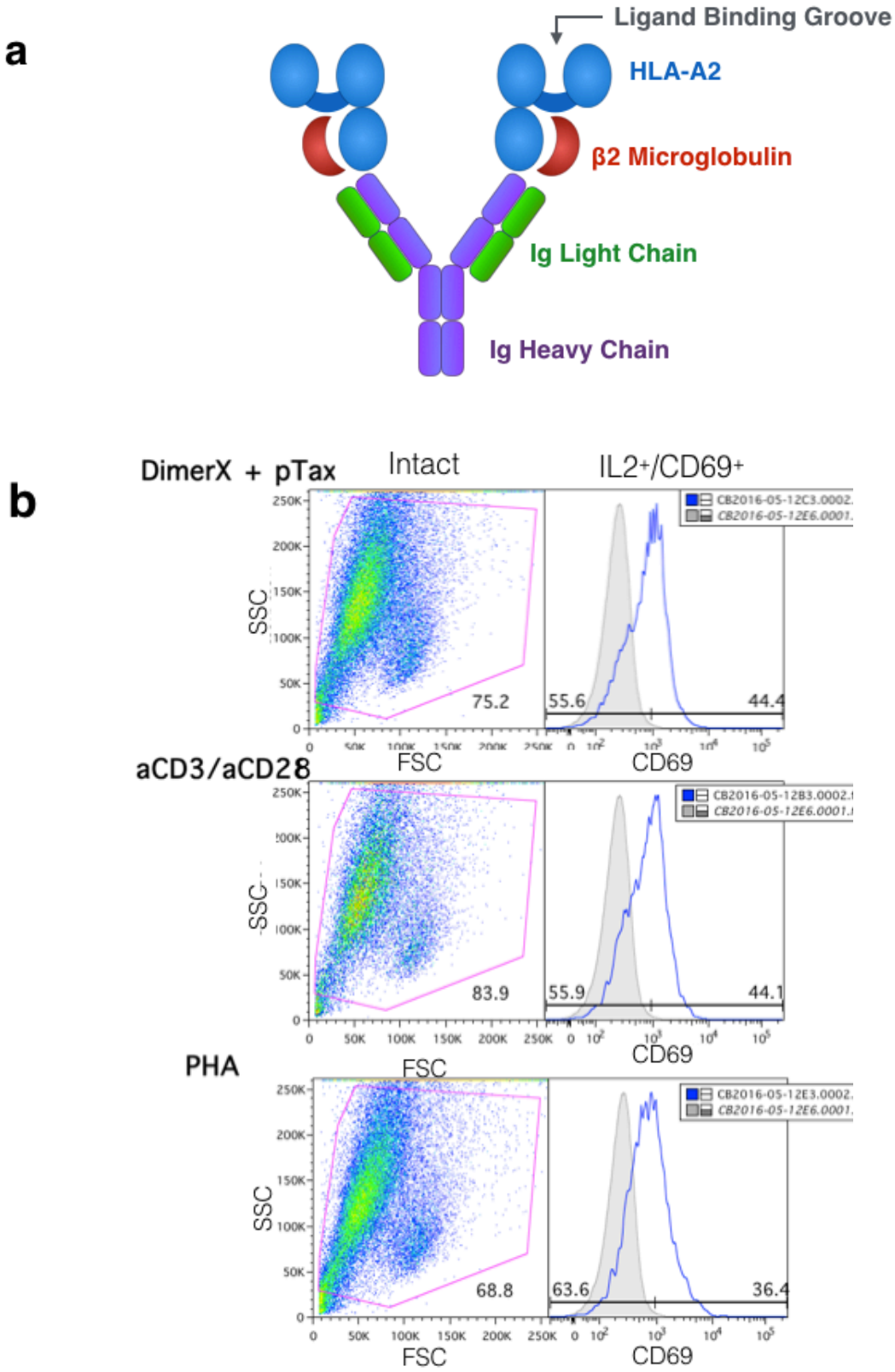

Figure 1. Stimulatory pTax peptide can be presented by DimerX. (**a**) Structure of DimerX, fusion molecule of mouse IgG and human HLA-A2 (**b**) Jurkat cells were analysed by flow cytometry for CD69 upregulation after 24-hour stimulation with DimerX loaded with pTax, with anti-CD3/anti-CD28, or with PHA. Grey fill: unstimulated cells, blue line: stimulated cells. Numbers indicate population frequency within the gates shown.

Based on these findings I concluded that the stimulus provided by DimerX+pTax was appropriate to analyse T cell responses in the Tax TCR-transduced Jurkat lines.

4.2.2 Increased IL-2 expression in PTPN22 KO clones

Studies from our lab comparing the responses of primary mouse CD8 T cells from WT and PTPN22 KO mice showed that there was increased IL-2 expression in cells lacking PTPN22, and was even found to contribute to the increased resistance of these cells to downregulation driven by TGF-β, an important factor in the tumour microenvironment[201]. I was therefore interested in testing whether IL-2 expression would be increased in human T cells lacking PTPN22.

I stimulated cells in a 96-well plate coated with a titration of DimerX+pTax for 6 hours in the presence of anti-CD28, or treated for the same time with PHA+PMA. Each clone was stimulated in an individual well, with six KO and six WT clones represented. Cells were treated with Brefeldin A within 10 minutes of plating to prevent secretion of IL-2 during the experiment. After the stimulation period, cells were stained with antibodies for surface CD3 and for intracellular CD69 and IL-2. Intracellular CD69 was measured intracellularly because Brefeldin A was also shown to completely inhibit export of CD69 to the surface[241]. IL-2 production was detectable by flow cytometry in a discrete subpopulation of cells, that was only seen in the presence of stimulus (Figure 2). This population was also positive for CD69, confirming that they were cells that had been activated in response to pTax stimulation.

In both WT and KO lines, a higher concentration of DimerX+pTax correlated with increased IL-2 production, however a significantly higher percentage of cells were positive for IL-2 in the PTPN22 KO clones compared to the WT lines in all stimulation conditions (Figure 3a). The MFI of the IL-2 positive populations allowed us to focus on the cells that have been activated to express IL-2, and compare the amount of IL-2 produced by these cells. We found that IL-2 positive PTPN22 KO cells expressed significantly more IL-2 than IL-2 positive PTPN22 WT cells (Figure 3b). Therefore, not only did a greater proportion of PTPN22 KO cells become

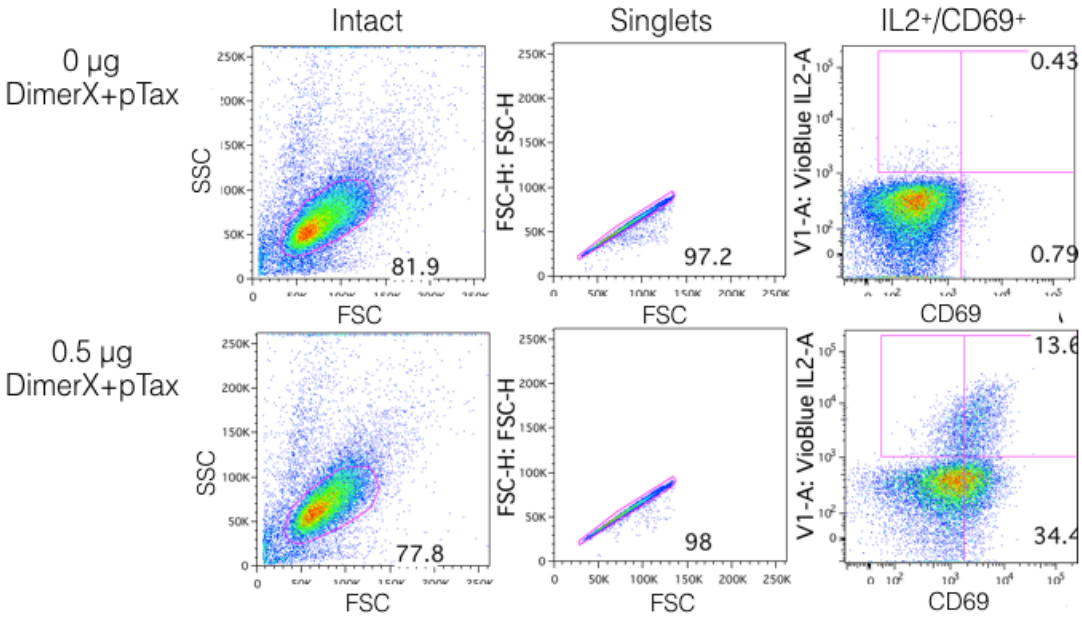

Figure 2. Gating strategy for intracellular staining by flow cytometry. Unstimulated Jurkat cells and Jurkat cells stimulated for 6 hours with DimerX+pTax were stained intracellularly for IL2 and CD69 expression and examined by flow cytometry. Numbers indicate population frequency within a gate.

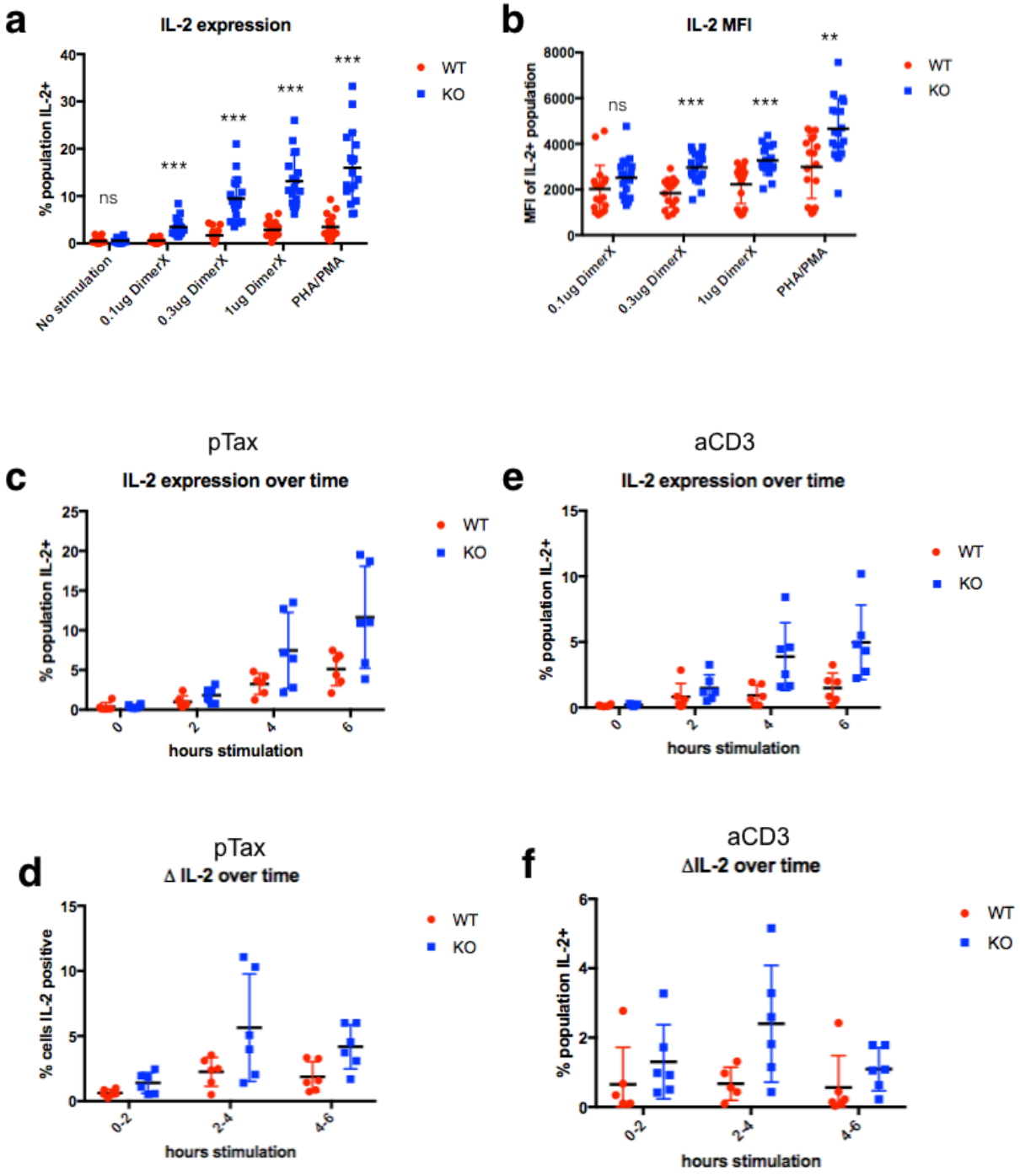

Figure 3. PTPN22 KO Jurkat clones express more IL-2 upon stimulation. IL-2 expression of Jurkat clones was determined by intracellular staining after 6 hours of stimulation in the presence of Brefeldin A with different concentrations of DimerX+pTax and anti-CD28, or with PHA/PMA. (**a**) Percentage of IL-2 positive cells among the population of intact cells. (**b**) MFI of IL-2 positive cells. Statistical significance for each condition was determined by unpaired T test and Holm-Sidak multiple comparisons correction. A p-value less than 0.05 was considered significant. ns = not significant, *p < 0.05, **p < 0.01, ***p < 0.001 (**c-f**) IL-2 expression was determined after 0-6 hours of stimulation with (**c,d**) 1 µg DimerX+pTax or (**e,f**) 1 µg aCD3. Anti-CD28 was always included in stimulation cultures. (**d**) and (**f**) show the change in IL-2 expression between time points.

activated to produce IL-2, on average these cells also produced more IL-2 than activated PTPN22 WT cells. These findings were repeated in three separate experiments with consistent results, each symbol on the graph represents a single well in an experiment.

To further investigate the timing of the increase in IL-2 expression PTPN22 KO cells, I conducted a time course using the highest concentration of DimerX+pTax stimulation (Figure 3c). I observed that for both PTPN22 WT and KO cells, IL-2 expression peaked between 2-4 hours, and the greatest increase in the percentage of IL-2 positive cells in PTPN22 KO populations over WT populations was found at this time period. There was also a slight increase in IL-2 positive cells in PTPN22 KO cells over WT cells prior to two hours, and between 4-6 hours (Figure 3d).

Interestingly, the same time course conducted using anti-CD3 showed slightly different timing in the maximum response from DimerX+pTax (Figure 3e). While the magnitude of IL-2 production in response to anti-CD3 was less across all cell lines compared to DimerX+pTax stimulation, the peak was still between 2-4 hours (Figure 3f). However, I observed that CD3-stimulated cells began producing IL-2 sooner, with more cells producing IL-2 within two hours of CD3 stimulation than in the same time period following DimerX+pTax stimulation. CD3-stimulated cells also downregulated IL-2 expression sooner: by 4-6 hours following CD3 stimulation, the percentage of IL-2 positive cells had fallen to be similar to 1-2 hours following CD3 stimulation, while cells stimulated for 4-6 hours with DimerX+pTax still had more IL-2 positive cells relative to the 1-2 hour time point. In summary, compared to CD3 stimulation, cells stimulated with DimerX produced IL-2 later but sustained production for longer, and more total cells produced IL-2 by 6 hours of stimulation. This pattern suggests that the timing of receptor stimulation like anti-CD3 is considerably different from that of cognate antigen stimulation, which is important when considering the context of many studies of T cell signalling.

4.2.3 Increased CD69 expression in PTPN22 KO clones

The readout of CD69 in the experiments described above revealed a significant effect of PTPN22 on CD69 expression. CD69 is an early indicator of activation, typically upregulated in the first four hours of stimulation. In contrast to IL-2, no

distinct CD69 positive population was formed; instead a shift in the population as a whole was observed (Figure 2). Compared to IL-2, more cells in both groups upregulated CD69 in response to all tested concentrations of DimerX+pTax, suggesting a lower threshold of activation was required for CD69 expression compared to IL-2. We observed a significant increase in the percentage of CD69 positive cells in PTPN22 KO clones compared to WT clones in all stimulation conditions (Figure 4a). Notably, there was also a slight increase in CD69 expression in resting PTPN22 KO cells, suggesting a small population of PTPN22 KO cells slightly upregulate CD69 in the absence of stimulation. We also observed an increase in the MFI of CD69 positive cells in PTPN22 KO cells, indicating that a lack of PTPN22 leads not only to more cells being activated to express CD69, but also to elevated CD69 expression on activated cells (Figure 4b).

We also looked at CD69 over a 6-hour time course. Similarly to IL-2 expression, the timing of peak CD69 expression did not vary much between PTPN22 WT and KO cells stimulated with DimerX+pTax (Figure 4c). Both upregulated the most CD69 between 2-4 hours, with similar low-level expression from 0-2 and 4-6 hours (Figure 4d). The 2-4 hour period was also the time period when the increase in CD69 expression in KO cells compared to WT cells was the greatest, with only a small increase at 0-2 hours and with KO cells having slightly fewer CD69 positive cells than WT cells after 4 hours. These data show that WT and KO cells follow a similar pattern of CD69 timing, but that KO cells produce more CD69 at the peak of expression.

Monitoring CD69 expression every 2 hours for 6 hours showed a markedly different pattern of CD69 upregulation between anti-CD3 and DimerX+pTax stimulation (Figure 4e). In contrast to more cells expressing CD69 between 2-4 hours than at 0-2 hours, as observed with DimerX+pTax stimulation, CD3 stimulated cells upregulated CD69 expression similarly in the 0-2 hours and 2-4 hours time points (Figure 4f). By 4-6 hours, the number of CD3-stimulated cells newly expressing CD69 had dropped below to nearly zero, while about 5% of DimerX+pTax-stimulated cells were still upregulating CD69. Again, these findings suggest a

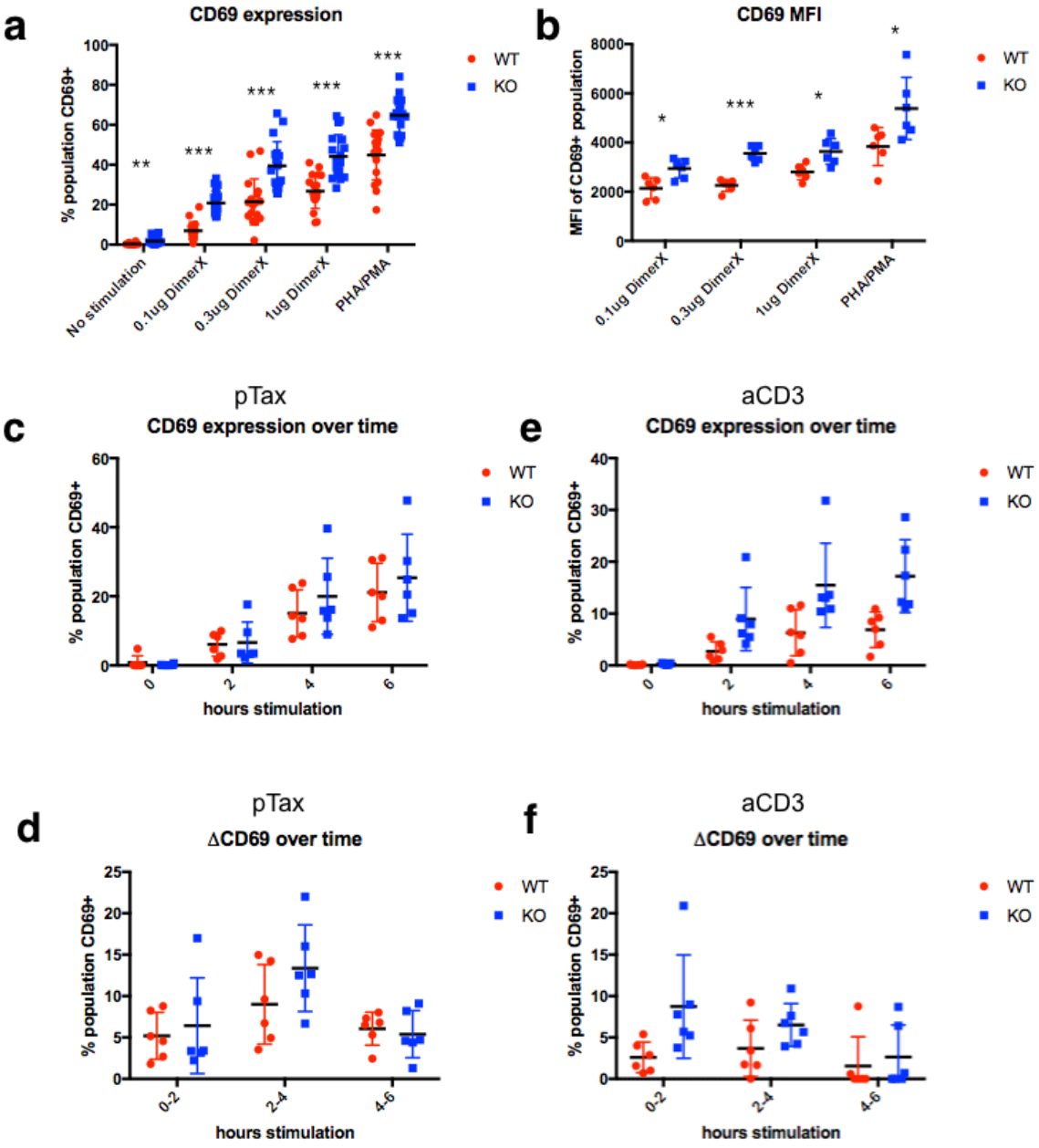

Figure 4. PTPN22 KO Jurkat clones express more CD69 upon stimulation. CD69 expression of Jurkat clones was determined by intracellular staining after 6 hours of stimulation in the presence of Brefeldin A with different concentrations of DimerX+pTax and anti-CD28, or with PHA+PMA. (**a**) Percentage of CD69 positive cells among population of intact cells. (**b**) MFI of CD69 positive cells. Data is representative of three experiments. Statistical significance for each condition was determined by unpaired T test and Holm-Sidak multiple comparisons correction. A p-value less than 0.05 was considered significant. ns = not significant, *p < 0.05, **p < 0.01, ***p < 0.001 (**c-f**) CD69 expression was determined after 0-6 hours of stimulation with (**c,d**) 1 µg DimerX+pTax or (**e,f**) 1 µg anti-CD3. Anti-CD28 was always included in stimulation cultures. (**d**) and (**f**) show the change in CD69 expression between time points.

different mechanism of response timing between CD3 and cognate antigen stimulation, in which the response to cognate antigen produces is delayed but sustained compared to CD3 stimulation.

While few new cells were upregulating CD69 after 6 hours, the cells that expressed CD69 maintained their expression through 6 hours. I also looked at CD69 after 24 hours to determine whether the relatively elevated CD69 levels in PTPN22 KO cells would be lost over time. Despite CD69 acting as an early activation marker, it remained easily detectable on the surface of cells after 24 hours of stimulation, and its expression was highly correlated with cells undergoing AICD, which were reduced in size (FSC) but still live/dead negative (Figure 5a and Figure 6a, blue population). Therefore dying cells could not be excluded from analysis, as responding cells were apoptotic after 24 hours, likely due to the strength of stimulation induced by plate-bound antigen. PTPN22 KO cells still had higher levels of CD69 expression after 24 hours of stimulation with the two lower concentrations of DimerX+pTax, as well as no stimulation (Figure 5b). However, 24 hours of stimulation with the higher concentrations of DimerX+pTax resulted in no significant differences, although PTPN22 KO cells still tended to have higher levels of CD69 expression. These findings indicate that loss of PTPN22 on CD69 observed in the hours immediately following activation continue to influence the cell by 24 hours, but that stronger stimulation may mask these effects.

4.2.4 Increased AICD after weak stimulation in PTPN22 KO clones

I observed massive cell death after stimulating Jurkat cells for 24 hours with anti-CD3 or DimerX+pTax. AICD is a well-established dose-dependent effect of stimulation in Jurkat cells[242], and can be considered a readout of activation. I used a live/dead marker to identify dead cells by flow cytometry (Figure 5a). Stimulated cells showed three populations when stained with the Live/Dead marker: a “live” population of larger cells that were live/dead negative, an “apoptotic” population of smaller cells that were live/dead negative, and a “dead” population of smaller cells that were live/dead positive. Live/Dead negative cells were included in the analysis of CD69 staining because the apoptotic population comprised the bulk of CD69 positive cells (Figure 6a). Dead cells, which were live/dead positive and susceptible to non-specific binding by fluorescent antibody, were excluded from CD69 analysis.

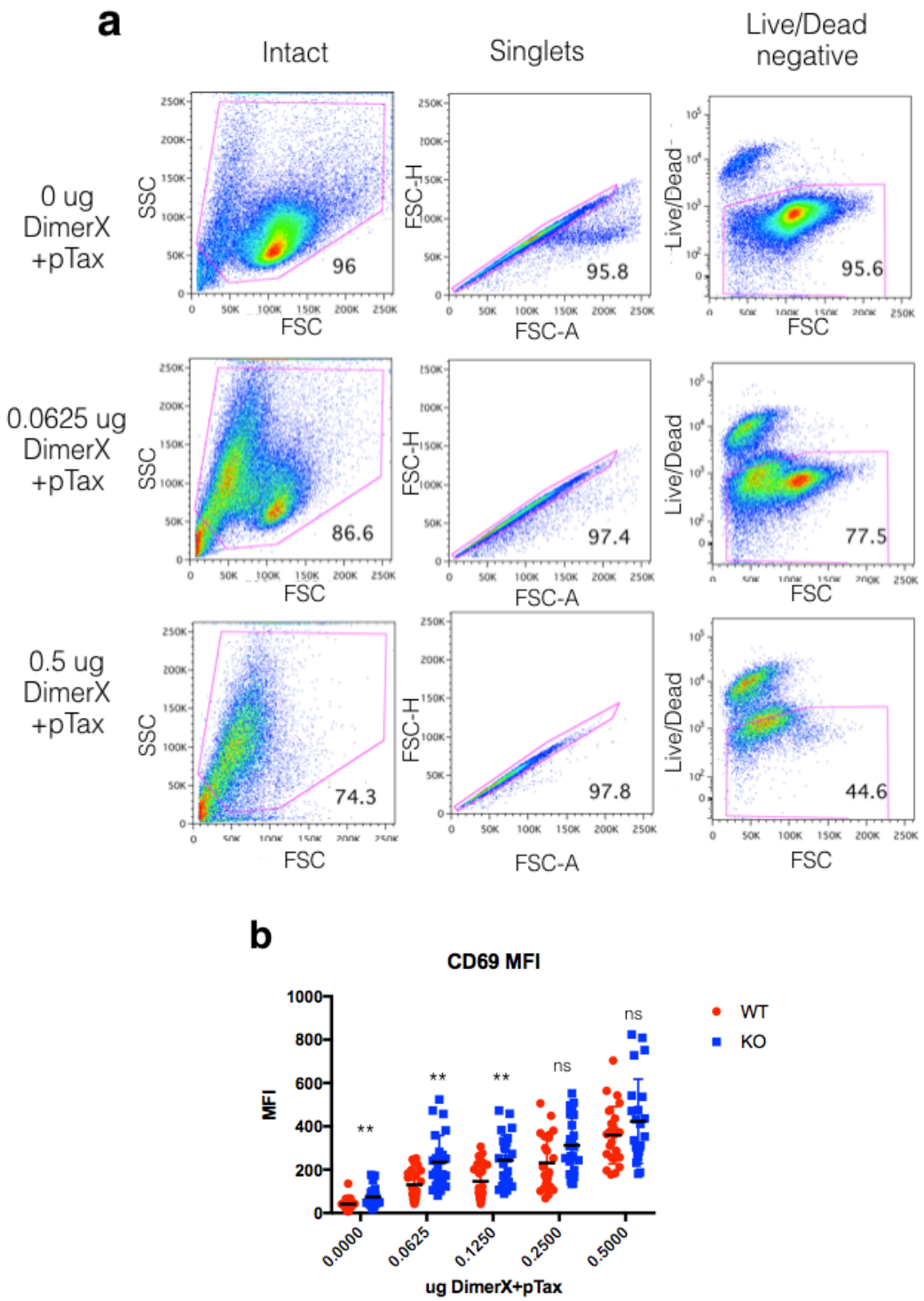

Figure 5. PTPN22 KO Jurkat clones express more CD69 after 24 hours of weak stimulation. (**a**) Gating strategy for Live/Dead staining after 24 hours of stimulation with DimerX+pTax. Jurkat cells were analysed by flow cytometry after surface staining and Live/Dead staining. Live/Dead negative cells were analysed for surface markers. Numbers indicate population frequency within a gate. (**b**) MFI of CD69 expression of Live/Dead population in PTPN22 WT and KO Jurkat cells after 24 hours of stimulation with DimerX+pTax. Statistical significance for each condition was determined by unpaired T test and Holm-Sidak multiple comparisons correction. A p-value less than 0.05 was considered significant. ns = not significant, *p < 0.05, **p < 0.01, ***p < 0.001

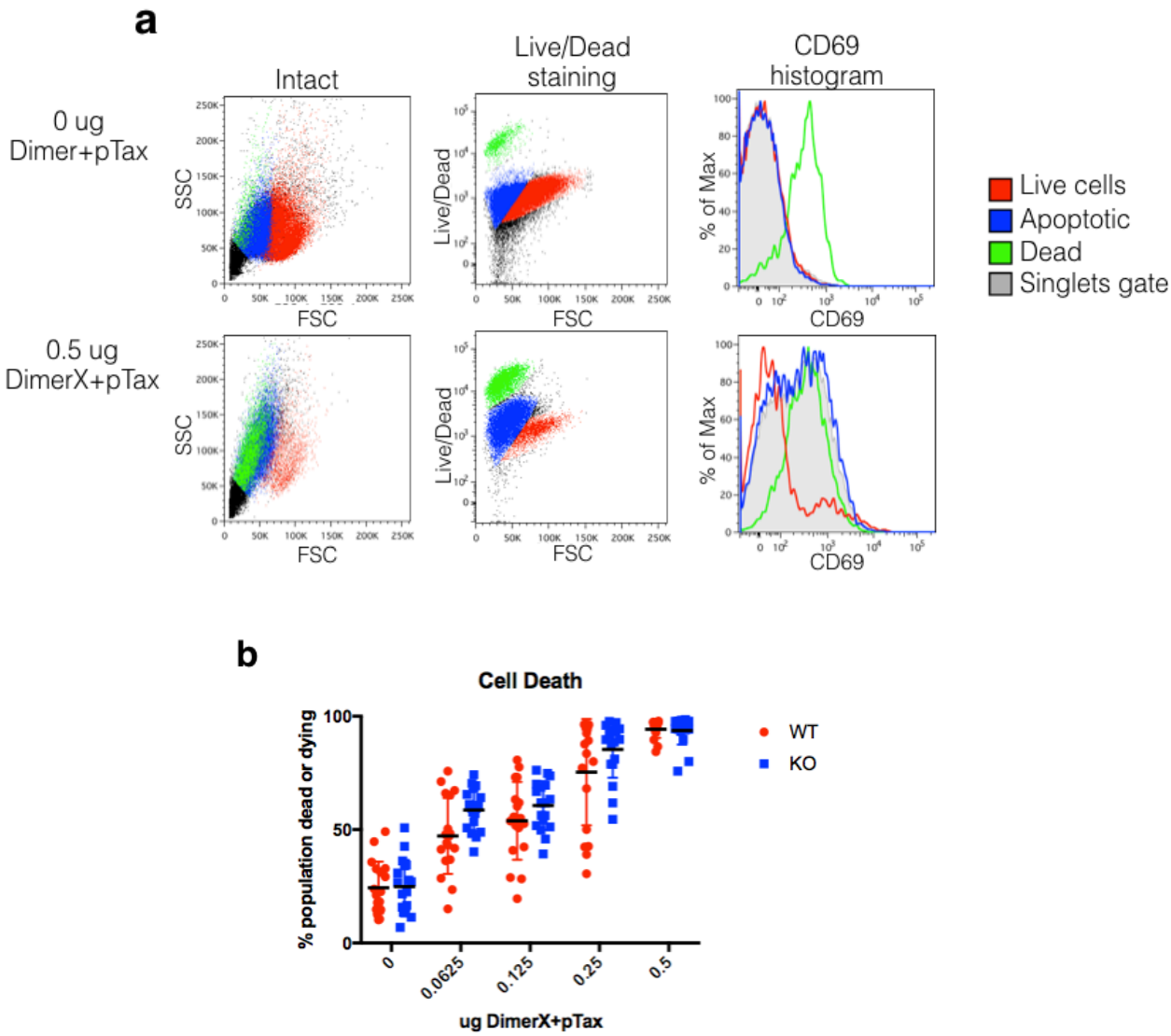

Figure 6. PTPN22 KO Jurkat clones experience more AICD after 24 hours of weak stimulation. (**a**) Jurkat cells were stimulated with DimerX+pTax for 24 hours, stained with aCD69 and a Live/Dead marker, and analysed by flow cytometry. Grey fill: all intact events, gated on singlets; red line: large, Live/Dead negative cells; blue line: small, Live/Dead negative cells; green line: Live/Dead positive cells. (**b**) Jurkat cell death following activation for 24 hours with DimerX+pTax was measured by the percentage of cells outside of the "Live" gate (panel a, red population). No significant differences between PTPN22 WT and KO clones were found. Statistical significance for each condition was determined by unpaired T test and Holm-Sidak multiple comparisons correction. A p-value less than 0.05 was considered significant.

PTPN22 KO Jurkat cells tended to have greater amounts of cell death than WT cells when stimulated for 24 hours with low concentrations of peptide, but this difference was not significant in any stimulation condition (Figure 6b). Dead cells were identified as cells outside the “live cell” gate, defined in red based on FSC and Live/Dead stain in Figure 6a, and therefore included smaller apoptotic cells as well as dead cells.

I used Annexin V/propidium iodide (PI) staining to more closely analyse the stages of apoptosis in 24-hour stimulated Jurkat clones. The Annexin V/PI staining protocol allows for differentiation of live cells from early apoptotic, late apoptotic, and dead cells (Figure 7). Annexin V/PI staining showed that PTPN22 WT cells had a greater proportion of live cells (Figure 8), and that PTPN22 KO cells tended to have a greater proportion of cells in early and late apoptosis, as well as dead cells. Notably, the strongest stimulation condition showed PTPN22 WT and KO clones to have the same proportion of live cells, suggesting that the negative regulatory role of PTPN22 has less of an effect under strong stimulation conditions, as has been shown in mice[200]. However, while the differences in number of live cells between stimulated PTPN22 WT and KO was significant (Figure 8c), the differences in the other groups were not. This is likely due to the fact that the non-live cells are distributed evenly through the other three groups, thus reducing the magnitude of the difference between PTPN22 WT and KO cells in each group. The trend for more cells in early apoptosis in PTPN22 KO clones was strongest ($p = 0.06$) (Figure 8d). In both PTPN22 WT and KO clones, the groups most strongly affected by stimulation were late apoptosis (increased as stimulation strength increased) and live cells (reduced as stimulation strength increased) (Figure 8b,c). Dead cells and early apoptotic cells were only slightly increased by stronger stimulation relative to the other groups (Figure 8a,d). Thus, stimulated Jurkat cells move quickly through the early apoptosis stage into the late apoptosis stage, but tend not to advance to dead cells from late apoptosis by 24 hours of stimulation. PTPN22 KO cells initiate the apoptotic process more readily than PTPN22 WT cells, resulting in slightly more cells in all stages of apoptosis.

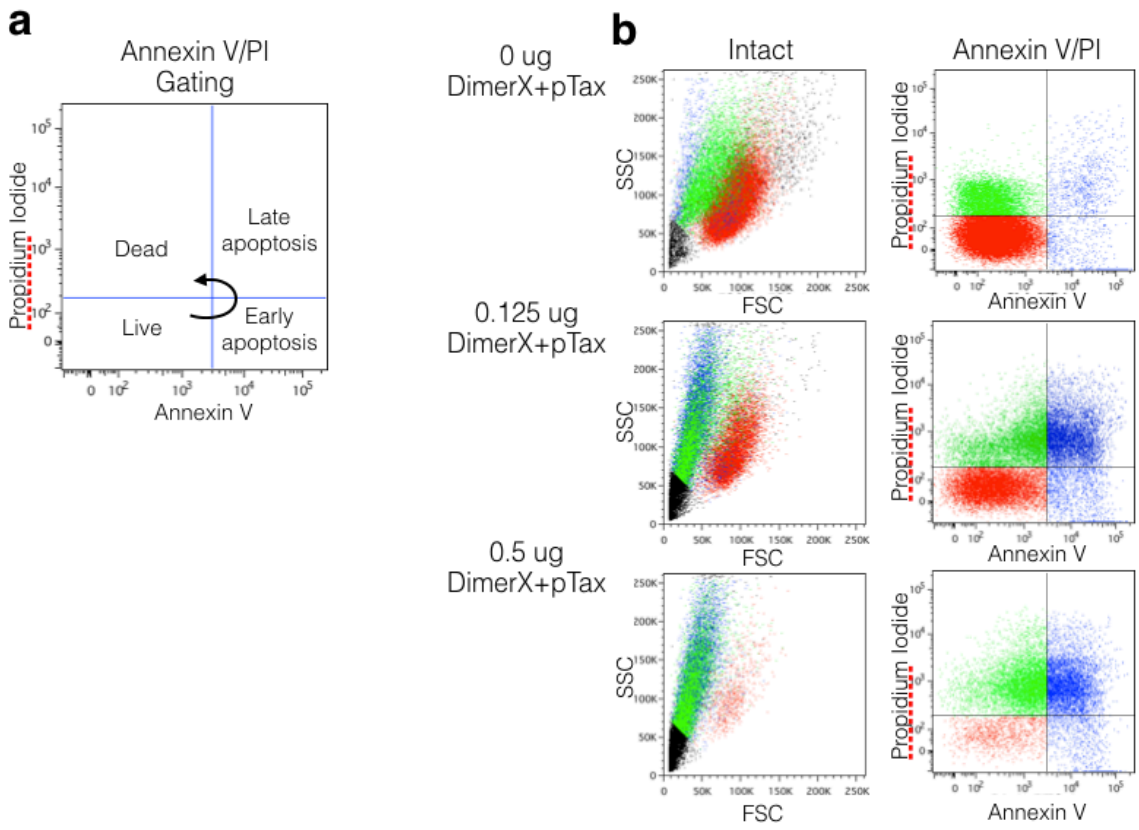

Figure 7. Gating strategy for Annexin V/Priopidium Iodide staining. (**a**) Annexin V/Propidium Iodide staining gating to differentiate between live cells, early apoptosis, late apoptosis, and dead cells. (**b**) Examples of dot plots of Jurkat cells stained with Annexin V and Propidium Iodide after 24 hours of stimulation with DimerX+pTax, and analysed by flow cytometry. All intact (colored) events were included in the analysis.

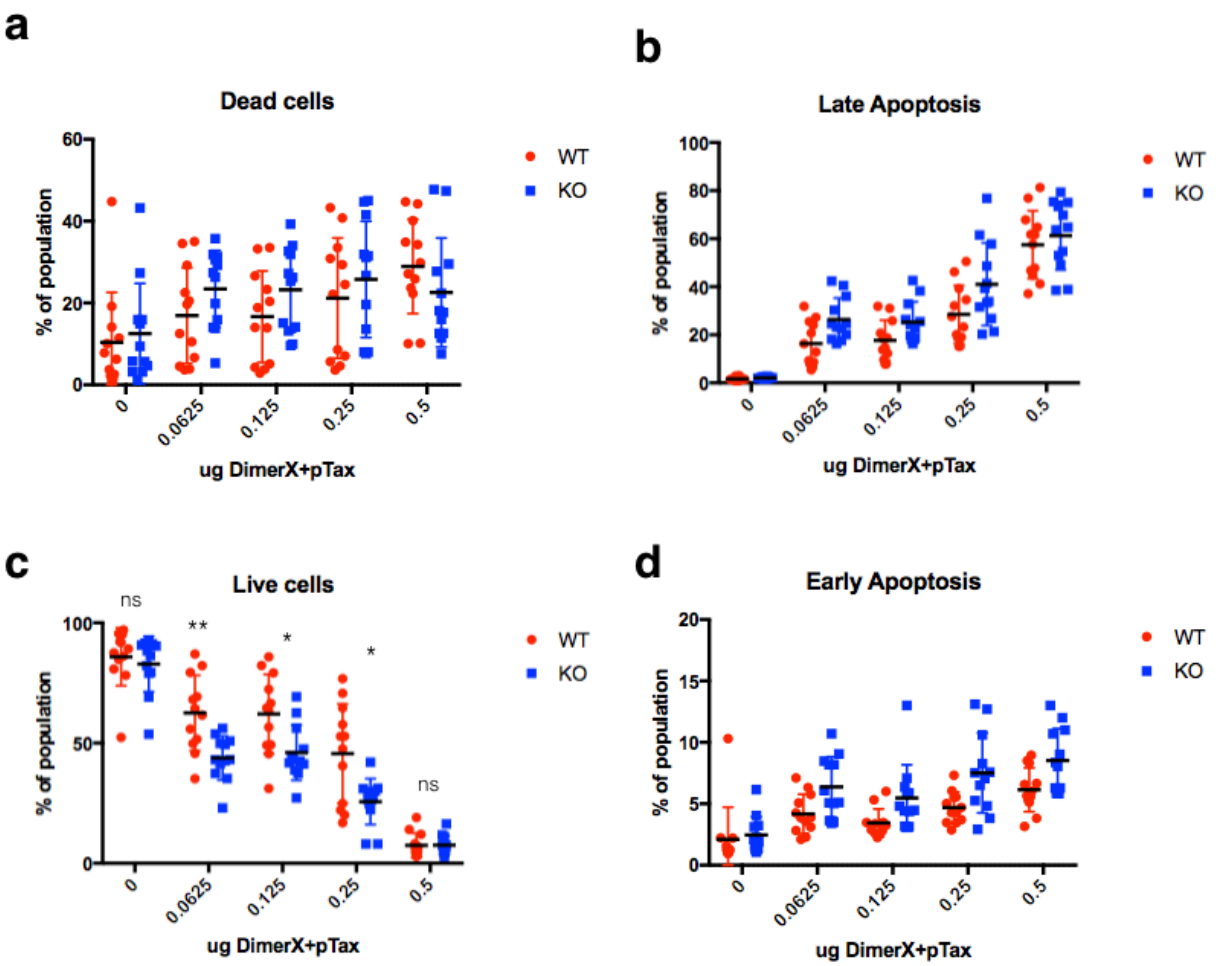

Figure 8. PTPN22 KO Jurkat clones have fewer live cells after 24 hours of weak stimulation. Annexin V/Propidium Iodide staining was used to determine the states of apoptosis in PTPN22 WT and KO Jurkat cells stimulated with DimerX+pTax for 24 hours. Cells were designated as (**a**) dead, (**b**) late apoptosis, (**c**) live, or (**d**) early apoptosis. Statistical significance for each condition was determined by unpaired T test and Holm-Sidak multiple comparisons correction. A p-value less than 0.05 was considered significant. ns = not significant, *p < 0.05, **p < 0.01, ***p < 0.001

4.3 Discussion

The purpose of the work presented in this chapter was to investigate the impact of loss of PTPN22 on human T cell responses to antigen. We found that more PTPN22 KO clones became activated in response to stimulus, and that the activated PTPN22 KO cells produced more IL-2 and CD69 than activated PTPN22 WT cells. In addition, we found that certain effects of loss of PTPN22 on 24-hour stimulations were strongest when cells were stimulated with reduced concentration of stimulus, and that differences PTPN22 WT and KO cells could be reduced with high concentrations of stimulus. These results show that, like PTPN22 KO mouse T cells, PTPN22 KO human T cells are more responsive to weak antigen.

Notably, plate-bound antigen is distinct from the way antigen is likely to be encountered by presentation by APCs under physiological conditions. Although it is a common method of *in vitro* stimulation, some artificialities of plate-bound stimulation include a broad surface of antigen interaction, as opposed to the tight synapse formed upon interaction with an APC, greatly altering the morphology of the T cell as it binds to antigen and the plasma-membrane proximal signalling environment. Plate-bound antigens are therefore relatively potent, and can lead to excessive stimulation, which may account for the high rates of cell death observed after 24 hours in a cell type already susceptible to AICD[234]

When stimulating equivalent numbers of cells with a titration of antigen, a significantly greater proportion of PTPN22 KO clones upregulated IL-2 (Figure 3a) and CD69 (Figure 4a), and induced apoptosis (Figure 8c). Given that the entire population of cells was exposed to the same peptide stimulus, the decision in an individual cell to commit to activation or not was likely due to degree of exposure to the peptide, or how many DimerX+pTax molecules the cell came into contact with. A number of cells were settled onto the bottom of a cell culture plate coated with DimerX+pTax such that a single layer of cells could not cover the entire bottom of the well, so that amount of stimulus, not cell number, limited interactions. However, cells would not necessarily distribute evenly across the bottom, and therefore it was likely that certain cells within the population would have reduced access to stimulus,

creating heterogeneity across the population. Additional heterogeneity in responses may be due to the fact that Jurkat cells cycle continuously, as it has been suggested that cell cycle phase could influence susceptibility to AICD; however this hypothesis remains controversial[243,244].

While cell distribution and cell cycle phase possibly introduced differences to how individual cells within a population experienced stimulation, they are unlikely to account for the differences observed between PTPN22 WT and KO Jurkat cell responses. All clones were counted using a CASY counter and were seeded simultaneously on the same plate, meaning any effects that would influence the ability of the cells to access stimulus would be shared by all clones. Furthermore, I observed no changes to cell growth upon loss of PTPN22 (Chapter 3, Figure 12b), meaning it is unlikely that the greater proportion of responsive PTPN22 KO cells was due to the cells being in significantly different cell cycle phases from PTPN22 WT cells.

Given that the observation that more PTPN22 KO cells respond to stimulus than WT cells was reproducible across biological and technical replicates, as well as different stimulation conditions, the result most likely attributable to the effect of PTPN22 on regulating the decision of the T cell to respond to stimulus. Low concentrations of peptide molecules was insufficient stimulation for PTPN22 WT cells to express effector molecules, whereas PTPN22 KO cells exposed to the same interactions experienced a stronger signalling response, resulting in increased effector molecule expression. The stimulation threshold required for expression of IL-2 or CD69 varied for these two molecules; the greatest proportion of IL-2 expressing cells achieved was 30% (in the most responsive cell lines stimulated with PHA/PMA stimulation), whereas CD69 expression was recorded in up to 80% of cells in the same condition. Therefore, cells that were stimulated sufficiently to express CD69 did not necessarily reach the greater stimulation threshold needed to express IL-2[245]. For both IL-2 and CD69, as well as AICD, lack of PTPN22 reduced the stimulation threshold required by the cell, enabling more cells to be activated by the same amount of stimulus. The role of increasing the stimulation threshold required for effector function helps explain the role of PTPN22 in regulating T cell responses to self-antigen and preventing autoimmune disease.

In addition to a greater number of responsive cells, I found that PTPN22 KO cells expressed more IL-2 and CD69 than responsive PTPN22 WT cells (Figure 3b, 4b). PTPN22 therefore not only plays a role in the decision of the cell to respond, but also in the magnitude of the response.

The effect of lack of PTPN22 on the response of the cell was likely due to enhancement of the TCR signalling pathways initiated by pTax ligation; TCR pathways are dependent on the early Lck, Fyn, and Zap-70 phosphorylation events known to be regulated by PTPN22, and result in activation of transcription factors to upregulate effector molecules. The specific TCR pathways affected by loss of PTPN22 are investigated in Chapter 5. PTPN22 is shown here to play a role in downregulating the magnitude of T cell responses to a given antigen; dysregulation of this role could therefore contribute to the development of autoimmune responses to harmless self-antigen.

PTPN22 was shown to affect murine OT-1 T cell responses to weak peptide, but not strong peptide[200], but the effects of PTPN22 loss on human T cell responses to peptide have not previously been studied, as stimulating human cell lines or primary cells is typically done using antibodies to CD3 and CD28 and, as shown in Figures 3 and 4c-f, T cell responses to CD3 are not necessarily comparable to responses to peptide. The effects of peptide affinity and concentration on the role of PTPN22 in human T cells is therefore not yet clear. I observed that the difference between PTPN22 WT and KO cells at higher stimulation concentrations was lower after 24 hours of stimulation compared to 6 hours (Figures 4b and 5b). In the case of cell survival, it is likely that PTPN22 KO and WT cells behaved similarly after 24 hours of strong stimulation due to very few living cells remaining in either population (Figure 8c), in essence reaching a plateau for the readout. It is possible that a similar explanation may apply to the readout of CD69 expression (Figure 5b): as cells approach their maximum level of CD69 upregulation, the differences between populations become indistinguishable. These interpretations suggest that the negative regulatory activity of PTPN22 is simply overwhelmed by increasing signal strength, so that responses to strong stimulation are no longer susceptible to regulation by PTPN22. Alternatively, it is possible that PTPN22 activity itself is

negatively regulated in the context of strong stimulation, perhaps by interactions with other proteins that affect its localisation or phosphatase activity. Regardless of the mechanism, my data shows that PTPN22 has a more critical effect on regulating outcome of cell responses to weaker stimulus, and that absence of PTPN22 becomes less impactful as stimulatory signal increases.

My work in PTPN22 KO human T cells generally agrees with published data regarding mouse T cells lacking PTPN22. I observed an increase in IL-2 expression in PTPN22 KO cells, which was previously reported in T cells PTPN22 KO mice[165,201]. My data also reports increased CD69 expression in stimulated PTPN22 KO cells, similarly reported in both T and B cells derived from mice lacking PTPN22[164,200]. Taken together with previous studies in mouse, my results suggest that the effects of loss of PTPN22 are similar in human and mouse T cells.

The results I generated using PTPN22 KO human T cells provide a point of comparison for understanding the conflicting reports describing the effects of the PTPN22 R620W polymorphism in humans. I found that loss of PTPN22 increased CD69 expression, however Fiorillo et al's work on Jurkat cells transfected with R620 or W620 vector and stimulated with anti-CD3 showed minimal differences in the percentage of CD69-positive cells[151]. Whether the lack of effect of PTPN22 on CD69 was due to the overexpression of PTPN22, the confounding presence of both WT and variant proteins, or because the polymorphism indeed does not influence the CD69 pathway the same manner as the knockout remains to be seen.

I found that PTPN22 KO Jurkat cells had increased expression of IL-2. Vang et al reported a reduction in IL-2 response in human primary cells derived from T1D patients carrying the W620 polymorphism compared to those with R620, as well as a reduction when primary cells were transfected with a vector containing W620 PTPN22 instead of R620 PTPN22[192]. Their conclusion that R620W is a gain-of-function polymorphism is therefore consistent with my data showing that loss of PTPN22 increases IL-2 expression. However, the effect of the polymorphism in autoimmune disease is not as clear. Two groups studying the effects of PTPN22 polymorphism on IL-2 expression in myesthenia gravis (MG) reached divergent conclusions: a group studying thymocytes from MG thymoma reported reduced IL-2

production in patients carrying the W620[246], while another group studying PBMCs derived from MG patients showed an increase in IL-2-producing cells in patients carrying W620 compared to those with R620[247]. These studies are complicated by the fact that they are concerned with different cell types (thymocytes compared to PBMCs) derived from genetically diverse individuals in a disease setting. My work in PTPN22 KO Jurkats circumvents such challenges and clearly shows that loss of PTPN22 upregulates IL-2 production, but further work is needed to confirm the effects of the R620W polymorphism on the IL-2 pathway in human T cells.

The experiments presented in this chapter represent the first attempts to study the impact of loss of PTPN22 on human T cells. I found that PTPN22 KO Jurkat clones displayed enhanced responses to peptide stimulation, as evidenced by increased IL-2 and CD69 expression, and greater susceptibility to AICD than PTPN22 WT Jurkat clones. The following chapter describes subsequent work to investigate the specific T cell signalling pathways affected by PTPN22 KO to elicit increased IL-2 expression in response to stimulation.

5. Effect of PTPN22 on T cell signalling pathways

5.1 Introduction

My findings in Chapter 4 showed that PTPN22 knockout increased Jurkat T cell IL-2 production in response to antigen (Chapter 4, Figure 2). The work presented in this chapter attempts to identify the specific signalling pathways influenced by PTPN22 that lead to increases in IL-2 production.

The promoter region of the IL-2 gene contains binding sites for a number of transcription factors (Figure 1), and is highly conserved between human and mice (greater than 80% homology)[248]. Three well studied transcription factors that drive the IL-2 response are NFAT, AP-1, and NFκB; and cooperation between all three is required for optimal transcription of IL-2 in response to T cell stimulation[248].The activity of NFAT, AP-1, and NFκB is regulated by different pathways of TCR signalling, as well as by binding of additional transcription factors, and by epigenetic remodelling. The multitude of regulators involved in IL-2 transcription ensures that the IL-2 response depends on integration of information from various signalling pathways.

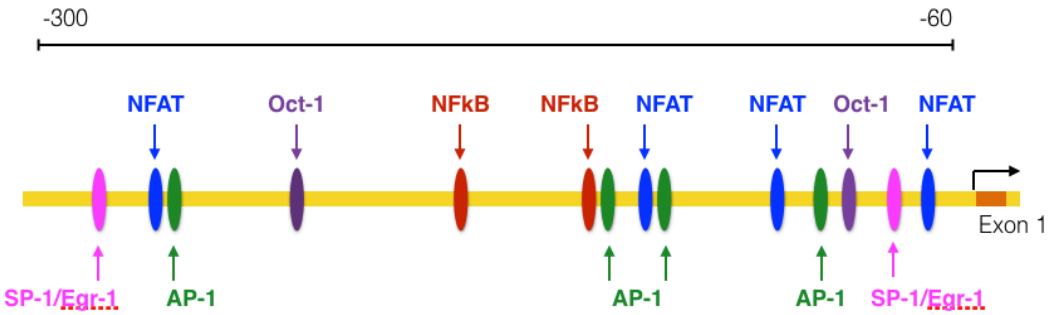

Figure 1. Regulatory elements and associated transcription factors of the human IL-2 promoter. Region shown spans -300 to -60 bp upstream of the *IL2* start codon. Adapted from Kim et al[228].

5.1.1 NFAT

NFAT is constitutively expressed but maintained in the cytoplasm in resting T cells. Calcium flux following TCR ligation leads to calcium ions binding to calmodulin, which activates the phosphatase calcineurin, which in turn dephosphorylates NFAT and exposes its nuclear-localisation signal, enabling NFAT to translocate into the nucleus[249]. NFAT translocation is inhibited by kinases such as GSK3, which is itself negatively regulated by Akt following CD28 costimulation.

Five members of the NFAT protein family have been identified, with NFAT1 and NFAT2 expressed primarily in T cells and corresponding to IL-2 expression[250]. T cells from NFAT1 or NFAT2 knockout mice showed either normal or increased expression of IL-2[251,252], suggesting that there may be compensatory mechanisms between NFAT proteins. Complete impairment of NFAT has a more dramatic effect: mice lacking both NFAT1 and 2 have severely impaired T cell cytokine production[253], a dominant-negative form of NFAT (able to inhibit four NFAT proteins) expressed in Jurkat cells significantly reduced IL-2 production[250], and studies of individuals within human families with deficient NFAT translocation suffered from severe immunodeficiency[254].

NFAT has been reported to interact synergistically with a number of transcriptional binding partners to drive IL-2 transcription, namely AP-1 (described below). Additionally, NFAT has been reported to cooperate with early growth response protein (EGR)1 in activated T cells to enhance IL-2 transcription[255]. The zinc-finger transcription factor EGR1 is upregulated upon TCR stimulation and displaces the constitutively-expressed SP-1 at a binding site on the IL-2 promoter adjacent to an NFAT binding site. In Jurkat cells, EGR1 showed little transactivating activity for IL-2, but its binding greatly enhanced transactivation by NFAT2[255]. The upregulation of IL-2 transcription by EGR1 has also been reported to be enhanced by CD28 costimulation through the activity of NGFI-A binding protein 2[256]. The cooperative effects of these proteins in IL-2 transcription highlight the integration of TCR pathways leading to IL-2 production.

5.1.2 AP-1

AP-1 is a heterodimer comprised of Fos and Jun family proteins and plays a role in

many cell types. Two well-described AP-1 genes, *c-fos* and *c-jun,* act as immediate early genes in T cells, transcription of which is rapidly induced by cell stimulation and activation of the PKC and calcium pathways[257]. Transcription of *c-fos* is also modulated by the MAP kinase ERK2 whereas the JNK family of MAP kinases enhances *c-jun* transcription[258]. The upregulation of transcription of both *c-fos* and *c-jun* promotes dimer formation, thus enhancing AP-1 DNA-binding activity[257].

The activity of c-Fos and c-Jun is also regulated post-transcriptionally through phosphorylation. JNK has been shown to potentiate the transactivation ability of c-Jun[259], while another MAPK called FRK serves a similar role for c-Fos[260]. There is also potential for negative regulation via phosphorylation; Erk was shown to phosphorylate a negative regulatory residue on c-Jun in vitro[261].

AP-1 cooperation with NFAT is critical for IL-2 transcription. Macián et al showed that mutating NFAT1 to prevent it from binding to AP-1 greatly reduced IL-2 promoter activity upon stimulation of Jurkat cells[262]. Of the four NFAT binding sites in the murine IL-2 promoter, at least two are composite NFAT:AP-1 sites, with binding by both NFAT and AP-1 improving stability of the interaction[263]. Cooperation between NFAT and AP-1 molecules integrates signalling through two main pathways of TCR signalling, calcium and MAPK signalling, to induce IL-2 gene transcription.

Oct-1 and Oct-2 are also reported to cooperate with AP-1 to enhance IL-2 transcription[264]. Oct-1 is constitutively active transcription factor, while Oct-2 is upregulated upon T cell stimulation, and shows greater transactivator activity for the IL-2 promoter than Oct-1[265]. However, Oct-2 has been reported to be absent in Jurkat cells, so it is not critical for transcription of IL-2[265].

5.1.3 NFκB

NFκB is present in an inactive form in the cytoplasm of resting cells while bound to an inhibitor IκB. Release of NFκB from IκB is mediated by IκB kinase complex, which phosphorylates IκB, resulting in ubiquitination of IκB and release of NFκB to enter the nucleus. Activation of the IκB kinase complex depends on the CBM complex, assembly of which is induced by PKCθ[266].

It has been shown that mutations to the NFκB binding sites in the IL-2 promoter have a less dramatic effect compared to those of other sites, but the inducible binding of NFκB to the IL-2 promoter in activated T cells indicates that it still has a role in IL-2 transcription[265]. The NFκB family contains five members: NFκB1, NFκB2, RelA, RelB, and c-Rel. The precise roles of each of these proteins are still being described. Binding different NFκB proteins to the IL-2 promoter may be time-dependent, as RelA was found to be the major component one hour after stimulation but was replaced by c-Rel by 6-hours following stimulation[267]. NFκB1 knockout mice were demonstrated to have elevated T cell IL-2 production, which would suggest that NFκB1 is a negative regulator of IL-2 signalling[268]. RelA knockout mice did not exhibit any change in T cell IL-2 levels[269], indicating that RelA is not critical for IL-2 expression, possibly due to redundancy with other NFκB members. Loss of RelB, normally constitutively expressed in the nucleus, also did not impair IL-2 transcription[270]. c-Rel knockout mice, however, did show deficiencies in IL-2 expression[271].

5.1.4 Epigenetics

In addition to the presence or absence of transcription factors, epigenetic regulation of the IL-2 gene was also shown to be necessary for IL-2 transcription in mouse and human T cells[272,273]. Attema et al. showed that the IL-2 promoter in resting Jurkat cells was assembled into a nucleosome that prevented binding of AP-1 and NFAT, but that activation of the cells caused the nucleosome to be remodelled[274]. The same group later showed this process to be dependent on c-Rel[269]. The IL-2 gene promoter was found to contain 15 CpG sites in mouse cells, all of which were methylated in both naive T cells and non-T cells. Upon stimulation of the T cells, CpG sites proximal to the IL-2 start codon were demethylated, which corresponded with IL-2 transcription. The state of demethylation was preserved after nine days, and blocking demethylation of the CpG sites prevented activity of the promoter in activated T cells[272]. Murayama et al identified a specific CpG site in the promoter-enhancer region of the human IL-2 gene which was demethylated upon T cell stimulation. Jurkat cells were shown to have reduced methylation of this site (20% of cells) compared to resting human CD4 cells (80% of cells). Methylation of the site in Jurkats was not changed by stimulation, however in human CD4 cells methylation of

the site was reduced to only 15% of cells. A transient reporter assay showed that methylation of the site reduced IL-2 promoter activity by 95%. Taken together, these studies demonstrate that epigenetics play an important role in control of IL-2 transcription, possibly by regulating the ability of activated transcription factors to access the IL-2 promoter.

The multitude of transcription factors that impact IL-2 transcription reflect the need to integrate the various TCR signalling pathways into an appropriate response. PTPN22 dephosphorylates targets involved in early TCR signalling events (Figure 2), so its effect on IL-2 signalling could be propogated via one or more of several branching paths of TCR signalling. To identify which pathways are being affected by loss of PTPN22, I assayed a number of different readouts of TCR signalling, including proximal phosphorylation events, calcium flux, immediate early gene transcription, transcription factor translocation, and Erk activation. These experiments are the first investigations of the effects of loss of PTPN22 on TCR signalling pathways in human T cells.

5.2 Results

5.2.1 Phosphorylation of Lck and Zap-70 is unchanged in PTPN22 KO Jurkat clones

The known substrates of PTPN22 are largely associated with early T cell signalling events. Lck, Fyn, and Zap-70 are particularly interesting targets of PTPN22 because of their vital role in initiating the phosphorylation events that drive early signalling. We expected PTPN22 KO Jurkat cells to have increased rates of phosphorylation on the activating residues of these proximal T cell signalling molecules.

To test the hypothesis that PTPN22 KO Jurkat cells would have increased phosphorylation of proximal T cell signalling molecules, I used phosphoprotein flow cytometry after stimulation (described in Chapter 2). This method was selected over traditional Western blotting for several reasons: (1) fewer cells for each condition were required, greatly reducing the quantity of DimerX required to stimulate the cells, (2) data allows us to see responses of individual cells, revealing variance within a population, percentage of responding cells, and the magnitude of individual

cell responses, and (3) flow cytometry has higher throughput than Western blotting, allowing many cell lines and conditions to be included in the same experiment.

Individual clones were labeled with different concentrations of CellTrace Violet so

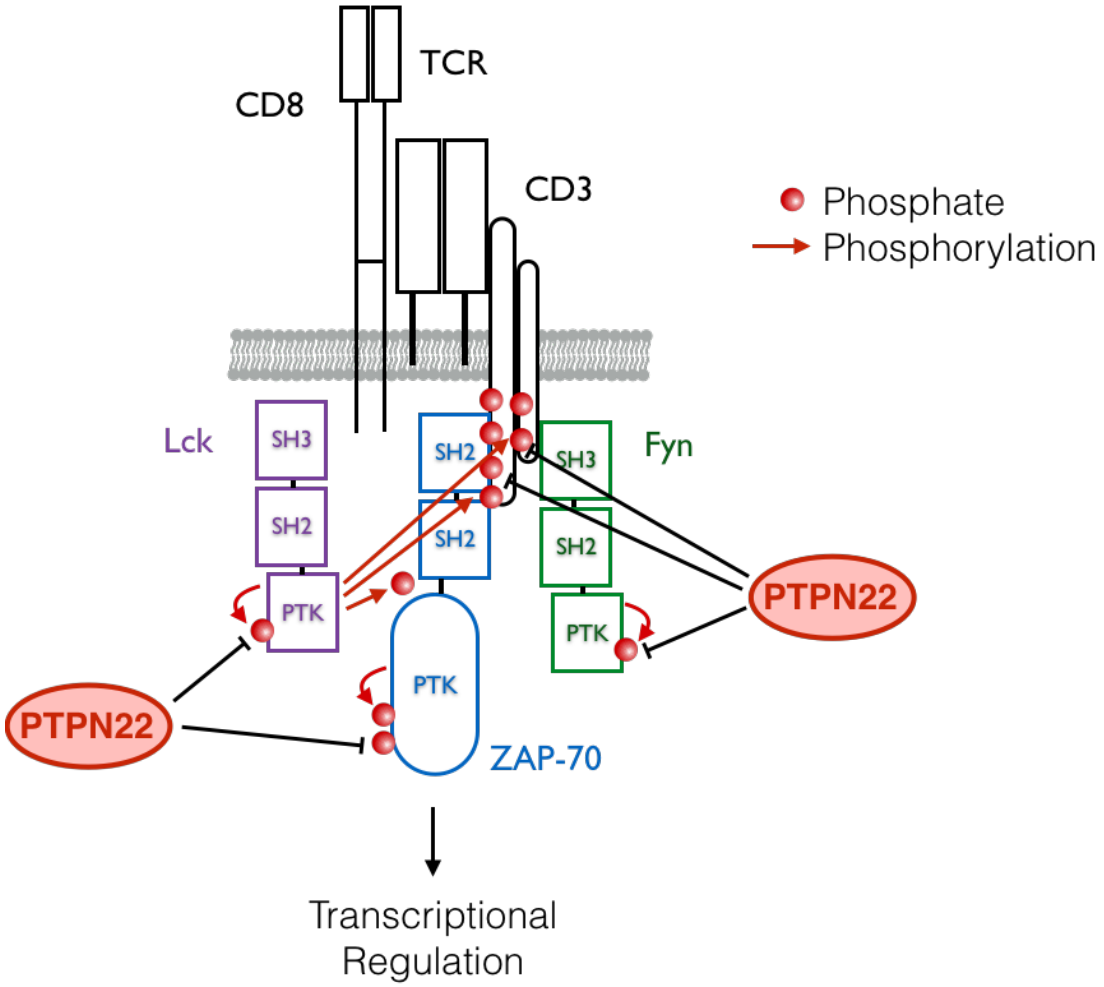

Figure 2. T cell substrates of PTPN22. Fyn Y420, Lck Y394, and Zap-70 Y495 are established substrates of PTPN22. TCR-CD3ζ and CD3ε are putative substrates. Adapted from Bottini et al {Bottini:2014kg}

that they could be distinguished after pooling for stimulation and processing. Stimulating and staining different clones in the same well greatly reduced potential technical variance in the treatment of the clones. The twelve clones (six WT and six KO) were split into three groups for stimulation and staining, with each group containing two WT and two KO clones. The grouping of the clones was randomised for each experiment. CD3 stimulation was used for these assays, because no phosphorylation could be detected within 30 minutes of DimerX+pTax stimulation, even at the highest concentrations. This may be due to the altered dynamics of signalling between anti-CD3 stimulation and peptide.

After stimulation, cells were divided into multiple wells and stained with antibody. I stained with antibodies that indicated the total amount of Lck and Zap-70 protein, as well as with antibodies specific for phosphorylated tyrosine residues Lck Y394, Lck Y505, and Zap-70 Y493. The primary antibodies were not directly conjugated, and thus required a secondary detection antibody. As each primary antibody had been raised in a rabbit, each staining was performed separately. An example of a flow cytometry plot and the gating strategy used in these experiments is shown in Figure 3a.

Using this assay, I was able to detect a trend of increased in phosphorylation of all three sites following stimulation relative to unstimulated phosphorylation levels (Figure 3b and c). The total abundance of protein appeared to change slightly upon stimulation (Figure 3b and c). I was unable to find any report of increased expression of these proteins in the literature, perhaps because protein phosphorylation is often detected by Western blot, which may not be sensitive enough to detect these subtle changes. It is also possible that the binding of antibody I used to detect total Lck levels is affected by phosphorylation of the protein. The total Lck antibody is polyclonal and recognises residues at the c-terminus, so phosphorylation of Lck Y505 could change the conformation of the protein in a way that affects the antibody's binding affinity. Another explanation could be that certain clones have elevated background binding, however Figure 3d shows that the clones which had a higher total protein signal did not necessarily also show elevated phosphorylation signal, indicating that the total protein signal is specific to

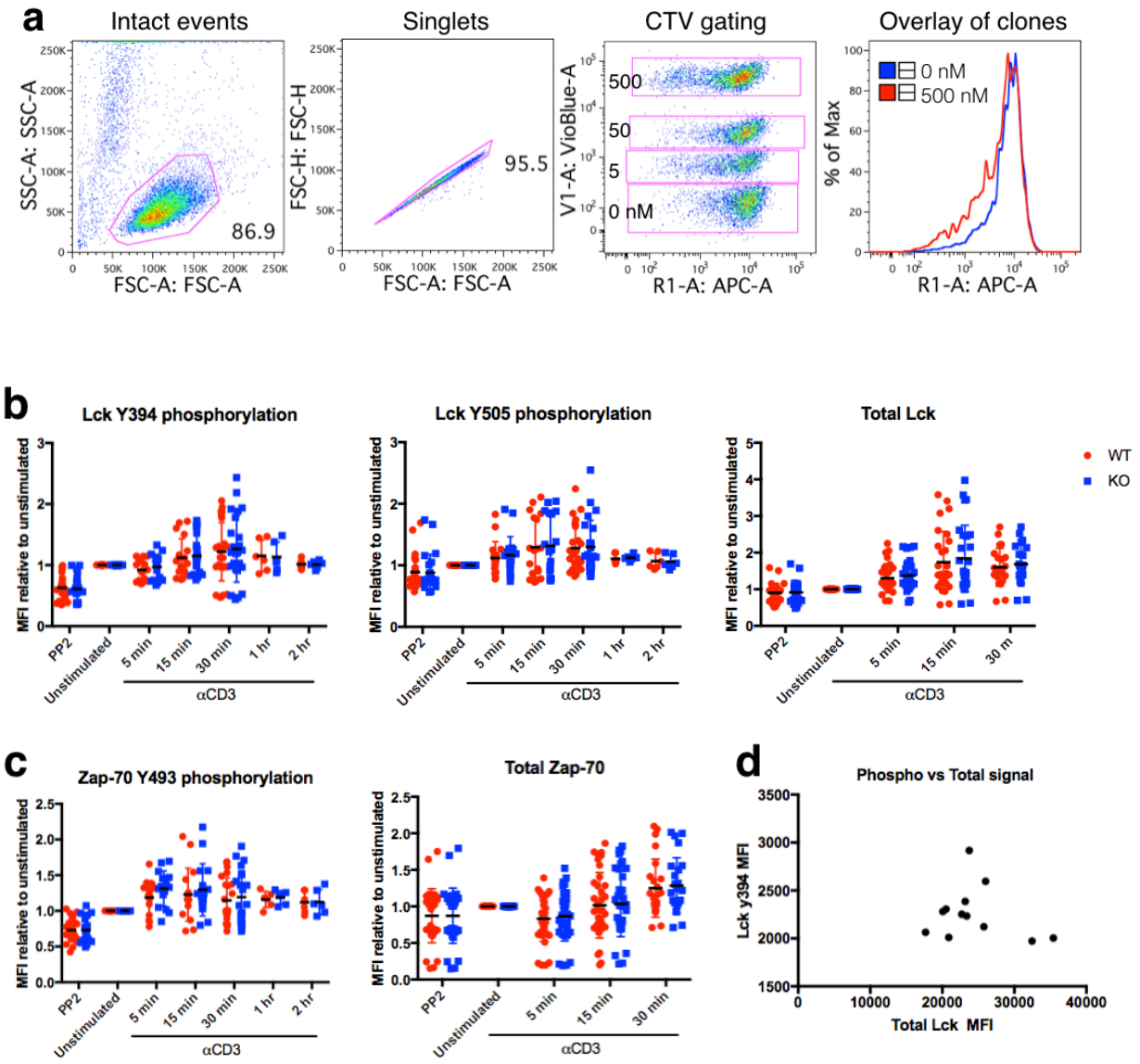

Figure 3. No changes in Lck or Zap-70 phosphorylation in PTPN22 KO T cells upon stimulation. (**a**) Gating strategy for detection of phosphorylation by flow cytometry. (**b**) Lck and (**c**) Zap-70 phosphorylatyion or total protein was measured in Jurkat cells treated with PP2, unstimulated, or stimulated with anti-CD3 for the indicated times. Each dot represents a single well in an experiment, data represents four independent experiments. (**d**) Example plot of relation between MFI of total Lck and Lck Y394 for individual cell lines stimulated with in anti-CD3 for 15 minutes in one experiment. No significant differences between PTPN22 WT and KO clones were found. Statistical significance for each condition was determined by unpaired T test and Bonferroni multiple comparisons correction. A p-value less than 0.05 was considered significant.

the primary total protein antibody.

Changes to Lck phosphorylation is notoriously difficult to detect consistently due to the highly transient nature of the phosphorylation events. Lck phosphorylation is a critical step in T cell signalling and is dynamically regulated by a number of phosphatases and kinases, therefore we would not expect to see dramatic global shifts in Lck phosphorylation upon T cell stimulation[57]. In accordance with this, I observed that the average phosphorylation of Lck increased only slightly upon stimulation (Figure 3b), but that there was a great deal of variance due to differences between the individual wells, potentially obscuring changes. Both residues Y394 and Y505 followed similar patterns of increasing stimulation upon activation, despite Y394 being an activating residue and Y505 being inhibitory. The average amount of phosphorylation for Y505 did peak earlier, perhaps reflecting the commitment of the cell to activation by 30 minutes. Y394, on the other hand, showed reduced phosphorylation on average after 5 minutes of stimulation, but continued to increase up to 30 minutes. The role of Lck appears to be less important after one hour of stimulation, as phosphorylation of both residues returned to near baseline by this point.

No significant difference in Zap-70 phosphorylation was detected between PTPN22 WT and KO clones, however the trend of elevated phosphorylation of Zap-70 Y493 in PTPN22 KO cells was more distinct than for either Lck tyrosine residue. Greater levels of phosphorylation of Zap-70 in PTPN22 KO cells may be due to the fact that Zap-70 is a downstream target of Lck, so subtly increased Lck activity could result in proportionally greater increases in Zap-70 phosphorylation, and that Zap-70 itself is also a target of dephosphorylation by PTPN22. Differences in Zap-70 phosphorylation between PTPN22 WT and KO cells were not statistically significant, but they may be indicative of the subtle biological effect of PTPN22 on early signalling molecules.

5.2.2 Calcium flux is unchanged in PTPN22 KO Jurkat clones

Given that only very subtle changes in the phosphorylation of early signalling molecules Lck and Zap-70 were detectable, I decided to check if any downstream effects of enhanced signalling could be detected in my PTPN22 KO clones.

Overexpression studies and experiments in primary cells have reported that the human R620W polymorphism decreases the magnitude of calcium flux in human T cells[192]. These results suggest that human PTPN22 plays a role in regulating calcium flux, so I tested whether the pathway was affected by removal of PTPN22 from Jurkat cells.

Indo-1 staining was used to measure calcium flux in real time. The blue Indo-1 stain is converted into a violet colour in the presence of calcium ions, so the ratio of violet:blue emission is an indicator of the amount of calcium present at any given point in time (a ratio is used to control for variances in the amount of dye taken up by the cells). After stimulation with anti-CD3, I added a saturating amount of ionomycin[165] to check that each cell line had a similar maximum potential for calcium flux (Figure 4b).

Similarly to the phosflow setup, each sample contained two independent clones differentially stained with a cell dye (Figure 4a,c,d). In this case I used CFSE, as the CellTrace Violet channel was needed for the Indo-1 stain. I tested different concentrations of CFSE on the same cell line to check for any effects of CFSE on calcium flux (Figure 4e). I detected a very slight increase in violet:blue ratio when using 50nM CFSE but not when using 5 nM, so I opted to use only two lines in each sample tube, one unstained and the other stained with CFSE at 5nM. For each experiment, I randomised the KO and WT lines that were paired together, as well as which line would be stained in each tube (either the WT or KO line could be $CFSE^{+}$). These steps ensured that CFSE staining would have a minimal overall effect on the results.

The amount of calcium in the cell reached its peak within 1-2 minutes of adding anti-CD3, and then gradually declined back to baseline over the course of 10-60 minutes. I stimulated cells in 600 µL media and ran samples for 16 minutes on the flow cytometer before adding ionomycin. We followed a strict timing protocol for each tube that allowed 15 seconds without data recording for the addition of reagents (Figure 5a).

I used three different values from each sample analysis plot: peak value, the

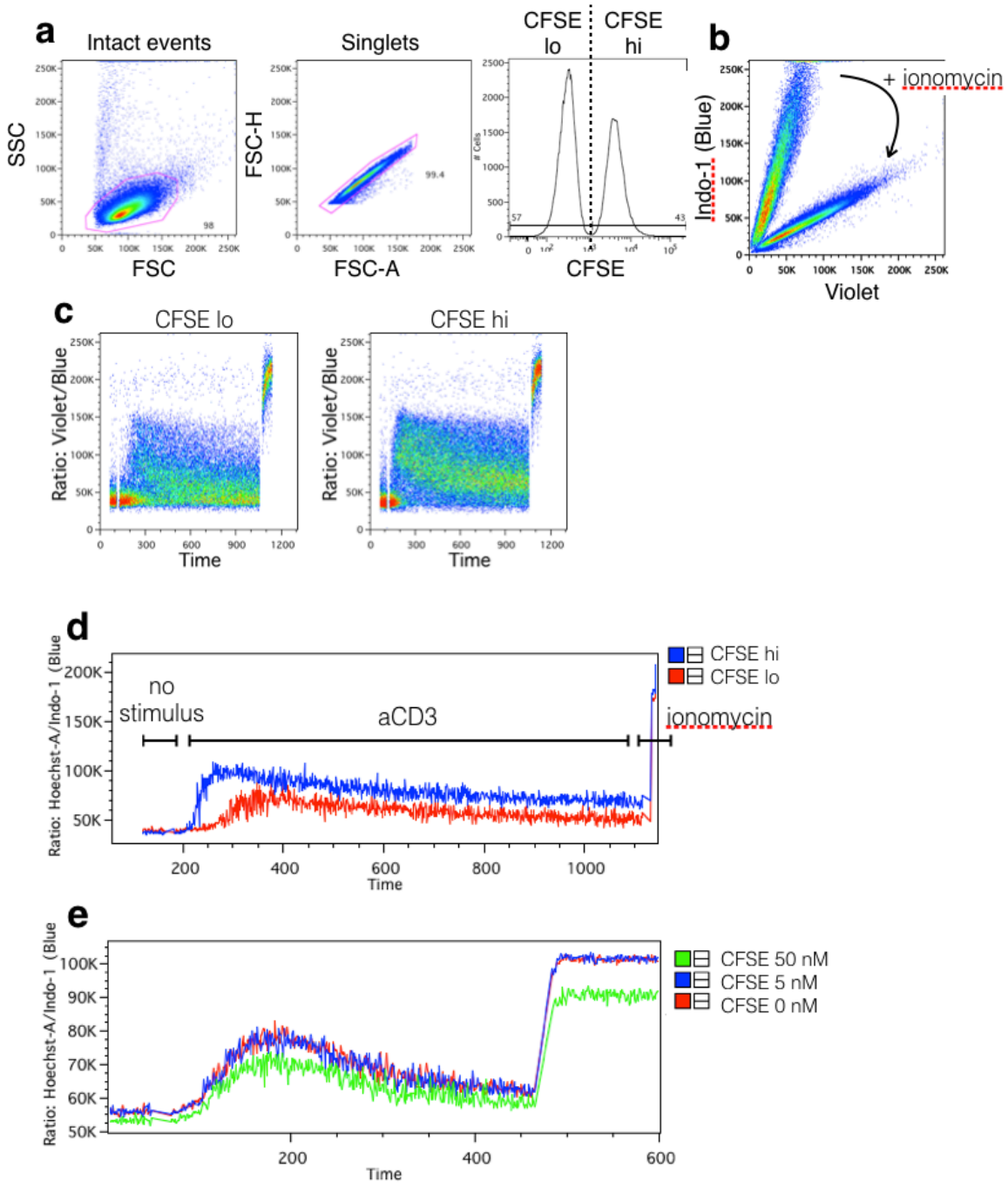

Figure 4. Calcium flux experimental set-up (**a**) Gating strategy for Indo-1 detection of CFSE-labelled cells by flow cytometry. (**b**) Example of shift of cell population from Indo-1 signal to violet signal upon addition of ionomycin. (**c**) Example dot blots of Indo-1 loaded, CFSE-labelled Jurkat cells without stimulus (0-60 seconds), upon anti-CD3 stimulation (60-1200 seconds) and subsequent ionomycin stimulation (1200 seconds) (**d**) Graphical representation of data in (c) overlayed onto one graph. (**e**) The effect of CFSE labelling on flux signal was determined by labelling a single clone with different concentrations of CFSE. Green: 50 nM CFSE, blue: 5 nM CFSE, red: 0 nM CFSE.

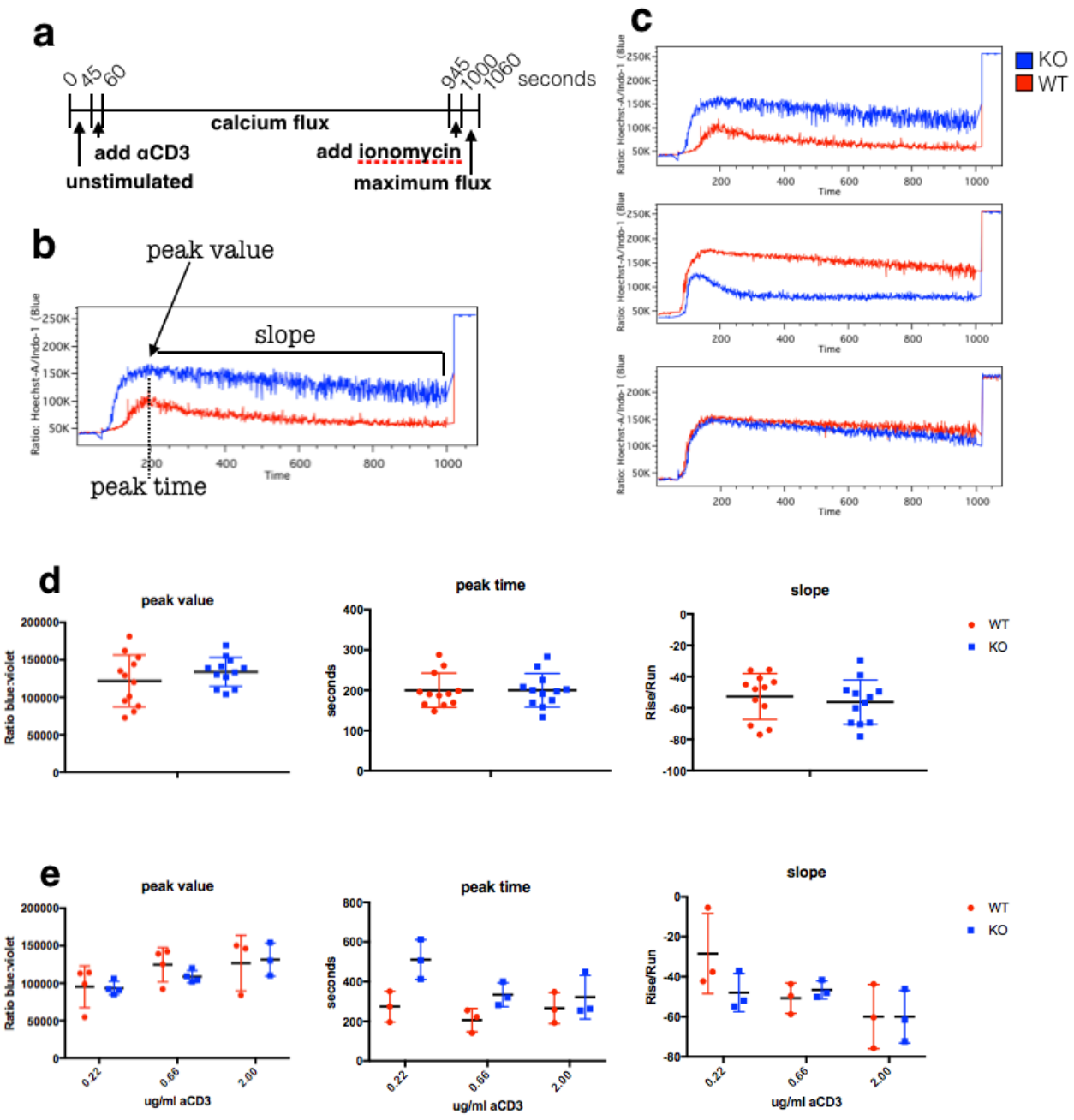

Figure 5. No significant changes in calcium flux in PTPN22 KO (**a**) Schematic of stimulation timing protocol. (**b**) Example of values represented in (**d**) and (**e**). (**c**) Examples of additional WT/KO pairings for calcium flux. (**d**) Calcium flux was recorded in PTPN22 WT and KO Jurkat cells stimulated with saturating amounts of αCD3. Data represents two independent experiments. (**e**) Calcium flux was recorded in Jurkat cells stimulated with titrated amounts of anti-CD3. Data represents two independent experiments. No significant differences between PTPN22 WT and KO clones were found. Statistical significance for each condition was determined by unpaired T test and Bonferroni multiple comparisons correction. A p-value less than 0.05 was considered significant.

numerical ratio of violet signal to blue; peak time, the number of seconds since beginning of data collection that the peak value was reached; and slope, the rate of decrease in the value of the violet:blue ratio from the peak time to the end of the experiment (Figure 5b). The slope is negative, so a greater absolute value indicates a faster return to baseline. The violet:blue ratio is given in arbitrary units, and the starting ratio for each sample was adjusted to 50,000 on the flow cytometry software before recording data, in accordance with the flow cytometer manufacturer recommendations. All six cell lines for each group were represented in each experiment, and the experiment was repeated twice.

There was a clear increase of intracellular calcium upon CD3 stimulation, but no consistent difference was found between the PTPN22 KO clones and the WT clones. There was variance between individual clones, so in any given pairing either the KO or the WT sample might have showed slightly greater Ca^{2+} flux as illustrated in Figure 3c, but the experiments as a whole showed no significant difference between the groups in any parameter measured (Figure 5d). In fact, when using low concentrations of anti-CD3 stimulation, there was a trend that PTPN22 KO cells took longer to reach the same peak flux value, and returned more quickly to baseline than PTPN22 WT cells did (Figure 5e). However, these differences were not significant. Notably, each individual clone was very consistent between the experiments, indicating that the Ca^{2+} flux characteristics of a given cell line was intrinsic to the clone and unlikely to change day to day. Based on my findings, I concluded that PTPN22 KO did not have an affect on calcium flux in Jurkat cells.

5.2.3 Transcription of early activation genes is unchanged in PTPN22 KO Jurkat clones

No effects of loss of PTPN22 on upstream signalling were detected to explain the increase in IL-2 production in PTPN22 KO clones (Chapter 4, Figure 2). To check for downstream effects of PTPN22 KO signalling in the form of altered gene expression, I investigated the transcription of early activation genes. I selected the genes cFos, cJun, and EGR 1 because they are highly upregulated within 30 minutes of TCR stimulation [275]. A number of housekeeping genes were also tested. I used qPCR to measure mRNA transcript levels after stimulation with anti-CD3, and ran the qPCR products of my primer pairs for each mRNA on a gel to ensure that a single product

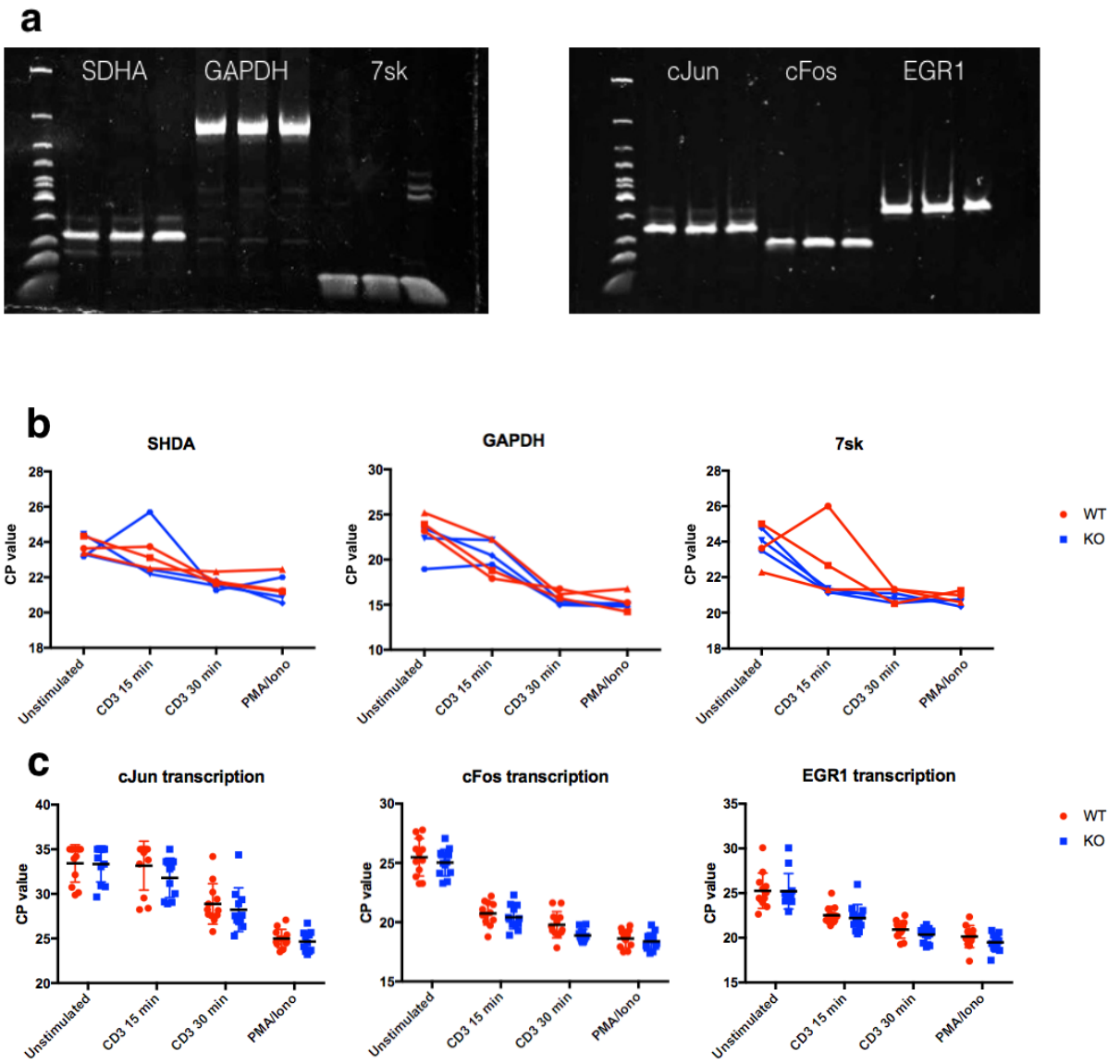

Figure 6. No significant changes in immediate early gene transcription in PTPN22 KO (**a**) qPCR products from each primer pair used were run on a DNA gel. Each gene is represented in triplicate. qPCR was performed using mRNA isolated from Jurkat cell lines stimulated with anti-CD3 or PMA+Ionomycin stimulation. Primers amplified (**b**) housekeeping or (**c**) immediate early gene transcripts. No significant differences between PTPN22 WT and KO clones were found. Statistical significance for each condition was determined by unpaired T test and Bonferroni multiple comparisons correction. A p-value less than 0.05 was considered significant.

was being detected (Figure 6a).

I stimulated cells with PMA/Ionomycin or anti-CD3 for 0, 15, and 30 minutes. RNA was immediately isolated after the stimulation period using trizol chloroform extraction, followed by isopropanol precipitation. I measured the concentration of the RNA preparations by Nanodrop, and loaded 1 µg of RNA for the cDNA reactions. qPCR was carried out on these samples using SYBR green mastermix. Three clones of each group were tested in each experiment, and the experiment was repeated four times.

It is standard practice when using qPCR to normalise crossing point-PCR-cycle (Cp) values of genes of interest to the Cp values of a housekeeping gene to account for variance in the amount of cDNA in each sample. It is assumed that the expression of house keeping genes remains constant under various treatment conditions. However, in my testing of commonly used and recommended housekeeping genes for T cells, I found that each of them was highly upregulated, i.e. showed lower Cp value, upon CD3 stimulation in Jurkat cells (Figure 6b). Attempting to normalise other upregulated genes based on these changing control values could potentially mask any differences in gene expression from baseline. Based on this finding, I decided not to use housekeeping genes in my analysis, and to instead load a consistent amount of RNA in each cDNA reaction.

The results of these experiments showed clear upregulation of mRNA expression of the early activating genes upon stimulation, but there were no significant differences observed between PTPN22 WT and KO cell lines at any time points (Figure 6c). There was a very slight trend for PTPN22 KO cells to have higher levels of mRNA for cJun, cFos and EGR1 upon CD3 stimulation, but it is unclear if such a slight difference would have a biological effect. Based on these findings, I concluded that PTPN22 had no readily detectable affect on the up-regulation of the immediate early activation genes cFos, cJun, or EGR1.

5.2.4 Nuclear translocation of transcription factors is unchanged in PTPN22 KO Jurkat clones

Having been thus far unable to identify the pathways that explained the increased

IL-2 production in PTPN22 KO cells (Chapter 4, Figure 2), I investigated changes in the transcription factors relevant for IL-2 expression: NFAT, NFκB, and AP-1 (cFos). If a single factor could be identified as changing, it could help indicate the nature of the specific molecular pathways regulated by PTPN22 signalling. Alternatively, upregulation of all three transcription factors could indicate that PTPN22 KO has an effect on an early signalling event, which influences a number of downstream pathways.

I used flow cytometry to address the question of whether or not NFAT, cFos, or NFκB were more active in PTPN22 WT or KO clones. Berg et al. describe a protocol to isolate nuclei from cells and stain them for flow cytometric analysis (unpublished). The advantage of looking at the isolated nuclei themselves is that NFAT, cFos and NFκB are only translocated into the nucleus upon activation, at which point they are able to affect transcription. Flow cytometry of nulcei allowed us to detect active NFAT, cFos, and NFκB on an individual cell basis across large populations.

I used DimerX+pTax stimulation combined with anti-CD28, the same stimulation conditions used to induce IL-2 expression (Chapter 4, Figure 2). The peak of IL-2 expression after DimerX+pTax stimulation was between 2 and 4 hours, so I chose the time points 0.5, 1, and 3 hours to capture the change in transcriptional activity. Each experiment was performed using three clones from each group, and was repeated three times (except for NFκB, which was excluded from one experiment).

The protocol to isolate nuclei results in loss of 90% of nuclei when lysing $1x10^6$ cells, and this percentage yield is further reduced with even less starting material. The number of cells used ($3x10^5$) for the stimulated samples was limited by the availability of DimerX reagent, whereas $1.8x10^6$ cells were used in staining controls. Thus the nuclei yields of the stimulated samples were lower than nuclei yields of control samples. Control samples were therefore used to set the Forward/Side-scatter gate, and the same gate was applied to the stimulated samples (Figure 7a).

Fig 5b and c shows that in unstimulated cells nuclei were negative for cFos and NFAT, however there was a substantial population that was positive for NFκB (Figure 7b). This population was present in every clone tested, although the

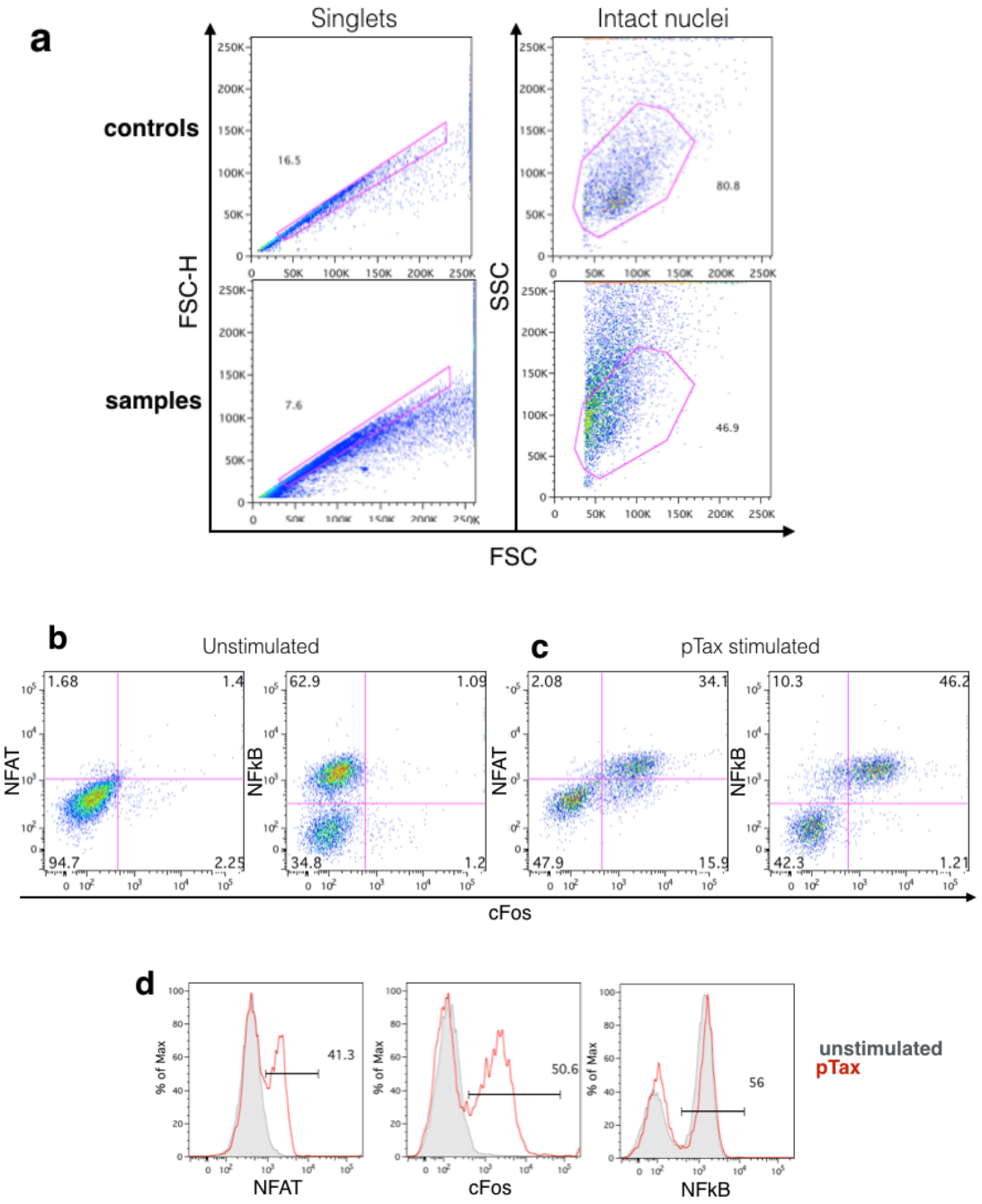

Figure 7. Gating strategy for nuclear flow cytometry (**a**) Nuclei gates were drawn on controls and applied to samples. Nuclei were isolated from Jurkat cells that were (**b**) unstimulated or (**c**) stimulated with DimerX+pTax, and stained for NFAT, cFos, or NFkB. (**d**) Histograms of data shown in (b) and (c). Grey = unstimulated cells, red = pTax stimulated cells.

frequency of positive cells varied from 16-90%. Interestingly, the population that was NFκB positive before stimulation was the same population that became positive for cFos and NFAT upon stimulation (Figure 7c). In samples with CD3 stimulation, NFκB negative populations did not upegulate cFos or NFAT. It is possible that some nuclei were simply constitutively positive for NFκB, although this result has not been reported in Jurkat cells previously. Alternatively, the NFκB negative population could not be nuclei at all, but be comprised of debris, or it could be nuclei from cells within the population that are resistant to activation for an unknown reason. It's also possible that the NFκB antibody, although it has been verified by the manufacturer as negative for staining on NFκB knockout cells, is binding non-specifically to an unknown nuclear marker; however the strong correlation between NFκB signal and NFAT and cFos signal upon stimulation makes this possibility seem unlikely. The histograms in Figure 5d show the gating used to generate the graphs in Figure 6.

NFκB notwithstanding, we observed an increase in nuclear translocation of NFAT and cFos upon stimulation with DimerX+pTax (Figure 8a and b). Both MFI and frequency of NFAT and cFos were reduced slightly from their peak by 3 hours, but remained elevated compared to baseline. I did not observe any significant differences between PTPN22 WT and KO cells. There is a slight trend for KO cells to have fewer cells positive for each transcription factor (Figure 8a), and for the fluorescence of those positive cells to be reduced (Figure 8b) compared to WT. These findings suggest that the increase in IL-2 in KO Jurkat cells compared to WT cells cannot be attributed to differences in the translocation of transcription factors. It is possible that regulation of IL-2 translation is more relevant in this effect.

5.2.5 Erk phosphorylation is increased upon weak stimulation in PTPN22 KO Jurkat clones

Erk phosphorylation is one of the most sensitive readouts of T cell activation that I tested, giving signal well above background even under weak conditions of stimulation. It is also shown to be elevated under certain stimulation conditions in T cells isolated from PTPN22 KO mice[200]. I was therefore interested in determining whether the Erk pathway was affected in my PTPN22 KO Jurkat clones.

Using phosflow as described above, I found that CD3 stimulation did produce a

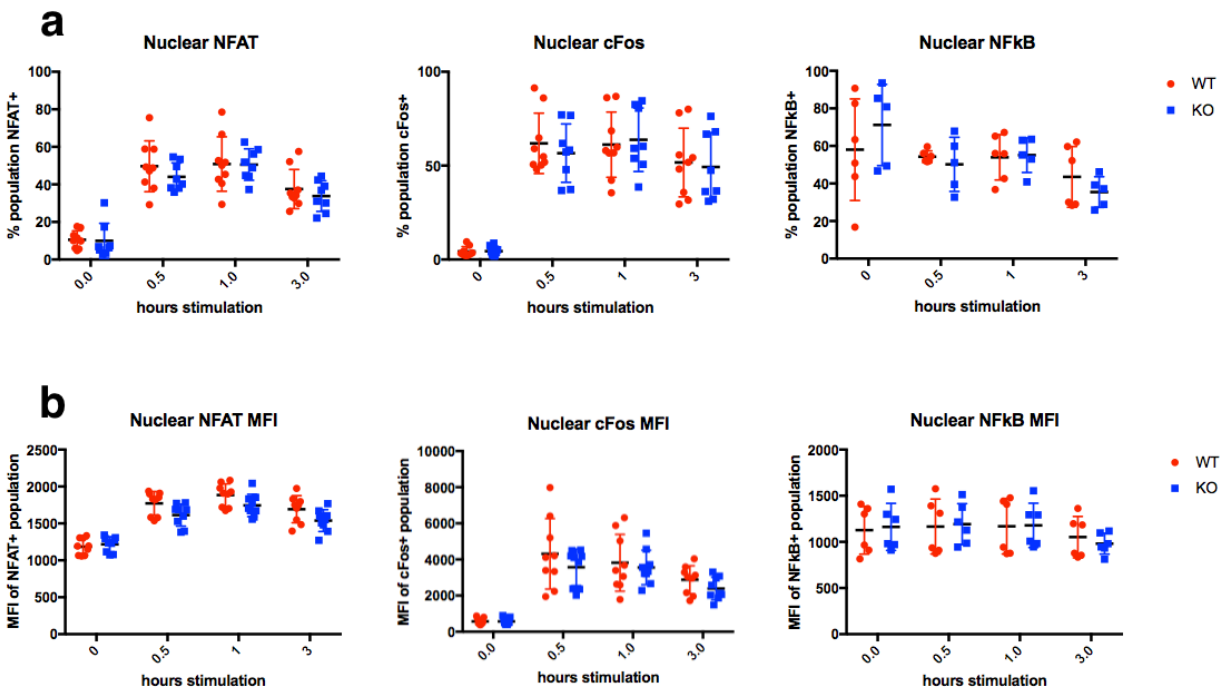

Figure 8. No significant difference in nuclear localisation of transcription factors in PTPN22 KO. Isolated nuclei from Jurkat cells stimulated with DimerX+pTax for the indicated number of hours, and presence of NFAT, cFos, and NFkB was detected by flow cytometry. (**a**) Percentage of nuclei positive for indicated transcription factor, (**b**) MFI of population positive for indicated transcription factor. No significant differences between PTPN22 WT and KO clones were found. Statistical significance for each condition was determined by unpaired T test and Bonferroni multiple comparisons correction. A p-value less than 0.05 was considered significant.

trend of increased Erk phosphorylation in PTPN22 KO cells. However this result was only significant after 30 minutes of stimulation, as phosphorylated Erk (pErk) in WT cells was dephosphorylated more quickly than KO cells (Figure 9a). Because pErk had not returned to baseline by two hours, I extended the experiment to six hours to observe whether pErk in PTPN22 KO cells would remain elevated over the entire period (Figure 9b). Using saturating concentrations of plate-bound CD3 showed a greater trend for PTPN22 KO clones to have higher pErk at one and two hours, though this difference was reduced by later time points. However, saturating concentrations of plate-bound DimerX+pTax showed no difference between the groups at any of the time points (Figure 9c). Additionally, the percent of pErk positive cells had decreased from its peak after one hour of CD3 stimulation, whereas with DimerX+pTax the percentage of pErk positive cells both higher than with anti-CD3 and sustained up to two hours. This once again reflects the inherent differences between CD3 and peptide stimulation, and also suggests that the effect of PTPN22 on pErk depends on the type of stimulation used.

To further test the effects of PTPN22 on pErk upregulation after stimulations with different strengths of ligand, I titrated DimerX+pTax for stimulation and also tested saturating amounts of DimerX+pHuD, the weaker affinity peptide (Figure 9d). I found that the percentage of pErk positive cells corresponded with stimulation strength, but also that a greater proportion of PTPN22 KO cells upregulated pErk than WT cells at weaker stimulations, and that this difference was reduced as signal strength increased (Figure 9e). This result is in line with the findings from PTPN22 KO mice, and also suggests an explanation for why many of my previous assays have produced negative results: when a strong stimulus is necessary to obtain a readout, the role of PTPN22 may be overshadowed. pErk is a sufficiently sensitive readout that, even though pHuD stimulation had never elicited a response significantly above baseline in any other assay I tested, pHuD caused upregulation of pErk detectable to sufficient levels for analysis of subtle differences. Based on these findings, I conclude that PTPN22 does affect Erk signalling in human T cells upon stimulation with weak affinity peptide, but that the strength of this effect is reduced upon increased activating signal strength. Further investigations into the role of PTPN22 on T cell signalling should employ highly sensitive assays that are able to detect the more subtle signal changes elicited by weaker stimulation conditions.

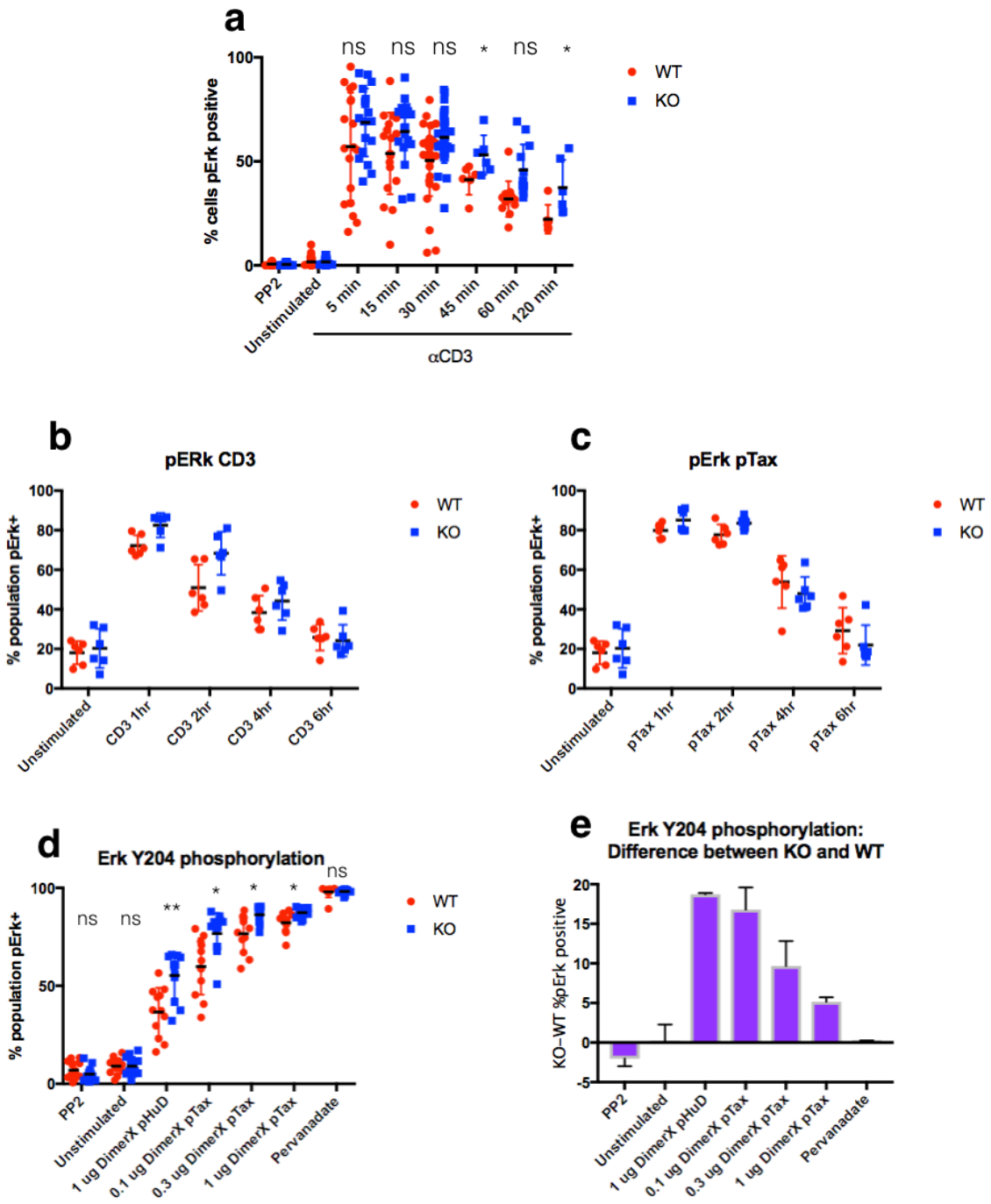

Figure 9. PTPN22 KO enhances Erk signalling upon weak stimulation. (**a**) and (**b**) Jurkat cells were stimulated with saturating anti-CD3 for the indicated time periods, or treated with PP2 or pervanadate, and pErk phosphorylation was measured by flow cytometry. (**c**) pErk levels were measured in Jurkat cells stimulated with saturating DimerX+pTax for the indicated time periods. (**d**) pErk levels were measured in Jurkat cells stimulated for one hour with DimerX+pHuD or different concentrations of DimerX+pTax or treated with PP2 or pervanadate. (**e**) Difference between average levels of pErk in PTPN22 WT and KO cells for each stimulation condition. Data represents two independent experiments. Statistical significance for each condition was determined by unpaired T test and Bonferroni multiple comparisons correction. A p-value less than 0.05 was considered significant. ns = not significant, *p < 0.05, **p < 0.01, ***p < 0.001

5.3 Discussion

The work presented in this chapter aimed to identify the pathways affected by loss of PTPN22 that lead to increased IL-2 and CD69 expression in Jurkat cells (Chapter 4, Figure 2 and 3). To this end, I compared PTPN22 WT and PTPN22 KO Jurkat clones in phosphorylation of Lck and Zap-70, calcium flux, early activation gene transcription, transcription factor nuclear localisation, and Erk phosphorylation.

PTPN22 is largely considered to have a role in TCR-proximal signalling, however we found no effect of loss of PTPN22 on early phosphorylation events (Figure 3). This may be due to the challenge of detecting subtle differences in phosphorylation using traditionally available signalling assays. For this reason, we expanded the readouts to include downstream effects at later time points (>15 minutes); while PTPN22 may not have a direct effect on these readouts, their increase may reflect slightly stronger proximal signalling made more pronounced by signal amplification. However, expanding our view of the signalling pathway not only complicates the system observed but also includes activity of additional signalling regulators, and results may no longer by directly attributable to PTPN22 activity. Future studies wishing to isolate the role of PTPN22 on TCR-proximal signalling may use techniques such as immunoprecipitation detected by flow cytometry[276] which has much improved sensitivity of phosphorylation events compared to phosphoprotein flow cytometry. Additionally, it is possible that PTPN22 KO Jurkat cells maintained in culture may have reduced differences to PTPN22 WT cells over just a few cell cycles, as tonic signalling effects may lead to adjustments to internal stoichiometry of TCR signalling regulators to maintain homeostasis. In this case, differences between the genotypes would be more readily detected if the period between transfection and assay is reduced as much as possible by eliminating the selection steps and simply performing the assays on the bulk transfected population.

Strong TCR:self-antigen interactions are selected against in the thymus, thus autoimmune responses in peripheral T cells are driven by weak self-antigens. A study using PTPN22 KO OT-1 mice showed that loss of PTPN22 had an impact on several readouts of T cell signalling, including Erk phosphorylation, under conditions

of weak peptide stimulation, but that loss of PTPN22 had less of an effect on T cell responses to high affinity peptide[200]. Similarly, in PTPN22 KO Jurkat clones, Erk phosphorylation was enhanced compared to WT clones under conditions of weak peptide stimulation, and the enhancement was reduced as peptide strength increased. These data demonstrated that the effect of human PTPN22 on regulating T cell signalling was greater in the context of weak antigen stimulation, such as may lead to autoimmune responses. The autoimmune-associated PTPN22 SNP may confer autoimmune susceptibility by inhibiting the ability of PTPN22 to regulate responses to weak self-antigen. Current literature suggests that human PTPN22 R620W acts as a gain-of-function mutation which inhibits T cell responses in response to CD3 or SAg (further described in Chapter 3), however the work presented here shows that the role of PTPN22 on T cell signalling is different in response to weak antigen, suggesting that the effects of the polymorphism might also be dependent on the type of stimulus. The observation that IL-2 production is increased in PTPN22 KO Jurkat clones (Chapter 4, Figure 2) was made following strong peptide stimulation, suggesting that even subtle signalling changes can lead to differences in effector molecule production. Further study is needed to fully understand the role of PTPN22 in different contexts of stimulation.

Using CD3 or strong peptide stimulation may have limited the role of PTPN22 in the pathways analysed by the other assays described in this chapter. We observed trends of PTPN22 KO clones having increased Lck and Zap-70 phosphorylation and immediate early gene transcription after stimulation with CD3, but the difference between PTPN22 KO and WT clones was not significant. It is possible that weaker stimulation would produce a greater difference between the PTPN22 KO and WT clone Lck and Zap-70 phosphorylation, however this difference could be difficult to detect using phosflow because the change in MFI from unstimulated cells, which is already less than two-fold on average when using strong stimulation, may be reduced to the point that it is indiscernible from background noise. The increase in immediate early gene transcription in activated cells compared to unstimulated cells is clearer, however if the difference in transcription of immediate early genes between PTPN22 WT and KO clones was less than two-fold, it would be difficult to detect by qPCR; a two-fold increase in transcript number only reduced the Cp value by one, so subtle changes could be easily masked by variance noise resulting from

analysis of numerous independent clones. Therefore, only a difference in transcription greater than two-fold would be likely to produce a significant result using this assay.

Calcium flux in response to stimulation had been shown previously to be dampened when PTPN22 R620W was overexpressed in human cell lines[192], and to be enhanced in thymocytes from PTPN22$^{-/-}$ mice on several different genetic backgrounds[160,162,165]. However, Rieck et al found a reduction in calcium flux in memory B cells of PTPN22 R620W homozygous individuals, but not in naive B cells[189], and Maine et al found that calcium flux in B cells was unaffected by PTPN22 in transgenic mice[161]. Taken together with the fact that lab mice are raised in a clean environment, these studies in B cells suggest that antigen experience may be important to observe the effect of PTPN22 on calcium signalling. If B cells experience a similar upregulation of PTPN22 upon antigen engagement to T cells[186], this phenomenon could be explained by differing amounts of PTPN22 expressed by naive lymphocytes compared to memory lymphocytes or thymocytes. In this model, the amount of PTPN22 expressed by naive lymphocytes is insufficient to downregulate calcium signalling. Therefore, as Jurkat cells are antigen-naive, they may simply not express enough PTPN22 to affect calcium signaling, as Chapter 3, Figure 11 showed that restimulated PBMCs express much more PTPN22 than unstimulated Jurkat cells. If this is the case, we would expect to see no difference between calcium flux in PTPN22 WT and KO Jurkat clones, which fits the results presented in this chapter. Regardless, the lack of difference in calcium flux indicates that the observed increase in IL-2 production in PTPN22 KO clones (Chapter 4, figure 2) was not due to enhanced calcium signalling.

Vang et al showed that increasing expression of PTPN22 in Jurkat cells lead to reductions of NFAT and AP-1 driven luciferase upon stimulation with anti-CD3, indicating that PTPN22 was able to inhibit activity of those transcription factors[149]. In addition, Brownlie et al showed a correlation between increased NFAT translocation and IL-2 production in PTPN22 KO mouse T cells in the context of TGFβ downregulation [201]. However, my data showed no significant changes in detection of NFAT, AP-1, and NFκB in the nucleus between PTPN22 KO Jurkat cells stimulated with strong peptide compared to PTPN22 WT cells, indicating that increased IL-2

production in PTPN22 KO clones was not due to increased activation and translocation of these factors. There are a few possible causes for this discrepancy: (1) I detected only one member of each transcription factor family (NFAT1, cFos, and RelA), so any differences mediated by related proteins would not be observed; (2) the presence of these transcription factors in the nucleus does not guarantee that they will drive transcription, which also depends on cooperative interactions between these and additional transcription factors, phosphorylation of transcription factors for full transactivation capacity, and epigenetic remodelling[277]; and (3) the assays did not account for activity of the transcriptional activity over time, due either to stabilizing phosphorylation or to targeted degradation of the proteins, either of which could significantly impact the transcriptional activity of the factors beyond their presence in the nucleus. Furthermore, Vang et al made their observations in the context of overexpression of PTPN22. By their description, overexpression of either variant of PTPN22 "blocked TCR signalling," thereby showing a clear divergence from the function of normal levels of PTPN22 in Jurkat cells. Overexpression of PTPN22 alters its stoichiometry relative to other proteins of TCR signalling, and may greatly overemphasize its negative regulatory abilities compared to physiological expression levels. In this case, we would expect to observe negative regulation by overexpressed PTPN22 that does not occur with normal expression of PTPN22. As my experiments are comparing the loss of PTPN22 to its normal expression, it is not surprising that I did not observe the loss of negative regulation of transcription factors since such negative regulation required more PTPN22 than was expressed in my PTPN22 WT cells.

It was recently shown that IL-2 is regulated nearly exclusively at the transcriptional level in mouse T cells[278], however there is evidence that IL-2 mRNA does not inevitably correlate with IL-2 protein expression, and polysome fractionation showed that TCR stimulated human peripheral blood T cells lacking co-stimulation failed to load IL-2 mRNA with high numbers of ribosome[279]. Ragheb et al found CD28 responsive elements in IL-2 mRNA that contributed to stabilisation of the transcript in a mouse T cell line[280]. It is therefore possible that the increase in IL-2 production in PTPN22 KO clones was due to differential translational regulation of IL-2, rather than changes to IL-2 transcription. Comparison of IL-2 transcript levels in PTPN22 WT and KO clones after stimulation would help identify how PTPN22 affects

transcriptional and translational regulations of IL-2.

Although I observed a clear increase of IL-2 expression by PTPN22 KO Jurkat cells, the data presented in this chapter showed little significant difference in many of the signalling molecules I assayed, although there was consistently a slight trend towards increased signalling in PTPN22 KO lines (Figures 3-8). This finding suggests that the effect of PTPN22 on individual signalling molecules is often too subtle to be detected using the methods described, but that the small differences culminate in a clear phenotype downstream. The assertion that PTPN22 has a subtle effect on T cell signalling is logical given the context in which PTPN22 was indicated as a gene important in autoimmunity: in GWAS studies, hundreds of individuals are needed in order for a significant gene to be identified due to the small contribution of each gene to the disease landscape. For example, a given individual homozygous for PTPN22 has a roughly 3-4% chance of developing rheumatoid arthritis[108], compared to 1% in the normal population. Thus PTPN22 R620W does not have a dramatic enough effect on TCR signalling to trigger autoimmunity on its own, but instead significantly contributes to a susceptible genetic background that, given certain environmental triggers, is more likely to lead to autoimmune disease.

Further study of T cell signalling pathways in PTPN22 WT and KO Jurkat cells is needed to conclusively identify the mechanisms by which loss of PTPN22 effects increased IL-2 production. Future work should focus on the effects of weak peptide stimulation, as PTPN22 may play a more significant role under conditions of weak stimulation. Erk phosphorylation was increased in PTPN22 KO cells (Figure 9), thus further investigation of pathways leading to Erk phosphorylation could explain how the increase is mediated by PTPN22. The data presented here and in the preceding chapters indicate that the effects of PTPN22 on signalling are subtle, but can lead to changes in effector molecule expression that may be biologically relevant.

6. Discussion

The advent of CRISPR technology has made it easier than ever to genetically engineer cells and organisms to address scientific questions. My work used CRISPR to create the first example of human T cells that lacked the phosphatase PTPN22. The ability to explore the effects of PTPN22 knockout in human T cells has helped elucidate the role of PTPN22 in human T cell signalling, which is of great interest due to the association of mutations in PTPN22 with human autoimmune disease. Additionally, studies in mouse models have demonstrated that loss of PTPN22 in T cells can increase the ability of those T cells to limit tumour growth; my work represents the first steps towards investigating CRISPR knockout of PTPN22 as a possible method to enhance adoptive T cell therapy in human cancers.

6.1 Effects of PTPN22 on T cell signalling

Knocking out PTPN22 in a Jurkat cell line provided a novel opportunity to understand the role of human PTPN22. My findings regarding human PTPN22 agree with the characterisation of PTPN22 in mice as a negative regulator of T cells[159], as its absence in Jurkat cells results in increased expression of the cytokine IL-2 and the marker for activation CD69 (Chapter 4, Figures 2 and 3). My data corroborates a previous report in which IL-2 production was increased reported in Jurkat cells in which PTPN22 expression was knocked down using siRNA[191]. The unabated growth of the PTPN22 KO lines (Chapter 3, Figure 12) also indicates that Baghbani et al's finding that PTPN22 knockdown in Jurkat cells caused apoptosis was likely due to off-target siRNA effects or experimental artefact[210]. My findings indicate that PTPN22 serves a similar negative regulatory function in human T cells as it does in mouse.

Many overexpression and primary cell studies indicate that human PTPN22 R620W dampens T cell responses more effectively than the major variant, including reduced IL-2 expression and Erk phosphorylation[149,189,190,192]. I found that loss of PTPN22 had the opposite effect in Jurkat cells, thereby supporting the classification of the R620W polymorphism as a gain-of-function effect. However, forcing PTPN22

R620W to fit into such a dichotomy ignores substantial data from mouse models as well as certain human studies that indicate it may have a gain-of-function effect in some contexts[155,247]. There exist a number of variables that have yet to be fully understood and may have a substantial effect on the interpretation of results, including how the role of PTPN22 may change in naive and memory cells, and before and after development of autoimmunity. For example, numerous splice variants described in humans have no defined function yet[281,282], and the one variant that has been described was reported to be a dominant negative isoform, overexpression of which increased IL-2 expression in Jurkat cells[145]. In addition, differences in splice form variant expression have been reported in individuals with including RA and SLE compared to healthy controls[146,147]. It is not clear whether these changes are a cause or effect of disease, and what role the polymorphism may play in the respective functions of variants of PTPN22. Splice variants are not reported in mouse PTPN22, and were not observed in PTPN22 WT Jurkat cells, although they seem to appear consistently in human primary T cells (unpublished observation). Splice variants may therefore someday explain some of the discrepancies between observations of PTPN22 made in human PBMCs and in other sources of T cells.

Another possible variable inhibiting the clear classification of PTPN22 R620W as gain-of-function is the fact that the role of the interaction between PTPN22 and Csk remains controversial. The SNP is known to reduce the interaction of these proteins, which was initially reported to involve 35-50% of PTPN22 and 5% of Csk in mouse T cells[158], to weak or undetectable levels[152]. Mouse and human Csk share 99% homology, however regulation of the interactions of Csk and PTPN22 appears to differ between the species: their interaction was reported to be constitutive in mouse T cells [154], but inducible by stimulation in human T cells[152,153]. Furthermore, the interaction was reported to correlate with inhibitory phosphorylation of PTPN22 in a Csk-dependent manner in human cells, but not in mouse cells[151]. The source of this possible discrepancy between mouse and human cells is yet unknown, but could help explain why the disassociation from Csk leads to an increase in PTPN22 function in humans but not in mice. My data demonstrates that the basic functionality of PTPN22 is similar between mouse and humans, so the difference in the effect of the polymorphism between the species may be due to additional

interactors, splice variants, or more subtle differences in PTPN22 localisation or regulation that have not yet been detected.

The driving question behind all PTPN22 research is of how the R620W polymorphism leads to autoimmunity. My work supports the hypothesis that the polymorphism leads to enhanced PTPN22 activity, and thus suppresses T cell functions; given the critical role T cells play in autoimmune responses, this conclusion seems counterintuitive. However, a single triggering event may be less important in autoimmunity than a constitutive dampening of peripheral tolerance mechanisms, and PTPN22 R620W may lead to the latter condition through the suppression of Treg cells. In addition, PTPN22 R620W may be associated with increased inflammation from immune responses by reduction of the expression of inflammation-limiting type-I interferons,[171] as well as with a B cell repertoire more likely to contain self-reactive BCRs[168]. It is likely a combination of these factors that increases autoimmune susceptibility.

To illustrate how these mechanisms may cooperate in a human individual with gain-of-function PTPN22 R620W mutation, consider first prolonged inflammation at the site of an innate response to pathogen. DCs are more likely to be activated and pick up environmental antigen, and a DC happens to process a self-antigen from surrounding damaged cells. Upon traveling to the lymph node, the DC encounters a naive T cell which recognises the self-antigen. Normally Treg cells maintain homeostasis despite the constant presence of self-reactive T cells, however, as the human PTPN22 R620W mutation leads to downregulation of T cell activity, Tregs have reduced functionality, and are less able to maintain suppression of self-reactive T cells. As a result, the naive self-reactive T cell receives sufficient stimulation to become activated and proliferate. Depending on whether it is a CD4 or CD8 T cell it may begin to express additional pro-inflammatory cytokines, become cytotoxic and begin to induce tissue damage, or directly stimulate B cell help. Additional T and B cell recruitment is likely in any scenario incurring ongoing inflammation, and in this case there are a greater number of self-reactive naive B cells, which begin to produce antibody directed against self-antigen derived from the site of inflammation. Thus, a full-blown immune response has been triggered, subtly circumventing different points of control to become activated against the self.

6.2 PTPN22 as a target in cancer therapy

In addition to the prevention of infectious disease, a function of the immune system is to prevent neoplastic growths from developing into cancer. In fact, many of the characteristics of auto-immune cells described above become desirable when considered in the context of fighting cancer. For this reason, we are interested in the possible enhancement PTPN22 may represent to immune therapy.

Recently, a number of therapeutic options have been explored to combat immune evasion and promote clearance of a tumour by the immune system, including cytokine treatment, therapeutic vaccines, checkpoint inhibition, and adoptive T cell therapy, with multiple treatment strategies able to be combined to produce promising results [283-286]. Cancer immunotherapy is still young, but the potential of this field has garnered a great deal of excitement and hope for future developments.

In recent developments of immune therapy, T cells are isolated from a patient or donor and modified to express a chimeric antigen receptor (CAR), which is an engineered antigen-recognition extracellular domain specific to a cancer antigen associated with intracellular T cell receptor signalling molecules[286]. CARs enable T cells to receive strong activating signals from tumour cells expressing the target antigen, increasing their cytotoxicity against tumour cells. However, CARs also result in severe side effects, including death, when CARs cross-react with non-tumour tissues[286,287].

We believe that knocking out PTPN22 may enhance the effectiveness of adoptively transferred T cells without the requirement of very strong CAR interactions, thereby limiting the severity of side effects. The same characteristics that predispose a T cell towards autoimmunity may also predispose it towards cancer immunity: enhanced responsiveness to weak antigen, increased cytokine production, and decreased sensitivity to negative regulation. Each of these traits has been demonstrated in PTPN22 KO mouse T cells, which were also shown to have improved tumour-killing capabilities in mice[200,201]. The work presented in this thesis also provides the first evidence that PTPN22 KO human T cells may also show enhanced responsiveness

to weak antigen and increased cytokine production (Chapter 5, Figure 9; Chapter 4, Figure 2). Increased IL-2 in particular has been shown to protect T cells against downregulation by TGF-β, commonly expressed in the tumour microenvironment, which may explain the ability of IL-2 to promote survival of adoptively transferred T cells and to regress melanomas and renal cell carcinomas[201,284]. PTPN22 KO mouse and human T cells have now been shown to display a similar phenotype; if these similarities remain consistent in the context of anti-tumour responses then knock out of PTPN22 could prove a useful tool in enhancing adoptive T cell therapy.

6.3 Future work

To further test whether or not PTPN22 R620W has a gain-of-function effect in a controlled cell line, CRISPR could be used to knock in the R620W polymorphism using the same Jurkat parent line as used in this project. The effects of the polymorphism would thus be directly comparable to the effects of the knockout, and could be tested in response to both weak and strong cognate peptide stimulation, thus potentially providing valuable insight into the role of the polymorphism in T cell signalling. More ambitiously, the functions of individual splice variants could by analysed by using CRISPR to replace the whole of the PTPN22 gene with a version of the gene containing only exons of the variant of interest, or selected exons could be targeted for deletion. If desired, clones could be chosen in which the splice variant is introduced on only one allele to investigate its interaction with the full-length protein.

The application of PTPN22 KO as a potential cancer therapy in humans would first need to be explored more thoroughly in animal models of disease, such as a humanised mouse tumour model. These studies would require the refinement of the CRISPR and TCR transduction protocols to suit a clinical setting, and would test whether human T cells that have had PTPN22 knocked out are better able to kill tumour cells when transferred into the physiological setting of a live animal.

7. Bibliography

1. Turvey, S. E. & Broide, D. H. Innate immunity. *J. Allergy Clin. Immunol.* **125,** S24–32 (2010).
2. Golubovskaya, V. & Wu, L. Different Subsets of T Cells, Memory, Effector Functions, and CAR-T Immunotherapy. *Cancers (Basel)* **8,** 36 (2016).
3. Schatz, D. G. & Ji, Y. Recombination centres and the orchestration of V(D)J recombination. *Nature Reviews Immunology* **11,** 251–263 (2011).
4. Klein, L., Kyewski, B., Allen, P. M. & Hogquist, K. A. Positive and negative selection of the T cell repertoire: what thymocytes see (and don't see). *Nature Reviews Immunology* **14,** 377–391 (2014).
5. Yang, Q., Jeremiah Bell, J. & Bhandoola, A. T-cell lineage determination. *Immunological Reviews* **238,** 12–22 (2010).
6. Kadish, J. L. & Basch, R. S. Hematopoietic thymocyte precursors. I. Assay and kinetics of the appearance of progeny. *J. Exp. Med.* **143,** 1082–1099 (1976).
7. Wu, L., Antica, M., Johnson, G. R., Scollay, R. & Shortman, K. Developmental potential of the earliest precursor cells from the adult mouse thymus. *J. Exp. Med.* **174,** 1617–1627 (1991).
8. Merkenschlager, M. *et al.* How many thymocytes audition for selection? *J. Exp. Med.* **186,** 1149–1158 (1997).
9. Huang, C.-Y., Sleckman, B. P. & Kanagawa, O. Revision of T cell receptor {alpha} chain genes is required for normal T lymphocyte development. *Proc. Natl. Acad. Sci. U.S.A.* **102,** 14356–14361 (2005).
10. Corthay, A., Nandakumar, K. S. & Holmdahl, R. Evaluation of the percentage of peripheral T cells with two different T cell receptor alpha-chains and of their potential role in autoimmunity. *J. Autoimmun.* **16,** 423–429 (2001).
11. Kurd, N. & Robey, E. A. T-cell selection in the thymus: a spatial and temporal perspective. *Immunological Reviews* **271,** 114–126 (2016).
12. Gascoigne, N. R. J. & Palmer, E. Signaling in thymic selection. *Curr. Opin. Immunol.* **23,** 207–212 (2011).
13. Daniels, M. A. *et al.* Thymic selection threshold defined by compartmentalization of Ras/MAPK signalling. *Nature* **444,** 724–729 (2006).
14. Mallaun, M., Zenke, G. & Palmer, E. A discrete affinity-driven elevation of ZAP-70 kinase activity initiates negative selection. *J.*

Recept. Signal Transduct. Res. **30,** 430–443 (2010).
15. Mallaun, M. *et al.* The T cell receptor's alpha-chain connecting peptide motif promotes close approximation of the CD8 coreceptor allowing efficient signal initiation. *J. Immunol.* **180,** 8211–8221 (2008).
16. Kakugawa, K. *et al.* A novel gene essential for the development of single positive thymocytes. *Mol. Cell. Biol.* **29,** 5128–5135 (2009).
17. Fu, G. *et al.* Themis sets the signal threshold for positive and negative selection in T-cell development. *Nature* **504,** 441–445 (2013).
18. Paster, W. *et al.* A THEMIS:SHP1 complex promotes T-cell survival. *EMBO J.* **34,** 393–409 (2015).
19. Ripen, A. M., Nitta, T., Murata, S., Tanaka, K. & Takahama, Y. Ontogeny of thymic cortical epithelial cells expressing the thymoproteasome subunit β5t. *Eur. J. Immunol.* **41,** 1278–1287 (2011).
20. Tomaru, U. *et al.* Exclusive expression of proteasome subunit {beta}5t in the human thymic cortex. *Blood* **113,** 5186–5191 (2009).
21. Nitta, T. *et al.* Thymoproteasome shapes immunocompetent repertoire of CD8+ T cells. *Immunity* **32,** 29–40 (2010).
22. Singer, A., Adoro, S. & Park, J.-H. Lineage fate and intense debate: myths, models and mechanisms of CD4- versus CD8-lineage choice. *Nature Reviews Immunology* **8,** 788–801 (2008).
23. Ehrlich, L. I. R., Oh, D. Y., Weissman, I. L. & Lewis, R. S. Differential contribution of chemotaxis and substrate restriction to segregation of immature and mature thymocytes. *Immunity* **31,** 986–998 (2009).
24. Naeher, D. *et al.* A constant affinity threshold for T cell tolerance. *Journal of Experimental Medicine* **204,** 2553–2559 (2007).
25. Zumer, K., Saksela, K. & Peterlin, B. M. The mechanism of tissue-restricted antigen gene expression by AIRE. *J. Immunol.* **190,** 2479–2482 (2013).
26. Giraud, M. *et al.* Aire unleashes stalled RNA polymerase to induce ectopic gene expression in thymic epithelial cells. *Proc. Natl. Acad. Sci. U.S.A.* **109,** 535–540 (2012).
27. Melichar, H. J., Ross, J. O., Herzmark, P., Hogquist, K. A. & Robey, E. A. Distinct temporal patterns of T cell receptor signaling during positive versus negative selection in situ. *Sci Signal* **6,** ra92–ra92 (2013).
28. Hadeiba, H. *et al.* CCR9 expression defines tolerogenic plasmacytoid dendritic cells able to suppress acute graft-versus-host disease. *Nature Immunology* **9,** 1253–1260 (2008).
29. Yu, W. *et al.* Clonal Deletion Prunes but Does Not Eliminate Self-Specific αβ CD8(+) T Lymphocytes. *Immunity* **42,** 929–941 (2015).

30. Tanchot, C., Lemonnier, F. A., Pérarnau, B., Freitas, A. A. & Rocha, B. Differential requirements for survival and proliferation of CD8 naïve or memory T cells. *Science* **276,** 2057–2062 (1997).
31. Kirberg, J., Berns, A. & Boehmer, von, H. Peripheral T cell survival requires continual ligation of the T cell receptor to major histocompatibility complex-encoded molecules. *J. Exp. Med.* **186,** 1269–1275 (1997).
32. Fry, T. J. & Mackall, C. L. The many faces of IL-7: from lymphopoiesis to peripheral T cell maintenance. *J. Immunol.* **174,** 6571–6576 (2005).
33. Tan, J. T. *et al.* IL-7 is critical for homeostatic proliferation and survival of naive T cells. *Proc. Natl. Acad. Sci. U.S.A.* **98,** 8732–8737 (2001).
34. Legoux, F. P. *et al.* CD4+ T Cell Tolerance to Tissue-Restricted Self Antigens Is Mediated by Antigen-Specific Regulatory T Cells Rather Than Deletion. *Immunity* **43,** 896–908 (2015).
35. Kaiko, G. E., Horvat, J. C., Beagley, K. W. & Hansbro, P. M. Immunological decision-making: how does the immune system decide to mount a helper T-cell response? *Immunology* **123,** 326–338 (2008).
36. Luckheeram, R. V., Zhou, R., Verma, A. D. & Xia, B. $CD4^+$T cells: differentiation and functions. *Clin. Dev. Immunol.* **2012,** 925135 (2012).
37. Weber, J. P. *et al.* ICOS maintains the T follicular helper cell phenotype by down-regulating Krüppel-like factor 2. *Journal of Experimental Medicine* **212,** 217–233 (2015).
38. Jogdand, G. M., Mohanty, S. & Devadas, S. Regulators of Tfh Cell Differentiation. *Front Immunol* **7,** 520 (2016).
39. Ouyang, W., Kolls, J. K. & Zheng, Y. The biological functions of T helper 17 cell effector cytokines in inflammation. *Immunity* **28,** 454–467 (2008).
40. Murphy, C. A. *et al.* Divergent pro- and antiinflammatory roles for IL-23 and IL-12 in joint autoimmune inflammation. *J. Exp. Med.* **198,** 1951–1957 (2003).
41. Cua, D. J. *et al.* Interleukin-23 rather than interleukin-12 is the critical cytokine for autoimmune inflammation of the brain. *Nature* **421,** 744–748 (2003).
42. Vignali, D. A. A., Collison, L. W. & Workman, C. J. How regulatory T cells work. *Nature Reviews Immunology* **8,** 523–532 (2008).
43. Cederbom, L., Hall, H. & Ivars, F. CD4+CD25+ regulatory T cells down-regulate co-stimulatory molecules on antigen-presenting cells. *Eur. J. Immunol.* **30,** 1538–1543 (2000).
44. Cao, O. *et al.* Induction and role of regulatory CD4+CD25+ T cells in tolerance to the transgene product following hepatic in vivo gene transfer. *Blood* **110,** 1132–1140 (2007).
45. Schmitt, E. G. & Williams, C. B. Generation and function of

induced regulatory T cells. *Front Immunol* **4,** 152 (2013).
46. MacLeod, M. K. L., Kappler, J. W. & Marrack, P. Memory CD4 T cells: generation, reactivation and re-assignment. *Immunology* **130,** 10–15 (2010).
47. Farber, D. L., Yudanin, N. A. & Restifo, N. P. Human memory T cells: generation, compartmentalization and homeostasis. *Nature Reviews Immunology* **14,** 24–35 (2014).
48. Berard, M. & Tough, D. F. Qualitative differences between naïve and memory T cells. *Immunology* **106,** 127–138 (2002).
49. Worbs, T., Hammerschmidt, S. I. & Förster, R. Dendritic cell migration in health and disease. *Nature Reviews Immunology* **17,** 30–48 (2017).
50. Bertram, E. M., Dawicki, W. & Watts, T. H. Role of T cell costimulation in anti-viral immunity. *Seminars in Immunology* **16,** 185–196 (2004).
51. Zheng, Y. *et al.* CD86 and CD80 differentially modulate the suppressive function of human regulatory T cells. *J. Immunol.* **172,** 2778–2784 (2004).
52. Sixt, M. *et al.* The Conduit System Transports Soluble Antigens from the Afferent Lymph to Resident Dendritic Cells in the T Cell Area of the Lymph Node. *Immunity* **22,** 19–29 (2005).
53. Gerner, M. Y., Torabi-Parizi, P. & Germain, R. N. Strategically localized dendritic cells promote rapid T cell responses to lymph-borne particulate antigens. *Immunity* **42,** 172–185 (2015).
54. Davis, S. J. & van der Merwe, P. A. The kinetic-segregation model: TCR triggering and beyond. *Nature Immunology* **7,** 803–809 (2006).
55. Bunnell, S. C. *et al.* T cell receptor ligation induces the formation of dynamically regulated signaling assemblies. *J. Cell Biol.* **158,** 1263–1275 (2002).
56. Boomer, J. S. & Green, J. M. An enigmatic tail of CD28 signaling. *Cold Spring Harb Perspect Biol* **2,** a002436 (2010).
57. Nika, K. *et al.* Constitutively active Lck kinase in T cells drives antigen receptor signal transduction. *Immunity* **32,** 766–777 (2010).
58. Ma, Z., Janmey, P. A. & Finkel, T. H. The receptor deformation model of TCR triggering. *FASEB J.* **22,** 1002–1008 (2008).
59. Alcover, A., Alarcón, B. & Di Bartolo, V. Cell Biology of T Cell Receptor Expression and Regulation. *Annu. Rev. Immunol.* **36,** 103–125 (2018).
60. Xu, C. *et al.* Regulation of T cell receptor activation by dynamic membrane binding of the CD3epsilon cytoplasmic tyrosine-based motif. *Cell* **135,** 702–713 (2008).
61. Kim, S. T. *et al.* TCR Mechanobiology: Torques and Tunable Structures Linked to Early T Cell Signaling. *Front Immunol* **3,** 76 (2012).

62. Dushek, O. Elementary steps in T cell receptor triggering. *Front Immunol* **2,** 91 (2011).
63. Zhang, W., Trible, R. P. & Samelson, L. E. LAT palmitoylation: its essential role in membrane microdomain targeting and tyrosine phosphorylation during T cell activation. *Immunity* **9,** 239–246 (1998).
64. Bubeck Wardenburg, J. *et al.* Regulation of PAK activation and the T cell cytoskeleton by the linker protein SLP-76. *Immunity* **9,** 607–616 (1998).
65. Kannan, A., Huang, W., Huang, F. & August, A. Signal transduction via the T cell antigen receptor in naïve and effector/memory T cells. *Int. J. Biochem. Cell Biol.* **44,** 2129–2134 (2012).
66. Gorentla, B. K. & zhong, X.-P. T Cell Co-inhibitory Receptors-Functions and Signalling Mechanisms. *J Clin Cell Immunol* **01,** (2013).
67. Fuller, D. M., Zhu, M., Koonpaew, S., Nelson, M. I. & Zhang, W. The importance of the Erk pathway in the development of linker for activation of T cells-mediated autoimmunity. *J. Immunol.* **189,** 4005–4013 (2012).
68. Lewis, R. S. Calcium signaling mechanisms in T lymphocytes. *Annu. Rev. Immunol.* **19,** 497–521 (2001).
69. Srikanth, S. & Gwack, Y. Orai1-NFAT signalling pathway triggered by T cell receptor stimulation. *Mol. Cells* **35,** 182–194 (2013).
70. Smith-Garvin, J. E., Koretzky, G. A. & Jordan, M. S. T Cell Activation. **27,** 591–619 (2009).
71. Ebinu, J. O. *et al.* RasGRP links T-cell receptor signaling to Ras. *Blood* **95,** 3199–3203 (2000).
72. Pollizzi, K. N. *et al.* mTORC1 and mTORC2 selectively regulate $CD8^+$ T cell differentiation. *J. Clin. Invest.* **125,** 2090–2108 (2015).
73. Delgoffe, G. M. *et al.* The mTOR kinase differentially regulates effector and regulatory T cell lineage commitment. *Immunity* **30,** 832–844 (2009).
74. Powell, J. D., Pollizzi, K. N., Heikamp, E. B. & Horton, M. R. Regulation of immune responses by mTOR. *Annu. Rev. Immunol.* **30,** 39–68 (2012).
75. Bartelt, R. R., Cruz-Orcutt, N., Collins, M. & Houtman, J. C. D. Comparison of T Cell Receptor-Induced Proximal Signaling and Downstream Functions in Immortalized and Primary T Cells. *PLoS ONE* **4,** e5430 (2009).
76. Finlay, D. K. *et al.* PDK1 regulation of mTOR and hypoxia-inducible factor 1 integrate metabolism and migration of CD8+ T cells. *Journal of Experimental Medicine* **209,** 2441–2453 (2012).
77. Zinzalla, V., Stracka, D., Oppliger, W. & Hall, M. N. Activation of mTORC2 by association with the ribosome. *Cell* **144,** 757–768 (2011).

78. Chen, C.-H. *et al.* ER stress inhibits mTORC2 and Akt signaling through GSK-3β-mediated phosphorylation of rictor. *Sci Signal* **4,** ra10–ra10 (2011).
79. Zoncu, R., Efeyan, A. & Sabatini, D. M. mTOR: from growth signal integration to cancer, diabetes and ageing. *Nat Rev Mol Cell Bio* **12,** 21–35 (2011).
80. Sharpe, A. H. & Abbas, A. K. T-cell costimulation--biology, therapeutic potential, and challenges. *N. Engl. J. Med.* **355,** 973–975 (2006).
81. Lerner, A., Jeremias, P. & Matthias, T. The World Incidence and Prevalence of Autoimmune Diseases is Increasing. *IJCD* **3,** 151–155 (2015).
82. Vojdani, A. A Potential Link between Environmental Triggers and Autoimmunity. *Autoimmune Dis* **2014,** 437231 (2014).
83. Schattner, A. Consequence or coincidence? The occurrence, pathogenesis and significance of autoimmune manifestations after viral vaccines. *Vaccine* **23,** 3876–3886 (2005).
84. Lyons, J. A., San, M., Happ, M. P. & Cross, A. H. B cells are critical to induction of experimental allergic encephalomyelitis by protein but not by a short encephalitogenic peptide. *Eur. J. Immunol.* **29,** 3432–3439 (1999).
85. Mok, C. C. Rituximab for the treatment of rheumatoid arthritis: an update. *Drug Des Devel Ther* **8,** 87–100 (2013).
86. Tuohy, V. K. & Kinkel, R. P. Epitope spreading: a mechanism for progression of autoimmune disease. *Arch. Immunol. Ther. Exp. (Warsz.)* **48,** 347–351 (2000).
87. Salinas, G. F., Braza, F., Brouard, S., Tak, P.-P. & Baeten, D. The role of B lymphocytes in the progression from autoimmunity to autoimmune disease. *Clin. Immunol.* **146,** 34–45 (2013).
88. Pillai, S. Rethinking mechanisms of autoimmune pathogenesis. *J. Autoimmun.* **45,** 97–103 (2013).
89. Olszak, T. *et al.* Microbial exposure during early life has persistent effects on natural killer T cell function. *Science* **336,** 489–493 (2012).
90. Belkaid, Y. & Hand, T. W. Role of the microbiota in immunity and inflammation. *Cell* **157,** 121–141 (2014).
91. Ivanov, I. I. *et al.* Induction of intestinal Th17 cells by segmented filamentous bacteria. *Cell* **139,** 485–498 (2009).
92. Frank, D. N. *et al.* Molecular-phylogenetic characterization of microbial community imbalances in human inflammatory bowel diseases. *Proc. Natl. Acad. Sci. U.S.A.* **104,** 13780–13785 (2007).
93. Wu, H.-J. *et al.* Gut-residing segmented filamentous bacteria drive autoimmune arthritis via T helper 17 cells. *Immunity* **32,** 815–827 (2010).
94. Cooper, G. S., Miller, F. W. & Pandey, J. P. The role of genetic factors in autoimmune disease: implications for environmental

research. *Environ. Health Perspect.* **107 Suppl 5,** 693–700 (1999).
95. Ramos, P. S., Shedlock, A. M. & Langefeld, C. D. Genetics of autoimmune diseases: insights from population genetics. *J. Hum. Genet.* **60,** 657–664 (2015).
96. Gough, S. C. L. & Simmonds, M. J. The HLA Region and Autoimmune Disease: Associations and Mechanisms of Action. *Curr. Genomics* **8,** 453–465 (2007).
97. Rizvi, S. M. & Raghavan, M. Mechanisms of function of tapasin, a critical major histocompatibility complex class I assembly factor. *Traffic* **11,** 332–347 (2010).
98. Pajewski, N. M. *et al.* The role of HLA-DR-DQ haplotypes in variable antibody responses to anthrax vaccine adsorbed. *Genes Immun.* **12,** 457–465 (2011).
99. Ovsyannikova, I. G. *et al.* Human leukocyte antigens and cellular immune responses to anthrax vaccine adsorbed. *Infect Immun* **81,** 2584–2591 (2013).
100. Sommer, S. The importance of immune gene variability (MHC) in evolutionary ecology and conservation. *Front. Zool.* **2,** 16 (2005).
101. Yamazaki, K. *et al.* Control of mating preferences in mice by genes in the major histocompatibility complex. *J. Exp. Med.* **144,** 1324–1335 (1976).
102. Boehm, T. & Zufall, F. MHC peptides and the sensory evaluation of genotype. *Trends Neurosci.* **29,** 100–107 (2006).
103. Kromer, J. *et al.* Influence of HLA on human partnership and sexual satisfaction. *Sci Rep* **6,** 32550 (2016).
104. Ráki, M. *et al.* Similar Responses of Intestinal T Cells From Untreated Children and Adults With Celiac Disease to Deamidated Gluten Epitopes. *Gastroenterology* **153,** 787–798.e4 (2017).
105. Eldershaw, S. A., Sansom, D. M. & Narendran, P. Expression and function of the autoimmune regulator (Aire) gene in non-thymic tissue. *Clin. Exp. Immunol.* **163,** 296–308 (2011).
106. Su, M. A. & Anderson, M. S. Monogenic autoimmune diseases: insights into self-tolerance. *Pediatr. Res.* **65,** 20R–25R (2009).
107. Witte, J. S. Genome-wide association studies and beyond. *Annu Rev Public Health* **31,** 9–20 4 p following 20 (2010).
108. Gregersen, P. K. & Olsson, L. M. Recent advances in the genetics of autoimmune disease. *Annu. Rev. Immunol.* **27,** 363–391 (2009).
109. Davies, H. T., Crombie, I. K. & Tavakoli, M. When can odds ratios mislead? *BMJ* **316,** 989–991 (1998).
110. Sjakste, T. & Kalnina, J. Disease-Specific and Common HLA and Non-HLA Genetic Markers in Susceptibility to Rheumatoid Arthritis, Type 1 Diabetes Mellitus and Multiple Sclerosis. *J Mol Genet Med* **10,** 1–6 (2016).

111. Fousteri, G., Liossis, S.-N. C. & Battaglia, M. Roles of the protein tyrosine phosphatase PTPN22 in immunity and autoimmunity. *Clin. Immunol.* **149,** 556–565 (2013).
112. Reich, N. C. STATs get their move on. *JAKSTAT* **2,** e27080 (2013).
113. Korman, B. D., Kastner, D. L., Gregersen, P. K. & Remmers, E. F. STAT4: genetics, mechanisms, and implications for autoimmunity. *Curr Allergy Asthma Rep* **8,** 398–403 (2008).
114. Fife, B. T. & Bluestone, J. A. Control of peripheral T-cell tolerance and autoimmunity via the CTLA-4 and PD-1 pathways. *Immunological Reviews* **224,** 166–182 (2008).
115. Kurkó, J. *et al.* Genetics of rheumatoid arthritis - a comprehensive review. *Clin Rev Allergy Immunol* **45,** 170–179 (2013).
116. Kristiansen, O. P., Larsen, Z. M. & Pociot, F. CTLA-4 in autoimmune diseases--a general susceptibility gene to autoimmunity? *Genes Immun.* **1,** 170–184 (2000).
117. Anzilotti, C., Pratesi, F., Tommasi, C. & Migliorini, P. Peptidylarginine deiminase 4 and citrullination in health and disease. *Autoimmun Rev* **9,** 158–160 (2010).
118. Sánchez-Zamora, Y. I. & Rodriguez-Sosa, M. The role of MIF in type 1 and type 2 diabetes mellitus. *J Diabetes Res* **2014,** 804519 (2014).
119. Cerosaletti, K. & Buckner, J. H. Protein tyrosine phosphatases and type 1 diabetes: genetic and functional implications of PTPN2 and PTPN22. *Rev Diabet Stud* **9,** 188–200 (2012).
120. Tsygankov, A. Y. TULA-family proteins: an odd couple. *Cell. Mol. Life Sci.* **66,** 2949–2952 (2009).
121. De Jager, P. L. *et al.* Meta-analysis of genome scans and replication identify CD6, IRF8 and TNFRSF1A as new multiple sclerosis susceptibility loci. *Nat. Genet.* **41,** 776–782 (2009).
122. Zoledziewska, M. *et al.* Variation within the CLEC16A gene shows consistent disease association with both multiple sclerosis and type 1 diabetes in Sardinia. *Genes Immun.* **10,** 15–17 (2009).
123. International Multiple Sclerosis Genetics Consortium. Genome-wide association study of severity in multiple sclerosis. *Genes Immun.* **12,** 615–625 (2011).
124. Furlan, G., Minowa, T., Hanagata, N., Kataoka-Hamai, C. & Kaizuka, Y. Phosphatase CD45 both positively and negatively regulates T cell receptor phosphorylation in reconstituted membrane protein clusters. *J. Biol. Chem.* **289,** 28514–28525 (2014).
125. Hermiston, M. L., Xu, Z. & Weiss, A. CD45: a critical regulator of signaling thresholds in immune cells. *Annu. Rev. Immunol.* **21,** 107–137 (2003).
126. Holmes, N. CD45: all is not yet crystal clear. *Immunology* **117,** 145–155 (2006).

127. Lorenz, U. SHP-1 and SHP-2 in T cells: two phosphatases functioning at many levels. *Immunological Reviews* **228,** 342–359 (2009).
128. Frank, C. *et al.* Effective dephosphorylation of Src substrates by SHP-1. *J. Biol. Chem.* **279,** 11375–11383 (2004).
129. Frearson, J. A., Yi, T. & Alexander, D. R. A tyrosine-phosphorylated 110-120-kDa protein associates with the C-terminal SH2 domain of phosphotyrosine phosphatase-1D in T cell receptor-stimulated T cells. *Eur. J. Immunol.* **26,** 1539–1543 (1996).
130. Nguyen, T. V., Ke, Y., Zhang, E. E. & Feng, G.-S. Conditional deletion of Shp2 tyrosine phosphatase in thymocytes suppresses both pre-TCR and TCR signals. *J. Immunol.* **177,** 5990–5996 (2006).
131. Zhang, T. *et al.* Loss of SHP-2 activity in CD4+ T cells promotes melanoma progression and metastasis. *Sci Rep* **3,** 2845 (2013).
132. Manz, B. N. *et al.* Small molecule inhibition of Csk alters affinity recognition by T cells. *eLife* **4,** e08088 (2015).
133. Naramura, M. *et al.* c-Cbl and Cbl-b regulate T cell responsiveness by promoting ligand-induced TCR down-modulation. *Nature Immunology* **3,** 1192–1199 (2002).
134. Bonnevier, J. L., Zhang, R. & Mueller, D. L. E3 ubiquitin ligases and their control of T cell autoreactivity. *Arthritis Res. Ther.* **7,** 233–242 (2005).
135. Bottini, N. *et al.* A functional variant of lymphoid tyrosine phosphatase is associated with type I diabetes. **36,** 337–338 (2004).
136. Begovich, A. B. *et al.* A missense single-nucleotide polymorphism in a gene encoding a protein tyrosine phosphatase (PTPN22) is associated with rheumatoid arthritis. *Am. J. Hum. Genet.* **75,** 330–337 (2004).
137. Kyogoku, C. *et al.* Genetic association of the R620W polymorphism of protein tyrosine phosphatase PTPN22 with human SLE. *Am. J. Hum. Genet.* **75,** 504–507 (2004).
138. Velaga, M. R. *et al.* The codon 620 tryptophan allele of the lymphoid tyrosine phosphatase (LYP) gene is a major determinant of Graves' disease. *J. Clin. Endocrinol. Metab.* **89,** 5862–5865 (2004).
139. Chen, Y.-F. & Chang, J. S. PTPN22 C1858T and the risk of psoriasis: a meta-analysis. *Mol. Biol. Rep.* **39,** 7861–7870 (2012).
140. Matesanz, F. *et al.* Protein tyrosine phosphatase gene (PTPN22) polymorphism in multiple sclerosis. *J. Neurol.* **252,** 994–995 (2005).
141. Bottini, N. & Peterson, E. J. Tyrosine phosphatase PTPN22: multifunctional regulator of immune signaling, development, and disease. *Annu. Rev. Immunol.* **32,** 83–119 (2014).

142. Baranathan, V. *et al.* The association of the PTPN22 620W polymorphism with Behcet's disease. *Ann. Rheum. Dis.* **66,** 1531–1533 (2007).
143. Barrett, J. C. *et al.* Genome-wide association defines more than 30 distinct susceptibility loci for Crohn's disease. *Nat. Genet.* **40,** 955–962 (2008).
144. Barr, A. J. *et al.* Large-scale structural analysis of the classical human protein tyrosine phosphatome. *Cell* **136,** 352–363 (2009).
145. Chang, H.-H. *et al.* PTPN22.6, a dominant negative isoform of PTPN22 and potential biomarker of rheumatoid arthritis. *PLoS ONE* **7,** e33067 (2012).
146. Ronninger, M., Guo, Y., Shchetynsky, K. & Hill, A. The balance of expression of PTPN22 splice forms is significantly different in rheumatoid arthritis patients compared with controls. *Genome …* (2012).
147. Chang, H.-H., Tseng, W., Cui, J., Costenbader, K. & Ho, I.-C. Altered expression of protein tyrosine phosphatase, non-receptor type 22 isoforms in systemic lupus erythematosus. *Arthritis Res. Ther.* **16,** R14 (2014).
148. Gjörloff-Wingren, A., Saxena, M., Williams, S., Hammi, D. & Mustelin, T. Characterization of TCR-induced receptor-proximal signaling events negatively regulated by the protein tyrosine phosphatase PEP. *Eur. J. Immunol.* **29,** 3845–3854 (1999).
149. Vang, T. *et al.* LYP inhibits T-cell activation when dissociated from CSK. *Nat. Chem. Biol.* **8,** 437–446 (2012).
150. Davidson, D., Bakinowski, M., Thomas, M. L., Horejsi, V. & Veillette, A. Phosphorylation-dependent regulation of T-cell activation by PAG/Cbp, a lipid raft-associated transmembrane adaptor. *Mol. Cell. Biol.* **23,** 2017–2028 (2003).
151. Fiorillo, E. *et al.* Autoimmune-associated PTPN22 R620W variation reduces phosphorylation of lymphoid phosphatase on an inhibitory tyrosine residue. *J. Biol. Chem.* **285,** 26506–26518 (2010).
152. la Puerta, de, M. L. *et al.* The autoimmunity risk variant LYP-W620 cooperates with CSK in the regulation of TCR signaling. *PLoS ONE* **8,** e54569 (2013).
153. Burn, G. L. *et al.* Superresolution imaging of the cytoplasmic phosphatase PTPN22 links integrin-mediated T cell adhesion with autoimmunity. *Sci Signal* **9,** ra99–ra99 (2016).
154. Cloutier, J. F. & Veillette, A. Cooperative inhibition of T-cell antigen receptor signaling by a complex between a kinase and a phosphatase. *J. Exp. Med.* **189,** 111–121 (1999).
155. Zhang, J. *et al.* The autoimmune disease-associated PTPN22 variant promotes calpain-mediated Lyp/Pep degradation associated with lymphocyte and dendritic cell hyperresponsiveness. *Nat. Genet.* **43,** 902–907 (2011).

156. Dai, X. *et al.* A disease-associated PTPN22 variant promotes systemic autoimmunity in murine models. *J. Clin. Invest.* **123,** 2024–2036 (2013).
157. Matthews, R. J., Bowne, D. B., Flores, E. & Thomas, M. L. Characterization of hematopoietic intracellular protein tyrosine phosphatases: description of a phosphatase containing an SH2 domain and another enriched in proline-, glutamic acid-, serine-, and threonine-rich sequences. *Mol. Cell. Biol.* **12,** 2396–2405 (1992).
158. Cloutier, J. F. & Veillette, A. Association of inhibitory tyrosine protein kinase p50csk with protein tyrosine phosphatase PEP in T cells and other hemopoietic cells. *EMBO J.* **15,** 4909–4918 (1996).
159. Hasegawa, K. *et al.* PEST domain-enriched tyrosine phosphatase (PEP) regulation of effector/memory T cells. *Science* **303,** 685–689 (2004).
160. Zikherman, J. *et al.* PTPN22 Deficiency Cooperates with the CD45 E613R Allele to Break Tolerance on a Non-Autoimmune Background. *J. Immunol.* **182,** 4093–4106 (2009).
161. Maine, C. J., Marquardt, K., Cheung, J. & Sherman, L. A. PTPN22 controls the germinal center by influencing the numbers and activity of T follicular helper cells. *J. Immunol.* **192,** 1415–1424 (2014).
162. Maine, C. J. *et al.* PTPN22 alters the development of regulatory T cells in the thymus. *J. Immunol.* **188,** 5267–5275 (2012).
163. Brownlie, R. J. *et al.* Lack of the phosphatase PTPN22 increases adhesion of murine regulatory T cells to improve their immunosuppressive function. *Sci Signal* **5,** ra87–ra87 (2012).
164. Zheng, P. & Kissler, S. PTPN22 silencing in the NOD model indicates the type 1 diabetes-associated allele is not a loss-of-function variant. *Diabetes* **62,** 896–904 (2013).
165. Sood, S. *et al.* Loss of the Protein Tyrosine Phosphatase PTPN22 Reduces Mannan-Induced Autoimmune Arthritis in SKG Mice. *J. Immunol.* **197,** 429–440 (2016).
166. Wu, D. J. *et al.* Autoimmunity-associated LYP-W620 does not impair thymic negative selection of autoreactive T cells. **9,** e86677 (2014).
167. Metzler, G. *et al.* The Autoimmune Risk Variant PTPN22 C1858T Alters B Cell Tolerance at Discrete Checkpoints and Differentially Shapes the Naive Repertoire. *J. Immunol.* **199,** 2249–2260 (2017).
168. Schickel, J.-N. *et al.* PTPN22 inhibition resets defective human central B cell tolerance. *Sci Immunol* **1,** aaf7153–aaf7153 (2016).
169. Menard, L. *et al.* The PTPN22 allele encoding an R620W variant interferes with the removal of developing autoreactive B cells in humans. *J. Clin. Invest.* **121,** 3635–3644 (2011).

170. Arechiga, A. F. *et al.* Cutting edge: the PTPN22 allelic variant associated with autoimmunity impairs B cell signaling. *J. Immunol.* **182,** 3343–3347 (2009).
171. Wang, Y. *et al.* The autoimmunity-associated gene PTPN22 potentiates toll-like receptor-driven, type 1 interferon-dependent immunity. *Immunity* **39,** 111–122 (2013).
172. Clarke, F. *et al.* Protein tyrosine phosphatase PTPN22 is dispensable for dendritic cell antigen processing and promotion of T-cell activation by dendritic cells. *PLoS ONE* **12,** e0186625 (2017).
173. Lins, T. C., Vieira, R. G., Grattapaglia, D. & Pereira, R. W. Allele and haplotype frequency distribution in PTPN22 gene across variable ethnic groups: Implications for genetic association studies for autoimmune diseases. *Autoimmunity* **43,** 308–316 (2010).
174. Cagliani, R. & Sironi, M. Pathogen-driven selection in the human genome. *Int J Evol Biol* **2013,** 204240 (2013).
175. Gomez, L. M., Anaya, J.-M. & Martin, J. Genetic influence of PTPN22 R620W polymorphism in tuberculosis. *Hum. Immunol.* **66,** 1242–1247 (2005).
176. Kouhpayeh, H.-R. *et al.* R620W functional polymorphism of protein tyrosine phosphatase non-receptor type 22 is not associated with pulmonary tuberculosis in Zahedan, southeast Iran. *Genet. Mol. Res.* **11,** 1075–1081 (2012).
177. Boechat, A. L., Ogusku, M. M., Sadahiro, A. & Santos, dos, M. C. Association between the PTPN22 1858C/T gene polymorphism and tuberculosis resistance. *Infect. Genet. Evol.* **16,** 310–313 (2013).
178. López-Cano, D. J. *et al.* The PTPN22 R263Q polymorphism confers protection against systemic lupus erythematosus and rheumatoid arthritis, while PTPN22 R620W confers susceptibility to Graves' disease in a Mexican population. *Inflamm. Res.* **66,** 775–781 (2017).
179. Orrú, V. *et al.* A loss-of-function variant of PTPN22 is associated with reduced risk of systemic lupus erythematosus. *Hum. Mol. Genet.* **18,** 569–579 (2009).
180. Rodríguez-Rodríguez, L. *et al.* The PTPN22 R263Q polymorphism is a risk factor for rheumatoid arthritis in Caucasian case-control samples. *Arthritis Rheum.* **63,** 365–372 (2011).
181. Lamsyah, H. *et al.* Association of PTPN22 gene functional variants with development of pulmonary tuberculosis in Moroccan population. *Tissue Antigens* **74,** 228–232 (2009).
182. Mestas, J. & Hughes, C. C. W. Of mice and not men: differences between mouse and human immunology. *J. Immunol.* **172,** 2731–2738 (2004).
183. Tao, L. & Reese, T. A. Making Mouse Models That Reflect

Human Immune Responses. *Trends Immunol.* **38,** 181–193 (2017).
184. Wang, Z., Turner, R., Baker, B. M. & Biddison, W. E. MHC allele-specific molecular features determine peptide/HLA-A2 conformations that are recognized by HLA-A2-restricted T cell receptors. *J. Immunol.* **169,** 3146–3154 (2002).
185. Stanford, S. M. & Bottini, N. PTPN22: the archetypal non-HLA autoimmunity gene. *Nat Rev Rheumatol* **10,** 602–611 (2014).
186. Burn, G. L., Svensson, L., Sanchez-Blanco, C., Saini, M. & Cope, A. P. Why is PTPN22 a good candidate susceptibility gene for autoimmune disease? *FEBS Lett.* **585,** 3689–3698 (2011).
187. Cope, A. P., Schulze-Koops, H. & Aringer, M. The central role of T cells in rheumatoid arthritis. *Clin. Exp. Rheumatol.* **25,** S4–11 (2007).
188. Suurmond, J. & Diamond, B. Autoantibodies in systemic autoimmune diseases: specificity and pathogenicity. *J. Clin. Invest.* **125,** 2194–2202 (2015).
189. Rieck, M. *et al.* Genetic variation in PTPN22 corresponds to altered function of T and B lymphocytes. *J. Immunol.* **179,** 4704–4710 (2007).
190. Aarnisalo, J. *et al.* Reduced CD4+T cell activation in children with type 1 diabetes carrying the PTPN22/Lyp 620Trp variant. *J. Autoimmun.* **31,** 13–21 (2008).
191. Perri, V. *et al.* Use of short interfering RNA delivered by cationic liposomes to enable efficient down-regulation of PTPN22 gene in human T lymphocytes. *PLoS ONE* **12,** e0175784 (2017).
192. Vang, T. *et al.* Autoimmune-associated lymphoid tyrosine phosphatase is a gain-of-function variant. **37,** 1317–1319 (2005).
193. Agrawal, S. & Kandimalla, E. R. Role of Toll-like receptors in antisense and siRNA [corrected]. *Nature Biotechnology* **22,** 1533–1537 (2004).
194. Ran, F. A. *et al.* Genome engineering using the CRISPR-Cas9 system. *Nat Protoc* **8,** 2281–2308 (2013).
195. Jinek, M. *et al.* A programmable dual-RNA-guided DNA endonuclease in adaptive bacterial immunity. *Science* **337,** 816–821 (2012).
196. Schumann, K. *et al.* Generation of knock-in primary human T cells using Cas9 ribonucleoproteins. *Proc. Natl. Acad. Sci. U.S.A.* **112,** 10437–10442 (2015).
197. Abraham, R. T. & Weiss, A. Jurkat T cells and development of the T-cell receptor signalling paradigm. *Nature Immunology* 1–8 (2004).
198. Gioia, L., Siddique, A., Head, S. R., Salomon, D. R. & Su, A. I. A Genome-wide Survey of Mutations in the Jurkat Cell Line. *bioRxiv preprint* 1–16 (2017). doi:10.1101/118117
199. Wu, J. *et al.* Identification of substrates of human protein-tyrosine

phosphatase PTPN22. *J. Biol. Chem.* **281,** 11002–11010 (2006).
200. Salmond, R. J., Brownlie, R. J., Morrison, V. L. & Zamoyska, R. The tyrosine phosphatase PTPN22 discriminates weak self peptides from strong agonist TCR signals. *Nature Immunology* 1–10 (2014). doi:10.1038/ni.2958
201. Brownlie, R. J. *et al.* Resistance to TGFβ suppression and improved anti-tumor responses in CD8+ T cells lacking PTPN22. *Nat Commun* **8,** 1343 (2017).
202. Ruella, M. & Kenderian, S. S. Next-Generation Chimeric Antigen Receptor T-Cell Therapy: Going off the Shelf. *BioDrugs* **31,** 473–481 (2017).
203. Thomas, S. *et al.* Human T cells expressing affinity-matured TCR display accelerated responses but fail to recognize low density of MHC-peptide antigen. *Blood* **118,** 319–329 (2011).
204. Bossi, G. *et al.* Examining the presentation of tumor-associated antigens on peptide-pulsed T2 cells. *Oncoimmunology* **2,** e26840 (2013).
205. Doench, J. G. *et al.* Rational design of highly active sgRNAs for CRISPR-Cas9-mediated gene inactivation. *Nature Biotechnology* **32,** 1262–1267 (2014).
206. Graham, D. B. & Root, D. E. Resources for the design of CRISPR gene editing experiments. *Genome Biol.* **16,** 260 (2015).
207. Cho, S. W. *et al.* Analysis of off-target effects of CRISPR/Cas-derived RNA-guided endonucleases and nickases. *Genome Res.* **24,** 132–141 (2014).
208. Liang, X. *et al.* Rapid and highly efficient mammalian cell engineering via Cas9 protein transfection. *J. Biotechnol.* **208,** 44–53 (2015).
209. Findlay, S. D., Vincent, K. M., Berman, J. R. & Postovit, L.-M. A Digital PCR-Based Method for Efficient and Highly Specific Screening of Genome Edited Cells. *PLoS ONE* **11,** e0153901 (2016).
210. Baghbani, E. *et al.* Suppression of protein tyrosine phosphatase PTPN22 gene induces apoptosis in T-cell leukemia cell line (Jurkat) through the AKT and ERK pathways. *Biomed. Pharmacother.* **86,** 41–47 (2017).
211. Schneider, U. & Bornkamm, G. **Characterization of EBV-genome negative "null" and ‘T’ cell lines derived from children with acute lymphoblastic leukemia and leukemic transformed non-Hodgkin lymphoma**. 1–6 (1977).
212. Kaur, G. & Dufour, J. M. Cell lines: Valuable tools or useless artifacts. *Spermatogenesis* **2,** 1–5 (2012).
213. Khalaf, H., Jass, J. & Olsson, P.-E. Differential cytokine regulation by NF-kappaB and AP-1 in Jurkat T-cells. *BMC Immunol.* **11,** 26 (2010).
214. Wiskocil, R., Weiss, A., Imboden, J., Kamin-Lewis, R. & Stobo, J.

Activation of a human T cell line: a two-stimulus requirement in the pretranslational events involved in the coordinate expression of interleukin 2 and gamma-interferon genes. *J. Immunol.* **134,** 1599–1603 (1985).
215. Henney, C. S., Kuribayashi, K., Kern, D. E. & Gillis, S. Interleukin-2 augments natural killer cell activity. *Nature* **291,** 335–338 (1981).
216. Kasakura, S. & Lowenstein, L. A factor stimulating DNA synthesis derived from the medium of leukocyte cultures. *Nature* **208,** 794–795 (1965).
217. Ruscetti, F. W., Morgan, D. A. & Gallo, R. C. Functional and Morphologic Characterization of Human T Cells Continuously Grown. *J. Immunol.* 1–9 (2018).
218. Oppenheim, J. J. IL-2: more than a T cell growth factor. *J. Immunol.* **179,** 1413–1414 (2007).
219. Zubler, R. H. *et al.* ACTIVATED B CELLS EXPRESS RECEPTORS FOR, AND PROLIFERATE IN RESPONSE TO, PURE INTERLEUKIN 2
. *Journal of Experimental Medicine* 1–14 (2018).
220. Lenardo, M. J. Interleukin-2 programs mouse alpha beta T lymphocytes for apoptosis. *Nature* **353,** 858–861 (1991).
221. Schorle, H., Holtschke, T., Hünig, T., Schimpl, A. & Horak, I. Development and function of T cells in mice rendered interleukin-2 deficient by gene targeting. *Nature* **352,** 621–624 (1991).
222. Sadlack, B. *et al.* Generalized autoimmune disease in interleukin-2-deficient mice is triggered by an uncontrolled activation and proliferation of CD4+ T cells. *Eur. J. Immunol.* **25,** 3053–3059 (1995).
223. Almeida, A. R. M., Legrand, N., Papiernik, M. & Freitas, A. A. Homeostasis of peripheral CD4+ T cells: IL-2R alpha and IL-2 shape a population of regulatory cells that controls CD4+ T cell numbers. *J. Immunol.* **169,** 4850–4860 (2002).
224. Cibrián, D. & Sánchez-Madrid, F. CD69: from activation marker to metabolic gatekeeper. *Eur. J. Immunol.* **47,** 946–953 (2017).
225. Testi, R., D'Ambrosio, D., De Maria, R. & Santoni, A. The CD69 receptor: a multipurpose cell-surface trigger for hematopoietic cells. *Immunol. Today* **15,** 479–483 (1994).
226. Lauzurica, P. *et al.* Phenotypic and functional characteristics of hematopoietic cell lineages in CD69-deficient mice. *Blood* **95,** 2312–2320 (2000).
227. Shiow, L. R. *et al.* CD69 acts downstream of interferon-alpha/beta to inhibit S1P1 and lymphocyte egress from lymphoid organs. *Nature* **440,** 540–544 (2006).
228. Esplugues, E. *et al.* Enhanced antitumor immunity in mice deficient in CD69. *J. Exp. Med.* **197,** 1093–1106 (2003).
229. Sancho, D. *et al.* CD69 downregulates autoimmune reactivity

through active transforming growth factor-beta production in collagen-induced arthritis. *J. Clin. Invest.* **112,** 872–882 (2003).
230. Martín, P. *et al.* The leukocyte activation antigen CD69 limits allergic asthma and skin contact hypersensitivity. *J. Allergy Clin. Immunol.* **126,** 355–65– 365.e1–3 (2010).
231. Radulovic, K. *et al.* CD69 regulates type I IFN-induced tolerogenic signals to mucosal CD4 T cells that attenuate their colitogenic potential. *J. Immunol.* **188,** 2001–2013 (2012).
232. González-Amaro, R., Cortés, J. R., Sánchez-Madrid, F. & Martín, P. Is CD69 an effective brake to control inflammatory diseases? *Trends Mol Med* **19,** 625–632 (2013).
233. la Fuente, de, H. *et al.* The leukocyte activation receptor CD69 controls T cell differentiation through its interaction with galectin-1. *Mol. Cell. Biol.* **34,** 2479–2487 (2014).
234. Brunner, T. *et al.* Cell-autonomous Fas (CD95)/Fas-ligand interaction mediates activation-induced apoptosis in T-cell hybridomas. *Nature* **373,** 441–444 (1995).
235. Volpe, E., Sambucci, M., Battistini, L. & Borsellino, G. Fas-Fas Ligand: Checkpoint of T Cell Functions in Multiple Sclerosis. *Front Immunol* **7,** 382 (2016).
236. Watanabe-Fukunaga, R., Brannan, C. I., Copeland, N. G., Jenkins, N. A. & Nagata, S. Lymphoproliferation disorder in mice explained by defects in Fas antigen that mediates apoptosis. *Nature* **356,** 314–317 (1992).
237. Takahashi, T. *et al.* Generalized lymphoproliferative disease in mice, caused by a point mutation in the Fas ligand. *Cell* **76,** 969–976 (1994).
238. Drappa, J., Vaishnaw, A. K., Sullivan, K. E., Chu, J. L. & Elkon, K. B. Fas gene mutations in the Canale-Smith syndrome, an inherited lymphoproliferative disorder associated with autoimmunity. *N. Engl. J. Med.* **335,** 1643–1649 (1996).
239. Depraetere, V. & Golstein, P. Fas and other cell death signaling pathways. *Seminars in Immunology* **9,** 93–107 (1997).
240. Norian, L. A. *et al.* The regulation of CD95 (Fas) ligand expression in primary T cells: induction of promoter activation in CD95LP-Luc transgenic mice. *J. Immunol.* **164,** 4471–4480 (2000).
241. Nylander, S. & Kalies, I. Brefeldin A, but not monensin, completely blocks CD69 expression on mouse lymphocytes: efficacy of inhibitors of protein secretion in protocols for intracellular cytokine staining by flow cytometry. *J. Immunol. Methods* **224,** 69–76 (1999).
242. Chwae, Y.-J. *et al.* Molecular mechanism of the activation-induced cell death inhibition mediated by a p70 inhibitory killer cell Ig-like receptor in Jurkat T cells. *J. Immunol.* **169,** 3726–3735 (2002).
243. Karas, M., Zaks, T. Z., Liu, J. L. & LeRoith, D. T cell receptor-induced activation and apoptosis in cycling human T cells occur

throughout the cell cycle. *Mol. Biol. Cell* **10,** 4441–4450 (1999).
244. Radvanyi, L. G., Shi, Y., Mills, G. B. & Miller, R. G. Cell cycle progression out of G1 sensitizes primary-cultured nontransformed T cells to TCR-mediated apoptosis. *Cell. Immunol.* **170,** 260–273 (1996).
245. Iezzi, G., Karjalainen, K. & Lanzavecchia, A. The duration of antigenic stimulation determines the fate of naive and effector T cells. *Immunity* **8,** 89–95 (1998).
246. Chuang, W.-Y. *et al.* The PTPN22gain-of-function+1858T(+) genotypes correlate with low IL-2 expression in thymomas and predispose to myasthenia gravis. *Genes Immun.* **10,** 667–672 (2009).
247. Lefvert, A. K. *et al.* PTPN22 R620W promotes production of anti-AChR autoantibodies and IL-2 in myasthenia gravis. *J. Neuroimmunol.* **197,** 110–113 (2008).
248. Rothenberg, E. V. & Ward, S. B. A dynamic assembly of diverse transcription factors integrates activation and cell-type information for interleukin 2 gene regulation. *Proc. Natl. Acad. Sci. U.S.A.* **93,** 9358–9365 (1996).
249. Nardozzi, J. D., Lott, K. & Cingolani, G. Phosphorylation meets nuclear import: a review. *Cell Commun. Signal* **8,** 32 (2010).
250. Chow, C. W., Rincón, M. & Davis, R. J. Requirement for transcription factor NFAT in interleukin-2 expression. *Mol. Cell. Biol.* **19,** 2300–2307 (1999).
251. Xanthoudakis, S. *et al.* An enhanced immune response in mice lacking the transcription factor NFAT1. *Science* **272,** 892–895 (1996).
252. Yoshida, H. *et al.* The transcription factor NF-ATc1 regulates lymphocyte proliferation and Th2 cytokine production. *Immunity* **8,** 115–124 (1998).
253. Peng, S. L., Gerth, A. J., Ranger, A. M. & Glimcher, L. H. NFATc1 and NFATc2 together control both T and B cell activation and differentiation. *Immunity* **14,** 13–20 (2001).
254. Feske, S., Draeger, R., Peter, H. H. & Rao, A. Impaired NFAT regulation and its role in a severe combined immunodeficiency. *Immunobiology* **202,** 134–150 (2000).
255. Decker, E. L., Skerka, C. & Zipfel, P. F. The early growth response protein (EGR-1) regulates interleukin-2 transcription by synergistic interaction with the nuclear factor of activated T cells. *J. Biol. Chem.* **273,** 26923–26930 (1998).
256. Collins, S. *et al.* Opposing regulation of T cell function by Egr-1/NAB2 and Egr-2/Egr-3. *Eur. J. Immunol.* **38,** 528–536 (2008).
257. Karin, M. The regulation of AP-1 activity by mitogen-activated protein kinases. *J. Biol. Chem.* **270,** 16483–16486 (1995).
258. Foletta, V. C., Segal, D. H. & Cohen, D. R. Transcriptional regulation in the immune system: all roads lead to AP-1. *J.*

Leukoc. Biol. **63,** 139–152 (1998).
259. Dérijard, B. *et al.* JNK1: a protein kinase stimulated by UV light and Ha-Ras that binds and phosphorylates the c-Jun activation domain. *Cell* **76,** 1025–1037 (1994).
260. Deng, T. & Karin, M. c-Fos transcriptional activity stimulated by H-Ras-activated protein kinase distinct from JNK and ERK. *Nature* **371,** 171–175 (1994).
261. Minden, A. *et al.* Differential activation of ERK and JNK mitogen-activated protein kinases by Raf-1 and MEKK. *Science* **266,** 1719–1723 (1994).
262. Macián, F., García-Rodríguez, C. & Rao, A. Gene expression elicited by NFAT in the presence or absence of cooperative recruitment of Fos and Jun. *EMBO J.* **19,** 4783–4795 (2000).
263. Macián, F., López-Rodríguez, C. & Rao, A. Partners in transcription: NFAT and AP-1. *Oncogene* **20,** 2476–2489 (2001).
264. Pfeuffer, I. *et al.* Octamer factors exert a dual effect on the IL-2 and IL-4 promoters. *J. Immunol.* **153,** 5572–5585 (1994).
265. Jain, J., Loh, C. & Rao, A. Transcriptional regulation of the IL-2 gene. *Curr. Opin. Immunol.* **7,** 333–342 (1995).
266. Paul, S. & Schaefer, B. C. A new look at T cell receptor signaling to nuclear factor-κB. *Trends Immunol.* **34,** 269–281 (2013).
267. Himes, S. R., Coles, L. S., Reeves, R. & Shannon, M. F. High mobility group protein I(Y) is required for function and for c-Rel binding to CD28 response elements within the GM-CSF and IL-2 promoters. *Immunity* **5,** 479–489 (1996).
268. Yang, L. *et al.* Essential role of nuclear factor kappaB in the induction of eosinophilia in allergic airway inflammation. *J. Exp. Med.* **188,** 1739–1750 (1998).
269. Rao, S., Gerondakis, S., Woltring, D. & Shannon, M. F. c-Rel is required for chromatin remodeling across the IL-2 gene promoter. *J. Immunol.* **170,** 3724–3731 (2003).
270. Sha, W. C., Liou, H. C., Tuomanen, E. I. & Baltimore, D. Targeted disruption of the p50 subunit of NF-kappa B leads to multifocal defects in immune responses. *Cell* **80,** 321–330 (1995).
271. Köntgen, F. *et al.* Mice lacking the c-rel proto-oncogene exhibit defects in lymphocyte proliferation, humoral immunity, and interleukin-2 expression. *Genes Dev.* **9,** 1965–1977 (1995).
272. Bruniquel, D. & Schwartz, R. H. Selective, stable demethylation of the interleukin-2 gene enhances transcription by an active process. *Nature Immunology* **4,** 235–240 (2003).
273. Murayama, A. *et al.* A specific CpG site demethylation in the human interleukin 2 gene promoter is an epigenetic memory. *EMBO J.* **25,** 1081–1092 (2006).
274. Attema, J. L. *et al.* The human IL-2 gene promoter can assemble a positioned nucleosome that becomes remodeled upon T cell activation. *J. Immunol.* **169,** 2466–2476 (2002).

275. Cheadle, C. *et al.* Control of gene expression during T cell activation: alternate regulation of mRNA transcription and mRNA stability. *BMC Genomics* **6,** 75 (2005).
276. Schrum, A. G. Visualization of Multiprotein Complexes by Flow Cytometry. *Current Protocols in Immunology* **6,** 287–18 (2009).
277. Crispín, J. C. & Tsokos, G. C. Transcriptional regulation of IL-2 in health and autoimmunity. *Autoimmun Rev* **8,** 190–195 (2009).
278. Salerno, F., Paolini, N. A., Stark, R., Lindern, von, M. & Wolkers, M. C. Distinct PKC-mediated posttranscriptional events set cytokine production kinetics in CD8+ T cells. *Proc. Natl. Acad. Sci. U.S.A.* **114,** 9677–9682 (2017).
279. Garcia-Sanz, J. A. & Lenig, D. Translational control of interleukin 2 messenger RNA as a molecular mechanism of T cell anergy. *J. Exp. Med.* **184,** 159–164 (1996).
280. Ragheb, J. A., Deen, M. & Schwartz, R. H. CD28-Mediated regulation of mRNA stability requires sequences within the coding region of the IL-2 mRNA. *J. Immunol.* **163,** 120–129 (1999).
281. Cohen, S., Dadi, H., Shaoul, E., Sharfe, N. & Roifman, C. M. Cloning and characterization of a lymphoid-specific, inducible human protein tyrosine phosphatase, Lyp. *Blood* **93,** 2013–2024 (1999).
282. Wang, S. *et al.* Identification of a variant form of tyrosine phosphatase LYP. *BMC Mol. Biol.* **11,** 78 (2010).
283. Dine, J., Gordon, R., Shames, Y., Kasler, M. K. & Barton-Burke, M. Immune Checkpoint Inhibitors: An Innovation in Immunotherapy for the Treatment and Management of Patients with Cancer. *Asia Pac J Oncol Nurs* **4,** 127–135 (2017).
284. Lee, S. & Margolin, K. Cytokines in cancer immunotherapy. *Cancers (Basel)* **3,** 3856–3893 (2011).
285. Guo, X. E., Ngo, B., Modrek, A. S. & Lee, W. H. Targeting tumor suppressor networks for cancer therapeutics. *Curr Drug Targets* **15,** 2–16 (2014).
286. Hartmann, J., Schüßler-Lenz, M., Bondanza, A. & Buchholz, C. J. Clinical development of CAR T cells-challenges and opportunities in translating innovative treatment concepts. *EMBO Mol Med* **9,** 1183–1197 (2017).
287. Lim, W. A. & June, C. H. The Principles of Engineering Immune Cells to Treat Cancer. *Cell* **168,** 724–740 (2017).